

MOLECULAR PATHOGENESIS OF J PARAMYXOVIRUS, A PROTOTYPE
FOR A NEW CLASS OF EMERGING PARAMYXOVIRUS

by

MATHEW ABRAHAM

(Under the Direction of Biao He)

ABSTRACT

J Paramyxovirus (JPV) was first isolated from moribund mice with hemorrhagic lung lesions in Australia in 1972. JPV is a paramyxovirus with a non-segmented, negative-strand RNA-genome. JPV is currently included in a proposed *jeilongvirus* genus within the *paramyxoviridae* family. Small hydrophobic (SH) protein is an integral membrane protein present in jeilongviruses, rubulaviruses, and pneumoviruses. SH has a role in blocking apoptosis by inhibiting the tumor necrosis factor-alpha (TNF- α)-mediated extrinsic apoptotic pathway. JPV caused severe disease in mice. We used JPV to study the role of SH in pathogenicity using laboratory mouse model. Deletion of SH resulted in the attenuation of JPV. We found that the SH of JPV can be replaced with SH of mumps virus (MuV) or respiratory syncytial virus (RSV) to restore the virulence of JPV- Δ SH. Similar functions of these SH proteins despite the lack of sequence similarity of JPV, MuV, and RSV SH genes, suggests the structural resemblance of the SH of paramyxoviruses. JPV genome is large when compared to other paramyxoviruses. The reverse genetics system of JPV allows us to incorporate foreign nucleic acid sequences into its genome to develop JPV-based vectored vaccines. We have replaced the SH gene of JPV with the hemagglutinin (HA) of a highly pathogenic

avian influenza H5N1. Recombinant JPV expressing HA protected mice from a lethal challenge with H5N1. Together, these results show that the deletion of genes or gene segments responsible for virulence is a safe and efficient way to develop JPV based vaccines.

INDEX WORDS: Paramyxovirus, JPV, jeilongvirus, apoptosis, virulence, SH protein, TNF- α , hemagglutinin, vaccine

MOLECULAR PATHOGENESIS OF J PARAMYXOVIRUS, A PROTOTYPE

FOR A NEW CLASS OF EMERGING PARAMYXOVIRUS

by

MATHEW ABRAHAM

BVSc & AH, Kerala Agricultural University, India, 2010

MS, The University of Georgia, 2013

A Dissertation Submitted to the Graduate Faculty of The University of Georgia in

Partial Fulfillment of the Requirements for the Degree

DOCTOR OF PHILOSOPHY

ATHENS, GEORGIA

2018

© 2018

Mathew Abraham

All Rights Reserved

MOLECULAR PATHOGENESIS OF J PARAMYXOVIRUS, A PROTOTYPE

FOR A NEW CLASS OF EMERGING PARAMYXOVIRUS

by

MATHEW ABRAHAM

Major Professor: Biao He
Committee: Zhen Fu
Jeremiah Saliki
Susan Sanchez
Wendy Watford

Electronic Version Approved:

Suzanne Barbour
Dean of the Graduate School
The University of Georgia
December 2018

DEDICATION

I dedicate this dissertation to the memory of Ms. Lini Puthussery (28), an Indian nurse who gave care to the first patient hospitalized with Nipah symptoms during the Nipah outbreak in May 2018 in Kerala state, India. She was exposed to the deadly virus while treating the affected patients and succumbed to the infection on May 21, 2018. Nipah outbreak in 2018 resulted in at least 17 deaths in India. I hope studies on the new and emerging paramyxoviruses will help us to develop strategies to prevent the spread of many zoonotic diseases.

ACKNOWLEDGMENTS

I would like to thank my major professor, Dr. Biao He, for his help and support through my time in his lab. He taught me how to self-motivate to excel in a situation which demands to multitask. I would like to thank Dr. Susan Sanchez and Dr. Jeremiah Saliki for their guidance and also for the opportunity to complete residency training in clinical microbiology together with my graduate studies. I appreciate the advice and guidance of Dr. Zhen Fu and Dr. Wendy Watford while I was working on my thesis work. I would like to thank all my lab members, past and present, for their help and friendship. I would like to thank Boehringer Ingelheim GmbH for their scholarship to support my combined Ph.D./clinical microbiology residency program at UGA. I also would like to thank my parents for their love and support. Last but not least, I would like to thank my wife, Rithu and our son, Noah for rejuvenating me with love, happiness, and motivation.

TABLE OF CONTENTS

	Page
ACKNOWLEDGMENTS	v
LIST OF FIGURES.....	viii
CHAPTER	
1 INTRODUCTION	1
2 LITERATURE REVIEW	4
History and Classification.....	4
Genome Structure and JPV proteins.....	5
Transmission and Pathogenesis	7
Transcription and Replication	8
Functions of Small Hydrophobic Protein.....	10
TNF- α -mediated extrinsic apoptotic pathway.....	12
Reverse genetic system of JPV.....	13
Importance of studying JPV and other Jeilongviruses.....	14
3 ROLE OF SMALL HYDROPHOBIC PROTEIN OF J PARAMYXOVIRUS IN VIRULENCE	21
Abstract	22
Importance	23
Introduction	24
Materials and Methods	27
Results	35

	Discussion	41
	Acknowledgments	44
4	A RECOMBINANT J PARAMYXOVIRUS EXPRESSING HEMAGGLUTININ OF INFLUENZA A VIRUS H5N1 PROTECTED MICE AGAINST LETHAL HIGHLY PATHOGENIC AVIAN INFLUENZA VIRUS H5N1 CHALLENGE.....	62
	Abstract	63
	Importance	64
	Introduction.....	65
	Materials and Methods	67
	Results	72
	Discussion	73
	Acknowledgments	76
5	CONCLUSIONS	83
	REFERENCES	87
	APPENDIX	
A	J PARAMYXOVIRUS (JPV) REPORTER VIRUSES GENERATED BY INCORPORATING A REPORTER GENE INTO THE VIRAL GENOME THROUGH THE INTERNAL RIBOSOMAL ENTRY SITE (IRES) REVEALS THE <i>IN VIVO</i> REPLICATION DYNAMICS OF JPV.....	105

LIST OF FIGURES

	Page
Figure 2.1: Schematic diagram of the JPV genome.....	17
Figure 2.2: TNF- α mediated extrinsic apoptotic pathway.....	18
Figure 2.3: Schematic of the rescue of rJPV-BH.....	19
Figure 2.4: Genome organization of jeilongviruses.....	20
Figure 3.1: Recovery of recombinant virus rJPV- Δ SH-EGFP.....	45
Figure 3.2: Comparison of rJPV and rJPV- Δ SH-EGFP <i>in vitro</i>	47
Figure 3.3: rJPV- Δ SH-EGFP induced more apoptosis in L929 cells.....	49
Figure 3.4: Inhibition of rJPV- Δ SH-EGFP-induced apoptosis by neutralizing antibody against TNF- α	51
Figure 3.5: rJPV- Δ SH-EGFP is attenuated in BALB/c mice.....	53
Figure 3.6: Recovery and growth characteristics of SH chimera viruses, rJPV-MuVSH and rJPV-RSVSH.....	55
Figure 3.7: MuV SH and RSV SH reduce the level of apoptosis and TNF- α production.....	57
Figure 3.8: rJPV-MuVSH and rJPV-RSVSH are pathogenic in mice.....	59
Figure 3.9: Infection of BALB/c mice with rJPV, rJPV- Δ SH-EGFP, rJPV-MuVSH, and rJPVRSVSH.....	61
Figure 4.1: Recovery of recombinant virus rJPV- Δ SH-H5.....	77
Figure 4.2: Gene expression of rJPV and rJPV- Δ SH-H5 <i>in vitro</i>	78
Figure 4.3: Comparison of rJPV and rJPV- Δ SH-H5 <i>in vitro</i>	80

Figure 4.4: Immunization of BALB/c mice with of PBS, rJPV-ΔSH-H5, and rPIV5-H5.....	81
Figure 4.5: Efficacy of rJPV-ΔSH-H5 against HPAI H5N1 challenge in mice.....	82
Figure A.1: Recovery of JPV reporter viruses, rJPV-SH-IRES-nL and rJPV-M-IRES-nL.....	120
Figure A.2: Growth characteristics and luciferase expression of rJPV-SH-IRES-nL	121
Figure A.3: Growth characteristics and luciferase expression of rJPV-M-IRES-nL	122
Figure A.4: Gene expression of JPV reporter viruses, rJPV-SH-IRES-nL and rJPV-M-IRES-nL in Vero cells.....	123
Figure A.5: Infection of BALB/c mice with of rJPV reporter viruses and visualization of JPV replication <i>in vivo</i>	126

CHAPTER 1

INTRODUCTION

J Paramyxovirus (JPV) is a member of the genus *Jeilongvirus* of the family *Paramyxoviridae*. JPV is a virus isolated from moribund mice in Australia in 1972. It has a genome size of 18,954 nucleotides consisting of eight genes in the order 3'-N-P/V/C-M-F-SH-TM-G-L-5'. *Jeilongvirus* is a newly proposed genus under the *Paramyxoviridae* family, which includes rodent viruses like JPV, Tailam virus (TlmPV), and Beilong virus (BeiPV). A new JPV strain (JPV-BH) behaved differently from the old isolate (JPV-LW) in both *in vitro* and *in vivo* conditions. JPV-LW did not cause disease in mice but induced cytopathic effects (CPE) in tissue culture. JPV-BH induced less CPE in tissue culture cells but caused severe disease in mice. As JPV can cause disease in laboratory mice (1), we have chosen JPV as a prototype of the genus to study the pathogenesis of Jeilongviruses in an animal model. Small hydrophobic (SH) protein is detected in many paramyxoviruses and pneumoviruses, but the role of SH in the pathogenicity has never been studied in a suitable animal model. Role of paramyxovirus SH in blocking the virus-induced apoptosis in tissue culture cells by inhibiting the tumor necrotic factor- α (TNF- α)-mediated extrinsic apoptotic pathway was previously determined (2–7). The function of JPV SH protein was studied previously using JPV-LW and revealed the apoptosis blocking function of SH. JPV-LW strain with its SH open reading frame (ORF) replaced with the ORF of *Renilla* luciferase (RLuc) had no growth defect in Vero cells. Due to the lack of pathogenicity of JPV-LW in mice, no difference in terms of mortality or morbidity was seen between

mice infected with JPV-LW and recombinant JPV-LW virus lacking SH (4). Lack of an ideal animal disease model simulating the mode of natural infection prevented studies to elucidate the role of SH in viral pathogenesis. As a rodent paramyxovirus containing SH, a pathogenic JPV-BH strain is very suitable to study the functions of SH of paramyxoviruses in a mouse model. Reverse genetics of JPV helps us to make mutant JPV viruses to investigate the roles of JPV genes and the pathogenic mechanism of Jeilongviruses.

This study includes the following aims:

Specific Aim 1. *To determine the role of SH protein in the pathogenesis of J Paramyxovirus (JPV-BH strain) in its natural host.* A recombinant JPV lacking the coding region of SH has been rescued. Also, the SH of JPV was replaced with the SH of Mumps virus (MuV) or Respiratory Syncytial Virus (RSV) to generate SH chimera viruses. These recombinant viruses were used to study the role of SH in viral replication and cytopathicity. Similarly, these recombinant viruses were tested *in vivo* to understand the role of SH in the pathogenesis of JPV. The working hypothesis is that the deletion of SH will attenuate JPV and the replacement of JPV SH with the SH of MuV or RSV will not alter the replication, cytopathic effect (CPE) and pathogenesis.

Specific Aim 2. *To develop and test the immunogenicity of JPV based vaccine candidates.* JPV is not known to cause disease in any species other than mice. However, JPV antibodies are identified in humans and swine. The large genome size of JPV will allow us to incorporate large foreign nucleic acid sequences into the JPV genome. The reverse genetic system of JPV helps us to modify the JPV genome by deleting virulent

genes and integrating other genes into the genome. Insertion and expression of reporter genes in JPV genome are (described in Appendix A) emphasizing the potential use of JPV to create safe and efficient vectored vaccines for humans and livestock. Deletion of genes or gene segments from JPV vector is safer than mutations in the genome, as latter has a possibility of reversion of virulence. We have used JPV as a vector to generate vaccine against highly pathogenic avian influenza (HPAI) H5N1. The working hypothesis is that JPV based vaccine will provide a protective immune response in animal models.

CHAPTER 2

LITERATURE REVIEW

History and Classification

Family *Paramyxoviridae* includes nonsegmented negative-sense single-stranded RNA viruses, classified under seven genera: *Aquaparamyxovirus*, *Avulavirus*, *Ferlavirus*, *Henipavirus*, *Morbillivirus*, *Respirovirus* and *Rubulavirus* (8, 9). *Jeilongvirus* is a newly proposed genus which includes J Paramyxovirus (JPV), Beilong virus (BeiPV) and Tailam virus (TImPV). These viruses were isolated either from a rodent source or as a contaminant from a rodent cell culture. JPV was first isolated from moribund mice with hemorrhagic lung lesions in Australia in 1972. JPV produced characteristic syncytia in kidney auticulture monolayers, and electron microscopy of the virus revealed the herring-bone shaped nucleocapsid typical of paramyxoviruses. Antibodies against JPV have been detected in mice, rats, pigs, bovines, and humans, suggesting that JPV has a wide host range. The name J was assigned to this virus in reference to M. H. Jun, the virologist who initially characterized this virus (10). In 2006, BeiPV was isolated from human kidney mesangial cells as a contaminant from a rat cell line (11). TImPV was isolated from Sikkim rats in Hong Kong in 2011. Both BeiPV and TImPV have similar genome structure of JPV, indicating that these three viruses are members of the new genus (11–13). Genome replication machinery of JPV and BeiPV can be interchanged, showing the close relationship between these two viruses (14).

Genome Structure and JPV proteins

The full-length genome of JPV has been sequenced and contains 18,954 nucleotides and eight genes in the order 3'-N-P/V/C-M-F-SH-TM-G-L-5' (Fig 2.1) (15). JPV genome is one of the largest among paramyxoviruses sequenced to date. JPV encodes integral membrane proteins, small hydrophobic (SH) and transmembrane (TM) genes which are 69 and 258 amino acids, respectively. JPV SH is a type I integral membrane protein located in the similar genome position of that of other paramyxoviruses, and its size and hydrophilicity profile is identical to MuV SH. There is no sequence homology observed between the JPV SH and SH of other paramyxoviruses. Subcellular localization of SH has not yet been determined. Like other SH proteins, JPV SH has a putative transmembrane domain at the N-terminus. TM is a type II glycosylated integral membrane protein, which promotes cell-to-cell fusion (16). TM is basic, which is a type II transmembrane glycoprotein. TM has two potential sites for O-linked glycosylation and has a putative transmembrane domain. JPV N protein contains 522 amino acids. P gene contains 499 amino acids with the RNA-editing site. Translation of P ORF after a faithful transcription produces Phospho (P) protein. JPV P protein is highly acidic and has potential sites for phosphorylation. The translation of alternative ORF produces C protein within the P gene. C protein contains 152 amino acids. V protein is produced by the addition of one non-templated G residue into the RNA editing site of the P gene. V protein contains 292 amino acids. Addition of two non-templated G residues to the editing site of P gene results in the transcription of mRNA

which codes for a putative W protein, with 310 amino acids. M protein of JPV has 340 amino acids and a similar structure of the M protein of other paramyxoviruses. JPV has a fusion protein (F) which is predicted to be a type I membrane protein containing 544 amino acids. The cleavage site of JPV F protein is monobasic with the sequence GVPGVR. JPV G is one of the largest paramyxovirus attachment proteins sequenced to date. The G gene encodes an attachment protein containing 709 amino acid residues. G has an untranslated region with 2115 nucleotides, and it is a distal second open reading frame termed as ORF-X. The ORF-X has not been detected in JPV-infected cells yet. Nucleotide probes specific to both the G-coding and ORF-X regions identified a mRNA species matching to the G gene (15, 17). Paramyxoviruses with HN attachment protein has a conserved neuraminidase active site which is also present in JPV G protein. The conserved hexapeptide sequence NRKSCS is thought to be an active site for sialic acid attachment, but in JPV this hexapeptide is changed to NRRSCS. JPV G protein has no hemagglutination or neuraminidase activities and contains a putative hydrophobic transmembrane domain (15, 17–19). L gene of paramyxoviruses is essential for the polymerase activity. Six conserved linear domains in the L gene of other paramyxoviruses are also conserved in JPV L (17, 20). JPV L gene has a conserved GDNQ sequence. Other viruses with large genomes – henipaviruses, Tupaia paramyxovirus (TPMV) and Mossman virus (MoV) have an altered GDNE sequence. Mutation of GDNQ sequence to GDNE did not affect the JPV replication in a minigenome system (17, 20–22).

Transmission and Pathogenesis

JPV was isolated on different occasions from four mice with extensive hemorrhagic lung lesions (10, 23). Based on a serological study conducted in Australian mammals, JPV neutralizing antibodies were detected in wild rodents, pigs, and humans. Experimental inoculation of mice and rats with JPV did not show any clinical signs, but autopsy after three weeks post-infection revealed varying degrees of interstitial pneumonia and isolation of virus from lungs, blood, liver, kidneys, and spleen. Experimental infection of JPV in pigs did not cause any clinical signs, but JPV antibodies were detected. (10, 24). Lin-Fa Wang's group performed complete genome sequencing of JPV in 2005 (17). A recombinant JPV-LW (rJPV-LW, named after Lin-Fa Wang) did not cause disease in mice but had a cytopathic effect (CPE) on tissue culture (4). A new JPV strain received from the University of Texas Medical Branch has been propagated in Vero cells, and a full genome sequencing of the new isolate (JPV-BH) was performed. JPV-BH has the same genome organization and number of nucleotides as JPV-LW with one nucleotide difference in the leader sequence and three nucleotide difference in the L gene. JPV behaved differently from the old isolate (JPV-LW) in both *in vivo* and *in vitro* conditions. JPV-BH had less CPE on tissue culture cells but caused severe disease in mice. rJPV-LW replicated faster than JPV-BH in Vero cells. The expression level of viral protein was more in Vero cells infected with rJPV-LW compared to JPV-BH-infected cells. Also, rJPV-LW infection produced more viral genome RNA and mRNA transcripts than JPV-BH. Experimental infection of mice with rJPV-LW or JPV-BH revealed that rJPV-LW is highly attenuated. Mice

infected with rJPV-LW had no detectable lung viral titer at five days post-infection and resulted in little weight loss. JPV-BH replicated steadily to 10^4 PFU/mL with a significant loss of body weight. Infection of lungs with JPV-BH also resulted in interstitial and alveolar infiltration with perivascular cuffing, while no histopathological changes were observed in the lungs of mice infected with rJPV-LW. This altered phenotype of JPV-LW and JPV-BH, suggests that JPV-LW is more adapted for growth in cell culture. It also suggests that JPV-LW was from a later laboratory passage and JPV-BH was from an earlier passage. Replacing the L gene of JPV-BH with the L gene of JPV-LW resulted in attenuation in mice, confirming the role of L gene in viral pathogenesis (1).

Transcription and Replication

All paramyxovirus RNA synthesis begins with the entry of viral RNA-dependent RNA polymerase (vRdRp) to the 3' promoter which transcribes the 3' leader before mRNA synthesis. Initiation of the mRNA synthesis is dependent on the distance between the 3' end of the genome and gene start signal. For *paramyxoviridae*, N gene is transcribed as the first coding gene, and vRdRp responds to the cis-acting sequences at the end of the N gene to produce capped and polyadenylated viral mRNAs. Then, the vRdRp reinitiates mRNA synthesis at the next downstream gene, and this sequential “stop-start” mechanism continues across the viral genome in a 3' to 5' direction (25). Initiation of the mRNA synthesis is also dependent on the strength of the replication promoter (26, 27). Monocistronic mRNA produced by vRdRp contains a 5' cap, which

is polyadenylated by a stuttering mechanism (28) and leads to the termination and release of mRNA. The viral gene junctions that modulate transcription is divided into three segments: Gene End (GE) region at the 3' end of the upstream gene, Intergenic Region (IGR), and a Gene Start (GS) region for the downstream 5' gene. The GE region contains a signal directing the vRdRp to terminate transcription and a stretch of U residues that act as a template for polyadenylation of mRNA by a mechanism that involves stuttering by vRdRp. After termination of transcription, vRdRp remains attached to the genome and reinitiates the transcription as directed by the sequences at the downstream of the GS site, which also directs the addition of methylated 5' guanine cap to the nascent mRNA. This stop-start mechanism is not perfect, and there is more chance for the genes located in the 3' region to get transcribed compared to the genes located away from the 3' end. mRNA production is inversely proportional to the distance from the 3' end of the genome, and this gradient of gene expression is maintained throughout the infection (29, 30). So N mRNAs are found more than the L mRNA. Initiation at downstream GS sites depends on termination at the upstream GE site. Conserved sequences at the gene borders control the stop and reinitiation of the transcription of individual paramyxovirus genes (8). Like henipavirus, morbillivirus, and respirovirus, JPV has a conserved trinucleotide IGR sequence. Paramyxovirus RNA is required to be bound by a helical nucleocapsid to be infectious. Most paramyxoviruses replicate efficiently only if they are a multiple of six nucleotides in length. It is because each nucleocapsid protein associates with precisely six nucleotides to form a helical nucleocapsid core that serves as the template for RNA synthesis (31). At 18,954 nt, the JPV genome adheres to this "rule of six." All paramyxovirus governed

by the rule of six edit their P gene (17, 32–35). The RNA genome of JPV contains eight open reading frames (ORF), but codes for 11 viral proteins. The unedited P mRNA encodes phosphoprotein, but edited P mRNA codes for C, V and W proteins. V protein of paramyxovirus is thought to be important in viral pathogenesis by blocking IL-6 signaling and interferon expression by degrading Signal Transducer and Activator of Transcription, STAT1 (36–41). Like other Paramyxovirus V protein, V protein of JPV and BeiPV interacts with the melanoma differentiation-associated protein 5 (mda5) and inhibits mda5-dependant activation of IFN- β promoter. In contrast to other paramyxoviruses, JPV and BeiPV V protein did not interact or impede STAT signaling, suggesting these two viruses included in the proposed *Jeilongvirus* genus have a V protein-independent strategy to target STAT (42).

Functions of Small Hydrophobic Protein

PIV5, Mumps virus, J paramyxovirus, Metapneumoviruses, and Respiratory Syncytial Virus (RSV) contain SH gene (5, 7, 43, 44). PIV5 SH is a type II membrane protein with 44 amino acids located between the F and HN genes (44, 45). A recombinant PIV5 lacking the coding region of SH (rPIV5 Δ SH) had no growth defect in tissue culture cells, but it induced more apoptosis in both MDBK and L929 cells through a TNF- α -mediated extrinsic apoptotic pathway (2, 3). Mumps SH protein is a type I membrane protein with 57 amino acids, and SH is not essential for the *in vitro* growth of Mumps virus (46). Even though there is no sequence homology between PIV5 SH and Mumps SH, replacement of PIV5 SH with Mumps SH did not change the functional properties

of the protein (5). RSV, a member of family *Pneumoviridae*, also encodes SH protein. RSV lacking SH (RSV Δ SH) was viable and exhibited similar growth pattern of wildtype RSV (47, 48). RSV Δ SH infection resulted in increased apoptosis in A549 cells and L929 cells (7). The function of the SH gene in blocking TNF- α -mediated apoptosis was described previously in MuV, PIV5, RSV, and JPV-LW. Deletion of the SH protein of these viruses did not affect the replication and gene expression *in vitro* (2–7). Recently it was reported that MuV SH inhibits TNF- α , IL-1 β and NF- κ B activation by interacting with TNF-R1, IL-1R1 and TLR3 complexes (49). These findings suggest the role of SH in evading the host immune response. The function of SH protein has not been studied in a suitable pathogenic animal model. PIV5 lacking SH was attenuated compared to wild-type in STAT1 KO mice (2). But STAT1 KO model is not ideal to study viral pathogenesis because PIV5 V protein targets STAT 1 for degradation. Laboratory mouse is not a perfect model to study RSV and MuV pathogenesis. Role of RSV SH in pathogenicity was previously reported. RSV lacking SH expression was attenuated in Chimpanzee and mice (50–52).

Similarly, MuV lacking SH expression was attenuated with reduced neurovirulence in neonatal rat intracerebral infection model (6). Poor systemic replication of MuV was the major limitation in using this model for pathogenesis studies. JPV SH is located between the F and TM genes. It is a type I membrane protein with 69 amino acid residues, a predicted N-terminal ectodomain of 5 residues, a transmembrane domain of 23 residues, and a C-terminal cytoplasmic domain of 41 residues. The function of JPV SH protein was studied previously using JPV-LW and revealed the apoptosis blocking function of SH. JPV-LW strain with its SH ORF replaced with the ORF of *Renilla*

luciferase (RLuc) had no growth defect in Vero cells (4, 17). Due to the lack of pathogenicity of JPV-LW in mice, no difference in terms of mortality or morbidity were seen between mice infected with JPV-LW and recombinant JPV-LW virus lacking SH.

TNF- α -mediated extrinsic apoptotic pathway

TNF- α is a member of the TNF family, identified in the 1980s by its activity in killing tumor cells *in vitro* and *in vivo* (53). TNF- α binds to tumor necrosis factor receptor 1 (TNFR1) on the cell surface and activates pathways that lead to apoptosis (Fig 2.2) or pathways that lead to the activation of NF- κ B (cell survival signaling) and subsequent production of anti-apoptotic proteins. In addition to the TNF- α pathway, binding of Fas to Fas Ligand (FasL) or TNF-related apoptosis-inducing ligand (TRAIL) to its receptors (DR4/DR5) also induces the activation of caspases responsible for the extrinsic apoptotic pathway (54). Upon binding of TNF- α with its receptor, TNFR1 interacts with TRADD through DD domain in its cytoplasmic domain. RIP1, TRAF2/5, and cIAP1/2 are recruited to TNFR1 through interaction with TRADD and forms a Complex 1. Complex 1 is endocytosed and dissociated from the TNFR1, which leads to the transduction of the death signal and activation of the caspase pathway. cIAP1/2 which signals cell survival detaches from TNFR1 leads to the recruitment of FADD, caspase-8, and caspase-10 to form Complex 2a. Complex 2a further activates the downstream effector caspases through a mitochondria-dependent pathway and leads to the activation of caspase-3 and caspase-7, and results in the programmed cell death

(55). TNF- α also signals cell survival through a canonical NF- κ B pathway. For the activation of this pathway Complex 1 remains in the cell membrane and cIAP1/2 is not degraded. RIP1 and TRAF2/5 are polyubiquitinated and provide a ubiquitin-binding site for NF-kappa-B essential modulator (NEMO)/inhibitor of nuclear factor kappa-B kinase subunit gamma (IKK- γ) leading to the recruitment of TAK1 (56, 57). TAK1 activates NF- κ B through the phosphorylation of NF- κ B inhibitor I- κ B (58).

Reverse genetic system of JPV

Development of a reverse genetic system of RNA viruses provided an efficient tool for genetic manipulation of viruses to study the functions of viral proteins and to study the pathogenesis. The reverse genetic system helps to recover infectious virus from a cDNA copy of non-segmented negative-sense single-stranded Virus (NNSV). Reverse genetics for paramyxovirus was first established in Measles Virus (MeV). Insertion of an additional ORF into the MeV genome did not reduce the infectivity of the virus (59). The reverse genetic system of NNSV involves the construction of a plasmid containing the viral anti-genome, and helper plasmids containing the N, P and L genes. Plasmids expressing these viral proteins are transfected into cells together with a plasmid encoding the full-length viral genome. All plasmids used for transfection are under the control of a T7 promoter. T7 polymerase is a bacteriophage-derived RNA polymerase used for the protein expression due to its high transcription efficiency and promoter specificity (60).

Reverse genetic system for JPV has been established for JPV-LW and JPV-BH strains (1, 4). A complete cDNA of the full-length JPV genome was constructed from plasmids carrying JPV genes for N, P, M, F, SH, TM, G, and L. genes together with leader and trailer sequences were cloned into a backbone plasmid from a parainfluenza virus 5 (PIV5) infectious cDNA clone (61). A plasmid with the full-length genome of JPV, together with helper plasmids carrying N, P and L genes were used to transfect 293-T cells. Transfected cells were later co-cultured with Vero cells to rescue recombinant JPV. JPV expressing Enhanced Green Fluorescent Protein (EGFP) was also viable and showed strong fluorescent signals in Vero cells (1, 4, 16). A schematic representation of the reverse genetics of JPV-BH is shown in Figure 2.3.

Importance of studying JPV and other Jeilongviruses

Extensive studies on Jeilongviruses have not been done yet. Recently, many other rodent paramyxoviruses with similar genome structure and phylogenetic relationship with JPV, BeiPV, and TImPV were sequenced. Pohorje Myodes paramyxovirus 1 (PMPV-1) was found in the kidney and lung of a bank vole (*Myodes glareolus*) in Slovenia. Mount Mabu Lophuromys paramyxovirus 1 (MMLPV-1) and Mount Mabu Lophuromys paramyxovirus 2 (MMLPV-2) were isolated from the kidney of a Rungwe brush-furred rat (*Lophuromys machangui*), captured in Mozambique (62). At 20,148 nucleotides, PMPV-1 is the largest mammalian paramyxovirus genus sequenced to date. MMLPV-1 and MMLPV-2 lack the SH gene but have sequence similarity to JPV. (44.31% and 52.55%, respectively). PMPV-1 has 51.51% sequence similarity with

TlmpV. MMLPV-1, MMLPV-2, and PMPV-1 genomes contain a putative RNA editing site (TTAAAAAAGGCA) within their P gene. This RNA editing sequence matches a conserved motif sequence (YTAAAARRGGCA) found in JPV, TlmpV, and BeiPV. Comparison of the genome of jeilongviruses is shown in Figure 2.4.

Jeilongviruses were not clustered with other unclassified paramyxoviruses like Black vole virus, Mossman virus, Nariva virus, and Tupaia paramyxovirus (11, 13, 63, 64). The large genome size of jeilongviruses can be attributed to the presence of SH and TM genes, as well as the large size of the G gene of these viruses. JPV, BeiPV, TlmpV, Rodent PV, MMLPV-1, MMLPV-2, and PMPV-1 have large G genes compared to other paramyxoviruses. G protein is involved in facilitating the cell entry by interacting with specific receptors in the cell membrane. This variation in the sizes of G protein and the presence of ORF-X in JPV, BeiPV, and TlmpV suggests that jeilongviruses utilize a wide variety of receptors to gain entry into the cells. This also indicates the evolutionary adaptation of jeilongviruses to infect multiple hosts. RNA sequences of Jeilongviruses are isolated from bats (65), demonstrating its zoonotic potential, as bats are the natural reservoirs of emerging zoonotic viruses like Ebola (66), SARS-CoV (67) and zoonotic paramyxoviruses like Nipah (68, 69) and Hendra (70). Investigations on JPV is critical because of following reasons: 1) a human pathogenic Jeilongvirus could emerge in the future, so knowledge about the pathogenic mechanism of this class of virus is essential 2) JPV is an excellent candidate to study the functions of the small hydrophobic (SH) protein of paramyxoviruses, 3) TM protein is unique for jeilongviruses, and it is the only paramyxovirus protein known for its role in cell-to-cell fusion, but not essential in virus-to-cell fusion, 4) Presence of JPV specific

antibodies in many species and the large genome size of JPV makes it a possible vector for expressing foreign genes, suggesting the potential use of JPV as a vaccine vector.

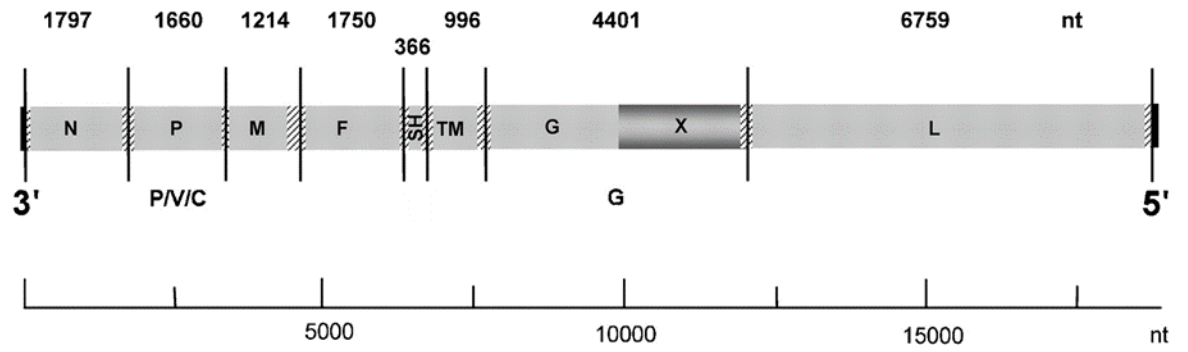


Figure 2.1. Schematic diagram of the JPV genome. Modified from Jack et al., 2008

(15)

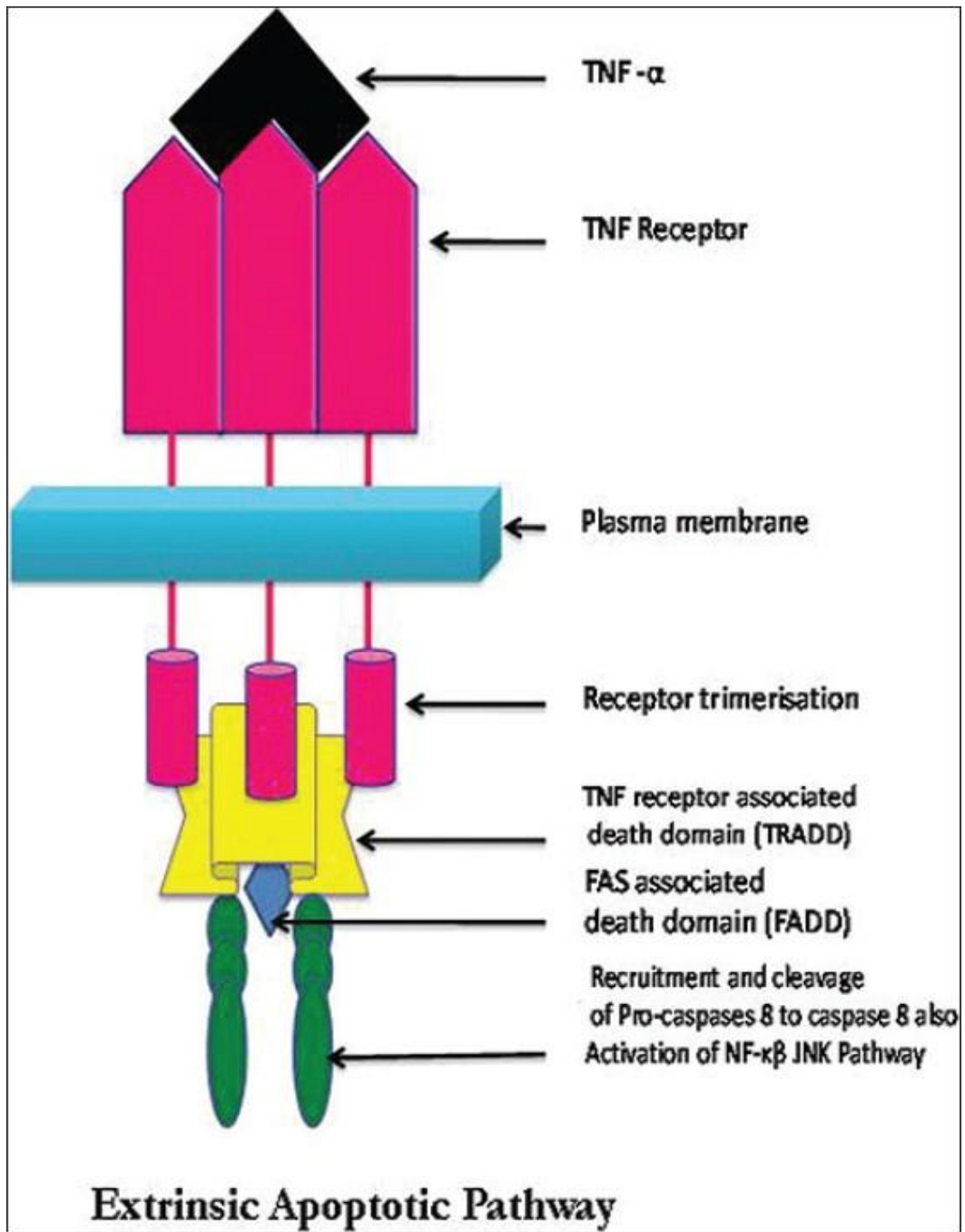


Figure 2.2. *TNF- α mediated extrinsic apoptotic pathway.* Modified from Ghatage et al., 2012 (71)

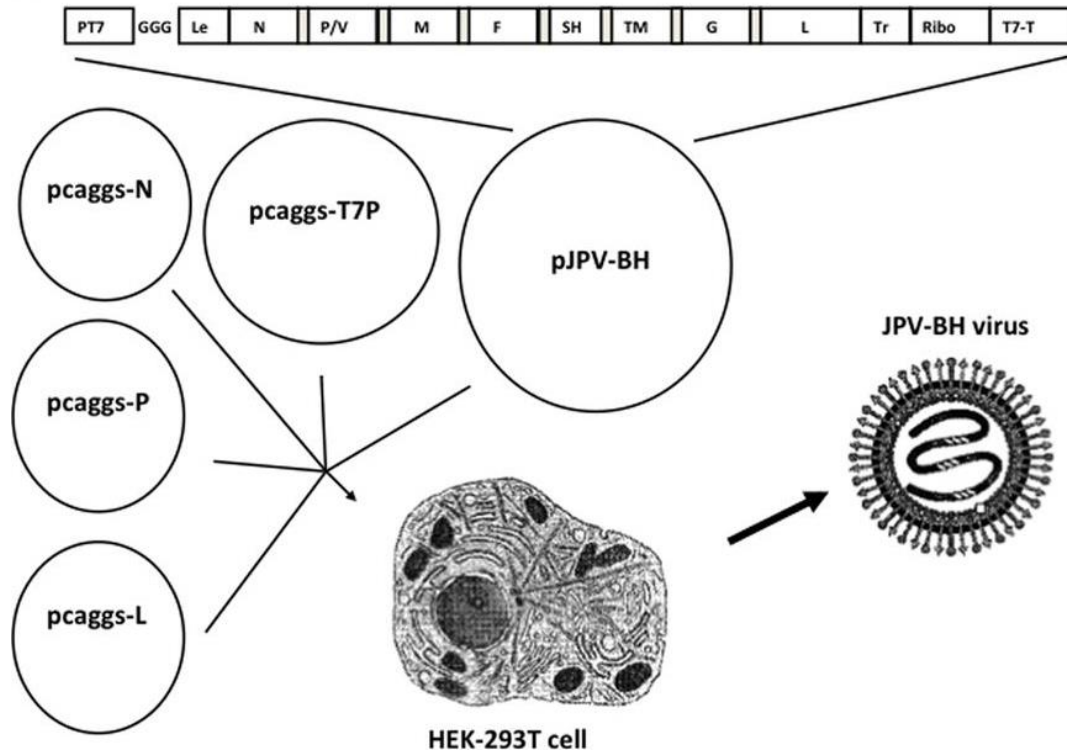


Figure 2.3. Schematic of the rescue of rJPV-BH. The JPV-BH plasmid containing the full-length genome of JPV-BH, a plasmid expressing T7 polymerase, and three helper plasmids encoding the N, P, and L proteins, respectively were cotransfected into HEK293T cells. HEK293T cells were co-cultured with Vero cells. Plaque assays performed on Vero cells were used to obtain single clones of recombinant JPV-BH strains. Modified from Li et al., 2013 (1).

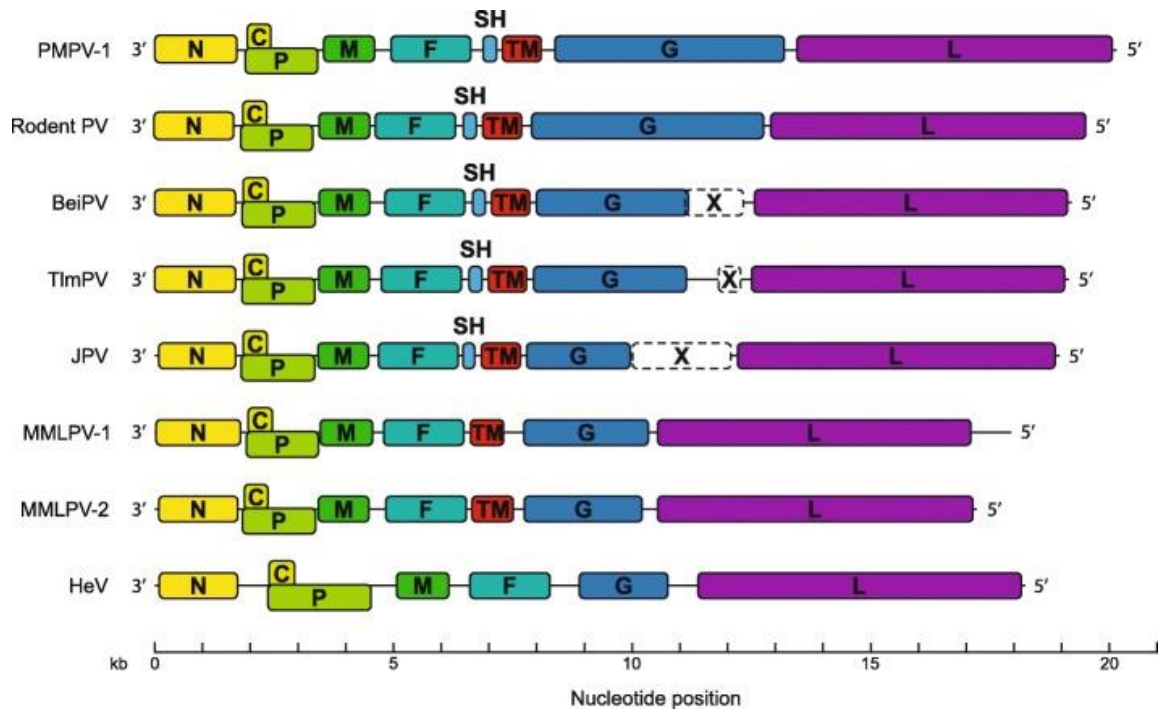


Figure 2.4. Genome organization of jeilongviruses. The genome of all known jeilongviruses was compared with a Hendra virus genome (HeV). Modified from Vanmechelen et al., 2018 (62).

CHAPTER 3
ROLE OF SMALL HYDROPHOBIC PROTEIN OF J PARAMYXOVIRUS IN
VIRULENCE¹

¹Abraham M, Arroyo-Diaz NM, Li Z, Zengel J, Sakamoto K, He B
Copyright © American Society for Microbiology, [*Journal of Virology*, Sept 26 2018,
92 (20) e00653-18; DOI: 10.1128/JVI.00653-18. Reprinted here with permission of the
publisher.

Abstract

J paramyxovirus (JPV) was first isolated from moribund mice with hemorrhagic lung lesions in Australia in 1972. It is a paramyxovirus classified under the newly proposed genus, *Jeilongvirus*. JPV has a genome of 18,954 nucleotides, consisting of eight genes in the order 3'-N-P/V/C-M-F-SH-TM-G-L-5'. JPV causes a little cytopathic effect (CPE) in tissue culture cells but severe disease in mice. The small hydrophobic (SH) protein is an integral membrane protein encoded by many paramyxoviruses such as mumps virus (MuV) and respiratory syncytial virus (RSV). However, the function of SH has not been defined in a suitable animal model. In this work, the functions of SH of JPV, MuV, and RSV have been examined by generating recombinant JPV lacking the SH protein (rJPV- Δ SH-EGFP) or replacing SH of JPV with MuV SH (rJPV-MuVSH) or RSV SH (rJPV-RSVSH). rJPV- Δ SH-EGFP, rJPV-MuVSH, and rJPV-RSVSH were viable and had no growth defect in tissue culture cells. However, more tumor necrosis factor-alpha (TNF- α) was produced during rJPV- Δ SH-EGFP infection, confirming the role of SH in inhibiting TNF- α production. rJPV- Δ SH-EGFP induced more apoptosis in tissue culture cells than rJPV, rJPV-MuVSH, and rJPV-RSVSH, suggesting that SH plays a role in blocking apoptosis. Furthermore, rJPV- Δ SH-EGFP was attenuated in mice compared to rJPV, rJPV-MuVSH, and rJPV-RSVSH, indicating that the SH protein plays an essential role in virulence. We investigated the functions of MuV SH and RSV SH and found that their functions are similar to that of JPV SH even though they have no sequence homology.

Importance

Paramyxoviruses are associated with many devastating diseases in animals and humans. J paramyxovirus (JPV) was isolated from moribund mice in Australia in 1972. Newly isolated viruses such as Beilong virus (BeiPV) and Tailam virus (TImPV) have similar genome structure of JPV. A new paramyxovirus genus, *Jeilongvirus*, which contains JPV, BeiPV, and TImPV, has been proposed. Small hydrophobic (SH) protein is present in many paramyxoviruses. Our present study investigates the role of SH protein of JPV in pathogenesis in its natural host. Understanding the pathogenic mechanism of *Jeilongvirus* is important to control and prevent a disease outbreak that could emerge from this group of viruses.

Introduction

J Paramyxovirus (JPV) is a member of genus *Jeilongvirus* of the *Paramyxoviridae* family. *Jeilongvirus* is a newly proposed genus which includes paramyxoviruses isolated from rodents or as a contaminant from rodent cell culture (11, 21). JPV was first isolated in northern Queensland, Australia in 1972. Extensive hemorrhagic lung lesions were reported in mice from which the virus was isolated. JPV produced characteristic syncytia in kidney auticulture monolayers, and electron microscopy of the virus revealed the herringbone-shaped nucleocapsid typical of paramyxoviruses (10). The full-length genome of JPV was sequenced and contains 18,954 nucleotides and eight genes in the order 3'-N-P/V/C-M-F-SH-TM-G-L-5'. JPV encodes integral membrane proteins, small hydrophobic (SH) and transmembrane (TM) genes, which are 69 and 258 amino acids (aa), respectively (15). TM is a type II glycosylated integral membrane protein, which promotes cell-to-cell fusion (16). JPV has a fusion protein (F), which is predicted to be a type I membrane protein. JPV G is the largest paramyxovirus attachment protein sequenced to date. The G gene encodes a putative 709 aa residue attachment protein and a distal second open reading frame termed, ORF-X, which has not yet been detected in infected cells. Nucleotide probes specific to both the G-coding and ORF-X regions identified a mRNA species matching to the G gene (15, 17). Beilong virus (BeiPV) and Tailam virus (TlmPV) are also included in the same proposed genus due to the identical genome organization and isolation from a rodent source. BeiPV was isolated from rat and human mesangial cell lines. TlmPV was isolated from Sikkim rats (*Rattus andamanensis*). Genomic and phylogenetic evidence supports the grouping of these viruses within the new genus

Jeilongvirus (11–13). *Jeilongviruses* are isolated from bats (65), demonstrating its zoonotic potential, as bats are the natural reservoirs of zoonotic paramyxoviruses like Nipah and Hendra viruses.

There are two different strains of JPV: JPV-LW and JPV-BH. JPV-LW is not pathogenic in mice, but JPV-BH is highly pathogenic in mice. Replacing the L gene of JPV-BH with the L gene of JPV-LW resulted in attenuation in mice, confirming the role of L gene in viral pathogenesis (1). These findings demonstrated that JPV-BH could be used as a model to study the pathogenic mechanisms of *Jeilongviruses*.

Some paramyxoviruses express the SH protein during infection. Parainfluenza virus 5 (PIV5), mumps virus (MuV), metapneumoviruses, and respiratory syncytial virus (RSV) contain the SH gene (7, 43, 44, 72). PIV5 SH is a type II membrane protein, contains 44 aa, and is located between the F and HN genes (44, 45). A recombinant PIV5 lacking the coding region of SH (rPIV5 Δ SH) had no growth defect in tissue culture cells, but it induced more apoptosis in both MDBK and L929 cells through a tumor necrotic factor- α (TNF- α)-mediated extrinsic apoptotic pathway (2, 3). MuV SH protein is a type I membrane protein with 57 aa, and SH is not essential for the *in vitro* growth of MuV (46). Although there is no sequence homology between PIV5 SH and MuV SH, MuV SH was able to functionally replace PIV5 in cell culture (72). RSV, a member of the family *Pneumoviridae*, also encodes SH protein. RSV lacking SH (RSV Δ SH) was viable and exhibited similar growth pattern as wild-type RSV (47, 48). RSV Δ SH infection caused more apoptosis in A549 cells and L929 cells (7). JPV SH is located between the F and TM genes. It is a type I membrane protein with 69 amino acid residues, a predicted N-terminal ectodomain of 5 residues, a transmembrane

domain of 23 residues, and a C-terminal cytoplasmic domain of 41 residues. JPV SH has no sequence similarity with any other paramyxovirus SH but has a similar hydrophilicity profile of the SH proteins of MuV and RSV (17). The function of JPV SH protein was studied previously using JPV-LW and revealed the apoptosis blocking function of SH. JPV-LW strain with its SH open reading frame (ORF) replaced with the ORF of *Renilla* luciferase (RLuc) had no growth defect in Vero cells (73). Due to the lack of pathogenicity of JPV-LW in mice, no difference in terms of mortality or morbidity were seen between mice infected with JPV-LW and recombinant JPV-LW virus lacking SH. Thus, definitive functions of JPV SH in an infection model have been not explored.

Recombinant RSV lacking the expression of SH was attenuated *in vivo* (50–52). RSV is a human virus, and the ideal animal model to study RSV pathogenesis is the Chimpanzee, so the study of RSV SH in a suitable animal model is difficult. Deletion of SH reduced the neurovirulence of MuV in a newborn rat intracerebral infection model (6), but MuV poorly replicates in this animal model and does not cause disease. Lack of an ideal animal disease model simulating the mode of natural infection prevented studies to elucidate the role of SH in viral pathogenesis.

Since JPV-BH is pathogenic in its natural host, we used laboratory mice to compare the pathogenicity of JPV mutant viruses to study the role of JPV genes in pathogenesis. In this work, we replaced the ORF of SH gene of JPV-BH with an enhanced green fluorescent protein (EGFP) without changing the gene start (GS) and gene end (GE) regions of the transcriptional unit. Similarly, we made recombinant chimera viruses, rJPV-MuVSH and rJPV-RSVSH, by replacing the SH of JPV-BH

with the SH of MuV or RSV. The role of the SH gene in pathogenesis was studied for the first time in the natural host of a virus.

Materials and methods

Cells

Human Embryonic Kidney 293T (HEK293T, ATCC, CRL-1573), mouse fibroblast L929 cells (ATCC N° CCL-1), and Vero cells (ATCC) were maintained in Dulbecco's modified Eagle's medium (DMEM) containing 10% fetal bovine serum (FBS), 100 IU/ml penicillin, and 100 µg/ml streptomycin. All cells were incubated at 37°C in 5% CO₂. Cells infected with viruses were grown in DMEM containing 2% FBS. Vero cells were used to perform plaque assays.

Mice

6-week-old, female, BALB/c mice (Envigo) were used for the studies. Mice were infected with JPV in enhanced Biosafety Level 2 facilities in HEPA-filtered isolators. All animal experiments were performed in accordance with the national guidelines provided by "The Guide for Care and Use of Laboratory Animals" and the University of Georgia Institutional Animal Care and Use Committee (IACUC). The Institutional Animal Care and Use Committee (IACUC) of the University of Georgia approved all animal experiments.

Construction of SH recombinant JPV plasmids

In this work, we are exclusively using the JPV-BH backbone. Hence, JPV-BH is referred to as JPV. Construction of a recombinant JPV plasmid with a PvuI restriction site at the N gene was previously described (1). By using standard molecular biology techniques, the ORF of the SH gene was replaced by an enhanced green fluorescent protein (EGFP) gene. The construct lacking the SH gene and containing the EGFP gene was designated as pJPV- Δ SH-EGFP plasmid. Similarly, the SH ORF of JPV was replaced with the ORFs of MuV SH or RSV (A2 strain) SH to generate pJPV-MuVSH and pJPV-RSVSH respectively.

Virus rescue and sequencing

To generate viable recombinant JPV without a SH gene (rJPV- Δ SH-EGFP), a full length pJPV- Δ SH-EGFP plasmid, a plasmid expressing T7 polymerase (pT7P), and three plasmids encoding the N, P, and L proteins of JPV (pJPV-N, pJPV-P, and pJPV-L) were co-transfected into HEK293T cells at 95% confluency in a 6-cm plate with Jetprime (Polypus-Transfection, Inc., New York, NY). The amount of plasmids used were as follows: 5 μ g of full-length pJPV- Δ SH-EGFP plasmid, 1 μ g of pT7P, 1 μ g of pJPV-N, 0.3 μ g of pJPV-P, and 1.5 μ g of pJPV-L. Two days post-transfection, 1/10th of the HEK293T cells were co-cultured with 1 x 10⁶ Vero cells in a 10-cm plate. Seven days after co-culture, media were centrifuged to remove the cell debris, and the supernatant was used for plaque assay in Vero cells to obtain single clones of recombinant JPV- Δ SH. Vero cells were used to grow the plaque-purified virus. Also, full-length pJPV-MuVSH and pJPV-RSVSH plasmids were used to rescue the SH

chimera viruses, rJPV-MuVSH and rJPV-RSVSH. The full-length genomes of plaque-purified rJPV- Δ SH-EGFP, rJPV-MuVSH, and rJPV-RSVSH viruses were sequenced. Total RNA of rJPV- Δ SH-EGFP-, rJPV-MuVSH- and rJPV-RSVSH- infected Vero cells were purified using the RNeasy minikit (Qiagen, Valencia, CA). cDNA was prepared by using random hexamers. PCR amplification of cDNA with primers MA12F and MA09R was used to identify rJPV- Δ SH-EGFP, rJPV-MuVSH, and rJPV-RSVSH. In addition, sequences of all primers used for sequencing the whole genome of rJPV- Δ SH-EGFP, rJPV-MuVSH, and rJPV-RSVSH are available upon request. DNA sequences were determined by an Applied Biosystems sequencer (ABI, Foster City, CA).

Fluorescence microscopy

To confirm the rescue of JPV- Δ SH-EGFP, Vero cells were mock infected or infected with rJPV or JPV- Δ SH. At 2 days post infection (d.p.i), the cells were photographed using a Nikon FXA fluorescence microscope to look for EGFP expression. Lack of SH in rJPV- Δ SH-EGFP was confirmed by immunofluorescence assay. Vero cells were mock infected or infected with rJPV or JPV- Δ SH-EGFP. At 2 d.p.i, cells were washed with phosphate-buffered saline (PBS) and fixed with 0.5% formaldehyde. The cells were permeabilized with 0.1% PBS-saponin solution and were incubated for 30 min with polyclonal anti-F or -SH rabbit serum at a 1:100 dilution (Genescript USA, Inc., Piscataway, NJ) and then Phycoerythrin (PE)-labelled goat anti-rabbit antibody was added to the cells. The cells were incubated for 30 min and were examined and photographed using a Nikon FXA fluorescence microscope.

To detect the NF- κ B P65 subunit, L929 cells on coverslips were mock infected or infected with rJPV, rJPV- Δ SH-EGFP, rJPV-MuVSH, or rJPV-RSVSH at an MOI of 5. At 1 d.p.i, cells were washed with PBS and then fixed with 1% formaldehyde for 15 min at room temperature. Cells were permeabilized using 0.1% Triton-X 100 for 10 min. Cells were washed 3 times with PBS. Anti-mouse JPV N monoclonal antibody conjugated with Zenon™ Allophycocyanin Mouse IgG2a (ThermoFisher Scientific) was used to stain cells for 1h. The cells were washed with PBS and then incubated for 1h in a 1:100 dilution of rabbit monoclonal antibody specific for the p65 subunit of NF- κ B. Cells were washed with PBS and incubated with goat anti-rabbit Cy3 for 1h. The cells were washed 3 times with PBS and stained with DAPI for 10 min. ProLong® Gold Antifade Mountant (Life technologies) was applied directly to the fluorescently-labeled cells. Fluorescence was examined and photographed using a Nikon FXA fluorescence microscope and a Nikon Eclipse Ti confocal microscope. Nuclear translocation of p65 was assessed based on the colocalization of anti-rabbit Cy3 into the DAPI region. Colocalization was expressed in terms of Mander's overlap coefficient using Nikon NIS-Elements software.

Electron Microscopy

rJPV and rJPV- Δ SH-EGFP were grown in Vero cells and concentrated in a 20% sucrose gradient. Concentrated JPV dissolved in PBS were adsorbed onto parlodion-coated grids for 30s. Grids were washed with Tris-buffered saline (TBS) and then stained with 2% phosphotungstic acid, pH 6.6. These grids were then examined using a JEOL 1230 transmission electron microscope (JEOL, Tokyo, Japan).

Growth Kinetics

Vero cells in 6-well plates were infected with rJPV, JPV- Δ SH-EGFP, rJPV-MuVSH, or rJPV-RSVSH at an MOI of 0.1 or 5. The cells were then washed with PBS and maintained in DMEM-2% FBS. The medium was collected at 0, 24, 48, 72, 96, and 120 hours post infection (h.p.i). The titers were determined by plaque assay on Vero cells.

Detection of viral protein expression

Expression of N and F in the virus-infected cells was compared. L929 cells in the six-well plates were mock infected or infected with rJPV or rJPV- Δ SH-EGFP at an MOI of 5. The cells were collected at 2 d.p.i and fixed with 0.5% formaldehyde for 1 h. The fixed cells were resuspended in FBS-DMEM (50:50) and permeabilized with 70% ethanol overnight. The cells were washed once with PBS and then incubated with mouse anti-N monoclonal antibody or mouse anti-F monoclonal antibody in PBS-1% BSA (1:200) for 1 h at 4°C. The cells were stained with APC Goat anti-mouse IgG from Biolegend (1:500) for 1 h at 4°C in the dark and then washed once with PBS-1% BSA. The fluorescence intensity was measured with a flow cytometer (Becton Dickinson LSR II).

To perform immunoblotting, Vero cells in a 6-well plate were mock infected or infected with rJPV, rJPV- Δ SH-EGFP, rJPV-MuVSH, or rJPV-RSVSH at an MOI of 1. At 2 d.p.i, cells were lysed with whole-cell extraction buffer (WCEB: 50 mM Tris-HCl

[pH8], 280 mM NaCl, 0.5% NP-40, 0.2 mM EDTA, 2 mM EGTA, and 10% glycerol). The lysates were run on SDS-PAGE gels and immunoblotted with primary antibody (anti-JPV SH, anti-MuV SH, anti-RSV SH, or anti-JPV N) and corresponding secondary antibodies conjugated to Cy3.

Enzyme-linked immunosorbent assay (ELISA) for TNF- α

L929 cells were mock infected or infected with rJPV, rJPV- Δ SH-EGFP, rJPV-MuVSH or rJPV-RSVSH at an MOI of 5. The medium was collected at 24 h, 48 h, and 72 h.p.i. The amounts of TNF- α were measured by using a mouse TNF- α detection kit (R&D Systems Inc. Minneapolis, MN, USA) according to the manufacturer's instructions. Fifty μ l of the medium from infected cells, standards, or controls were mixed with 50 μ l of assay diluent and added to strips pre-labeled with an antibody against TNF- α . The strips were incubated at room temperature for 2 h. After the strips were washed five times with wash buffer provided by the manufacturer, 100 μ l of a polyclonal antibody specific for mouse TNF- α conjugated to horseradish peroxidase was added, and they were incubated at room temperature for 2 h. The strips were then washed five times, and 100 μ l of tetramethylbenzidine substrate solution was added to each well. The strips were incubated in the dark at room temperature for 30 min, and 100 μ l of stop solution was added to each well. The optical density at 450 nm was measured within 30 min. The amounts of TNF- α were calculated using standard curves generated from known concentrations of TNF- α provided by the manufacturer.

To measure the amount of TNF- α in serum, 50 μ l of sera, standards, or controls were mixed with 50 μ l of assay diluent and added to strips pre-labeled with an antibody against TNF- α . ELISA was then performed as described above.

Apoptosis assay

Confluent L929 cells were mock infected or infected with rJPV or rJPV- Δ SH-EGFP at an MOI of 5. At 2 d.p.i, cells were washed twice with PBS without Mg²⁺ or Ca²⁺ and incubated in 0.5 ml of TTE buffer (0.2% Triton X-100, 10 mM Tris, 15 mM EDTA, pH 8.0) at room temperature for 15 min. Cell lysates were harvested and centrifuged at 14,000 rpm for 20 min. Supernatants were digested with 100 μ g of RNase A/ml at 37°C for 1 h. Samples were purified by phenol-chloroform extraction, precipitated, and washed with 70% ethanol. Pellets were air dried and resuspended in 10 μ l of Tris-EDTA. Electrophoresis was performed on 2% agarose gels with size markers.

For apoptosis assay, Pacific Blue™ Annexin V Apoptosis Detection assay with 7-amino-actinomycin D (7-AAD) from Biolegend (San Diego, CA, USA) was used. L929 cells were mock infected or infected with rJPV, rJPV- Δ SH-EGFP, rJPV-MuVSH, or rJPV-RSVSH at an MOI of 5. At 2 d.p.i, cells were trypsinized and combined with floating cells in the medium. Cells were washed twice with cold BioLegend's Cell Staining Buffer and then resuspended in Annexin V Binding Buffer at a concentration of 0.25-1.0 x 10⁷ cells/ml. One-hundred μ l of cell suspension was then transferred to a 5 ml test tube and mixed with 5 μ l each of Pacific Blue™ Annexin V and 7-AAD Viability Staining Solution. Cells were then vortexed and incubated for

15 min at room temperature (25°C) in the dark. The cells were analyzed by flow cytometry (Becton Dickinson LSR II).

Antibody treatment of infected cells

Confluent L929 cells were mock infected or infected with rJPV or rJPV- Δ SH-EGFP at an MOI of 5 and were incubated in 0.5 ml of DMEM-2% FBS with neutralizing antibody against TNF- α (BD Pharmingen, San Jose, CA) or isotype control at 30 μ g/ml. At 2 d.p.i, the cells were photographed using a light microscope, and an apoptosis assay was performed as described above.

Infection of mice with JPV

All animal experiments were carried out strictly following the protocol approved by the University of Georgia IACUC. To study the pathogenesis of JPV in animals, 6-week-old, female, BALB/c mice (Envigo) were infected with 100 μ l of PBS or 10^6 , 6×10^5 , or 2×10^5 PFU each of rJPV or rJPV- Δ SH-EGFP, intranasally. The weight of the mice was monitored for up to 14 d.p.i.

To study the pathogenesis of rJPV-MuVSH and rJPV-RSVSH, 6-week-old BALB/c mice (Envigo) were infected with 100 μ l of PBS or 8×10^5 of rJPV, rJPV- Δ SH-EGFP, rJPV-MuVSH, or rJPV-RSVSH, intranasally. The weight of the mice was monitored for up to 14 d.p.i. Blood was collected at 1, 3, 5, and 7 d.p.i to determine the serum level of TNF- α . Mice were euthanized at 3 and 7 d.p.i to collect lungs to determine the virus titer.

Histology studies

BALB/c mice from the infection study were euthanized at 3 d.p.i. The lungs were inflated with 4% paraformaldehyde and collected. Samples were processed, embedded, and sectioned for hematoxylin and eosin (H&E) staining. Interstitial pneumonia was scored from 1 (minimal) to 4 (severe) by a board-certified veterinary pathologist blinded to the study groups. Photomicrographs were taken using an Olympus BX41 microscope with an Olympus DP70 microscope digital camera and DP Controller imaging software.

Results

Recovery of recombinant virus rJPV- Δ SH-EGFP

To study the function of SH, we replaced the SH coding sequence in a full-length JPV-BH plasmid with EGFP (Fig. 3.1A). This plasmid, together with three other helper plasmids encoding N, P and L proteins, and a plasmid encoding T7 RNA polymerase, were co-transfected into HEK293T cells and co-cultured with Vero cells as described previously (1). After obtaining the rescued virus, PCR amplification of cDNA with primers MA12F and MA09R was used to identify rJPV- Δ SH-EGFP (Fig. 3.1B). Expression of EGFP in place of SH ORF was visualized with a fluorescence microscope (Fig. 3.1C). Also, the full-length genome sequence of plaque-purified rJPV- Δ SH-EGFP was confirmed by RT-PCR and Sanger sequencing. Recombinant virus lacking SH was further confirmed by immunofluorescence assay with antibodies against JPV SH and F protein (Fig. 3.1D).

Virus morphology and analysis of growth kinetics *in vitro*

To compare the growth kinetics of rJPV and rJPV- Δ SH-EGFP, growth rates at high MOI (Fig. 3.2A) and low MOI (Fig. 3.2B) were determined in Vero cells. Vero cells were infected with rJPV and rJPV- Δ SH-EGFP at the MOI of 5 and 0.1. The medium was harvested at different time points, and titers of virus in media were determined by plaque assay. A similar growth pattern was observed for rJPV and rJPV- Δ SH-EGFP. There was no difference in the plaque morphology of rJPV and rJPV- Δ SH-EGFP (Fig. 3.2C). Examination of virions by electron microscopy was not able to detect any difference in the structure of rJPV and rJPV- Δ SH-EGFP (Fig. 3.2D). Infection of L929 cells with rJPV and rJPV- Δ SH-EGFP produced similar levels of N and F proteins (Fig. 3.2E & 3.2F).

rJPV- Δ SH-EGFP induced more apoptosis in L929 cells than rJPV

To study the phenotype of rJPV and rJPV- Δ SH-EGFP in L929 cells, confluent cells were mock infected or infected with rJPV or rJPV- Δ SH-EGFP at an MOI of 5 (Fig. 3.3A). At 2 d.p.i, more dead cells were seen with rJPV- Δ SH-EGFP infection. To determine whether there was a difference in the apoptosis of rJPV and rJPV- Δ SH-EGFP infected cells, we examined cellular DNA fragmentation, a hallmark of apoptosis, in rJPV- and rJPV- Δ SH-EGFP- infected L929 cells. DNA was extracted from L929 cells infected with rJPV or rJPV- Δ SH-EGFP or mock infected. Extracted DNA was resolved by gel electrophoresis. Fragmented DNA was not visible in mock-infected cells, but both rJPV- and rJPV- Δ SH-EGFP- infected cells had DNA fragmentation. Increased DNA fragmentation was seen in rJPV- Δ SH-EGFP- infected

cells (Fig. 3.3B). To quantify the apoptosis induced by rJPV and rJPV- Δ SH-EGFP, we performed a Pacific Blue™ Annexin V Apoptosis Detection assay with 7-amino-actinomycin D (7-AAD) staining. L929 cells were mock infected or infected with rJPV or rJPV- Δ SH-EGFP. At 2 d.p.i, apoptotic cells were significantly more in cells infected with rJPV- Δ SH-EGFP (Fig. 3.3C). To investigate the role of SH gene of JPV in the production of TNF- α , L929 cells were mock infected or infected with rJPV or rJPV- Δ SH-EGFP at an MOI of 5. Supernatants were collected at various time points to measure the TNF- α production by ELISA. The amount of TNF- α was higher in rJPV- Δ SH-EGFP- infected cells than in rJPV- infected cells (Fig. 3.3D).

Inhibition of rJPV- Δ SH-EGFP-induced apoptosis by neutralizing anti-TNF- α antibody

To determine the role of TNF- α in apoptosis induced by rJPV and rJPV- Δ SH-EGFP infected cells, L929 cells were mock infected or infected with rJPV or rJPV- Δ SH-EGFP at an MOI of 5. Cells were incubated with DMEM-2% FBS containing no antibody, neutralizing antibody against TNF- α , or isotype control at 30 μ g/ml. At 2 d.p.i, cells were examined for CPE. More CPE was seen in cells infected with rJPV- Δ SH-EGFP than those infected with rJPV. CPE was inhibited in rJPV- Δ SH-EGFP- infected cells that were incubated with neutralizing antibody against TNF- α , while untreated cells and cells incubated with isotype control induced more CPE (Fig. 3.4A). The ability of TNF- α neutralizing antibody to inhibit apoptosis was quantified by flow cytometry (Fig. 3.4B). At 2 d.p.i, rJPV- Δ SH-EGFP induced less apoptosis in cells treated with TNF- α neutralizing antibody compared to the untreated cells or cells

treated with isotype control. Only 11.6% (10.9 - 12.3) of neutralizing antibody-treated cells infected with rJPV- Δ SH-EGFP were apoptotic, compared to 31.5% (28.9 - 34.1) apoptotic cells in untreated cells and 23.8% (21.4 - 26.2) apoptosis in cells treated with isotype control. However, the neutralizing antibody did not cause significant inhibition in the apoptosis induced by rJPV. Apoptosis induced by rJPV- Δ SH-EGFP was higher than rJPV. These results indicate that SH plays a role in blocking TNF- α -mediated apoptosis.

rJPV- Δ SH-EGFP is attenuated *in vivo*

BALB/c mice were infected with rJPV or rJPV- Δ SH-EGFP in three different doses at 10^6 , 6×10^5 , and 2×10^5 PFU, or 100 μ l of PBS intranasally. The mice were monitored for 14 days. rJPV infection caused more weight loss (Fig. 3.5A) and mortality (Fig. 3.5B) than rJPV- Δ SH-EGFP. LD₅₀ values of rJPV and rJPV- Δ SH-EGFP were calculated based on the Miller and Tainter method (74) using the back titration titer. LD₅₀ values of rJPV and rJPV- Δ SH-EGFP were determined to be 1.76×10^5 PFU and 6.7×10^5 PFU respectively, confirming that rJPV- Δ SH-EGFP was attenuated.

Recovery and growth characteristics of the SH chimera viruses, rJPV-MuVSH and rJPV-RSVSH

For a comparative study of the function of the SH gene of JPV, MuV and RSV on pathogenicity, recombinant JPV viruses were designed in such a way that the SH ORF of full-length JPV plasmid was replaced with the SH of MuV or RSV (Fig. 3.6A). rJPV-MuVSH and rJPV-RSVSH were rescued and sequenced as described in the Materials

and Methods. After obtaining the rescued viruses, PCR amplification of cDNA with primers MA12F and MA09R was used to identify rJPV-MuVSH and rJPV-RSVSH (Fig. 3.6B). SH proteins in Vero cells infected with rJPV, rJPV-MuVSH, or rJPV-RSVSH were detected by western blotting. JPV N was detected in all virus-infected cells (Fig. 3.6C). Both rJPV-MuVSH and rJPV-RSVSH have similar growth pattern as rJPV as shown in a low MOI (Fig. 3.6D) and high MOI (Fig. 3.6E) growth curve.

MuV SH and RSV SH reduce the level of apoptosis and TNF- α production

It was previously shown that the SH of MuV and RSV block apoptosis and the deletion of SH from either virus resulted in increased TNF- α production *in vitro* (6, 7). To determine the *in vitro* effect of rJPV-MuVSH and rJPV-RSVSH infection, L929 cells were mock infected or infected with rJPV, rJPV- Δ SH-EGFP, rJPV-MuVSH, or rJPV-RSVSH at an MOI of 5. The rJPV- Δ SH-EGFP infection produced a significantly higher level of apoptosis (Fig. 3.7A) and TNF- α production (Fig. 3.7B) than any of the other recombinant JPV infected groups. Interestingly, rJPV-MuVSH and rJPV-RSVSH behaved like wild-type rJPV in terms of apoptosis and TNF- α production. TNF- α activates NF- κ B and the nuclear translocation of the p65 subunit. It has been previously described that rJPV-LW- Δ SH infection increases nuclear translocation of p65. To study the effect of JPV SH, MuV SH and RSV SH on p65 nuclear translocation, L929 cells were mock infected or infected with rJPV, rJPV- Δ SH-EGFP, rJPV-MuVSH, or rJPV-RSVSH at an MOI of 5. There were an increased p65 expression and nuclear translocation in rJPV- Δ SH-EGFP infected cells compared to the other viruses (Fig.

3.7C & 3.7D). These results suggest the functional similarity of SH proteins of JPV, MuV, and RSV.

rJPV-MuVSH and rJPV-RSVSH are pathogenic in mice

MuV SH and RSV SH have not been studied in a suitable animal model to determine their role in pathogenesis. The rJPV-MuVSH and rJPV-RSVSH were used to infect mice to determine their role in pathogenesis. BALB/c mice were intranasally infected with 100 μ l of PBS or 8×10^5 PFU of rJPV, rJPV- Δ SH-EGFP, rJPV-MuVSH, or rJPV-RSVSH. Mice were monitored for 14 days. rJPV, rJPV-MuVSH, and rJPV-RSVSH infection resulted in greater weight loss (Fig. 3.8A) and mortality (Fig. 3.8B) than rJPV- Δ SH-EGFP. However, weight loss and mortality induced by infection with rJPV-MuVSH was intermediate between that induced by rJPV- Δ SH-EGFP and that induced by rJPV or rJPV-RSVSH. High virus load was observed in mice infected with rJPV, rJPV-MuVSH and rJPV-RSVSH at 3 d.p.i, but interestingly, no difference was observed in the virus loads between the groups at 7 d.p.i (Fig. 3.9A). Increased serum levels of TNF- α were detected in rJPV- Δ SH-EGFP-infected animals (Fig. 3.9B), suggesting that SH plays a role in reducing the production of TNF- α in JPV-infected animals. Reduced weight loss and a higher survival rate in rJPV- Δ SH-EGFP-infected mice was supported by histopathology, which showed less interstitial pneumonia in the lungs of mice infected with rJPV- Δ SH-EGFP (Fig. 3.9C).

Discussion

The families *Paramyxoviridae* and *Pneumoviridae* are in the order *Mononegavirales*, which has a non-segmented, negative-stranded RNA genome. Viruses in these two families have many similarities in gene order, gene expression strategies, and replication. *Jeilongvirus* is a newly proposed genus under the *Paramyxoviridae* family, which includes rodent viruses like JPV and BeiPV. JPV and BeiPV have similar genome organization, and it was previously shown that their genome replication machinery could be interchanged (17, 21). Unlike other paramyxoviruses, the inhibition of STAT1 translocation by JPV and BeiPV is V protein-independent, supporting the inclusion of these viruses in a new genus (42). The presence of two additional membrane proteins, SH and TM, in the genome of JPV, TImPV, and BeiPV makes these viruses unique in comparison to other paramyxoviruses (11, 12, 17). At present, very little is known about *Jeilongviruses*. JPV antibodies have been detected in wild mice, wild rats, pigs, and humans (10), suggesting a wide host range of JPV. JPV can cause severe disease in laboratory mice (1), which makes JPV an excellent model to study the pathogenesis of *Jeilongviruses in vivo*.

The function of the SH gene in blocking TNF- α -mediated apoptosis was described previously in MuV, PIV5, RSV, and JPV-LW. Deletion of the SH protein of these viruses did not affect the replication and gene expression *in vitro* (2, 7, 72, 73). Recently, it was reported that MuV SH inhibits TNF- α , IL-1 β , and NF- κ B activation by interacting with TNF-R1, IL-1R1 and TLR3 complexes (49). These findings suggest the role of SH in evading the host immune response. However, the role of SH protein has not been studied in a suitable pathogenic animal model, and the *in vivo* roles had

not been examined. The laboratory mouse is not an ideal model in which to study RSV and MuV pathogenesis. The role of RSV SH in pathogenicity has been previously reported (50–52). RSV lacking SH expression was attenuated in chimpanzees and mice. As RSV is a virus that affects humans, using chimpanzees for studying RSV pathogenicity is more relevant but difficult due to the ethical and financial concerns. Similarly, MuV lacking SH expression was attenuated with reduced neurovirulence in a neonatal rat intracerebral infection model (6). Poor systemic replication of MuV was the major limitation in using this model for pathogenesis studies. As a rodent paramyxovirus containing SH, JPV is very suitable to study the functions of SH of paramyxoviruses in mice. rJPV- Δ SH-EGFP had no growth defect in tissue culture cells. Plaque size and expression of viral proteins were similar in rJPV- and rJPV- Δ SH-EGFP- infected cells. Cells infected with rJPV- Δ SH-EGFP underwent greater apoptosis and TNF- α production. Neutralizing antibodies against TNF- α inhibited the apoptosis induced by rJPV- Δ SH-EGFP in L929 cells, confirming the role of SH protein in blocking the TNF- α -mediated apoptosis. No significant inhibition in apoptosis was seen in rJPV-infected cells incubated with TNF- α neutralizing antibody. Interestingly, L929 cells incubated with TNF- α neutralizing antibodies have been reported to inhibit the apoptosis induced by rJPV (LW strain) in a previous study (73). This might be due to the increased production of TNF- α and better sensitivity to TNF- α neutralizing antibodies in infection with the tissue culture-adapted JPV-LW strain. In contrast, JPV-BH is not a tissue culture adapted strain, causing less CPE than JPV-LW (1). We generated JPV-BH-based SH chimera viruses, rJPV-MuVSH and rJPV-RSVSH, to study the functional relationship between the SH of JPV, MuV, and RSV. rJPV-

MuVSH and rJPV-RSVSH infection in L929 cells resulted in reduced levels of apoptosis, inhibition of NF- κ B p65 translocation and decreased TNF- α production compared to the rJPV- Δ SH-EGFP infection. rJPV- Δ SH-EGFP was attenuated in mice with infection resulting in reduced weight loss. The LD₅₀ value of rJPV- Δ SH-EGFP was higher than rJPV in infection in BALB/c mice. We also observed increased serum levels of TNF- α in rJPV- Δ SH-EGFP-infected animals at 3 d.p.i and 5 d.p.i. The increased serum levels of TNF- α correlates with the decreased lung viral load and less interstitial pneumonia in rJPV- Δ SH-EGFP-infected animals at 3 d.p.i., suggesting the role of increased TNF- α in the attenuation of rJPV- Δ SH-EGFP. It is possible that increased TNF- α -mediated apoptosis of cells infected with rJPV- Δ SH-EGFP limited the cell-to-cell spread of virus infection and reduced the lung lesions. rJPV-MuVSH and rJPV-RSVSH were pathogenic in animals, and for the first time, we have demonstrated functions of MuV and RSV SH in an animal model. rJPV-RSVSH behaved like rJPV in mouse infection; replacing JPV SH with RSV SH completely rescued the JPV SH's phenotype. Even though there is no sequence homology between the JPV SH and the SH of MuV or RSV, the functions of the proteins are similar in a mouse model, suggesting that the SH proteins of various paramyxoviruses may have structural similarity, and/or that pathways affected by SH proteins are conserved in both mice and humans. Interestingly, rJPV-MuVSH was less pathogenic than rJPV-RSVSH and rJPV, indicating that MuV SH can only partially complement JPV SH functions. It is possible that this difference in pathogenicity might be due to the difference in the expression of various pro-inflammatory cytokines. Further

examination of the viruses *in vivo* may allow dissection of the different roles of JPV and MuV SH in the regulation of various cytokines.

Acknowledgments

We appreciate the members of He laboratory for their helpful discussion and technical assistance. We thank the Animal Facility and Flow Cytometry facility of the College of Veterinary Medicine at the University of Georgia for their help and support. This work was supported by grants from the NIH NIAID (R01AI128924) to B.H.

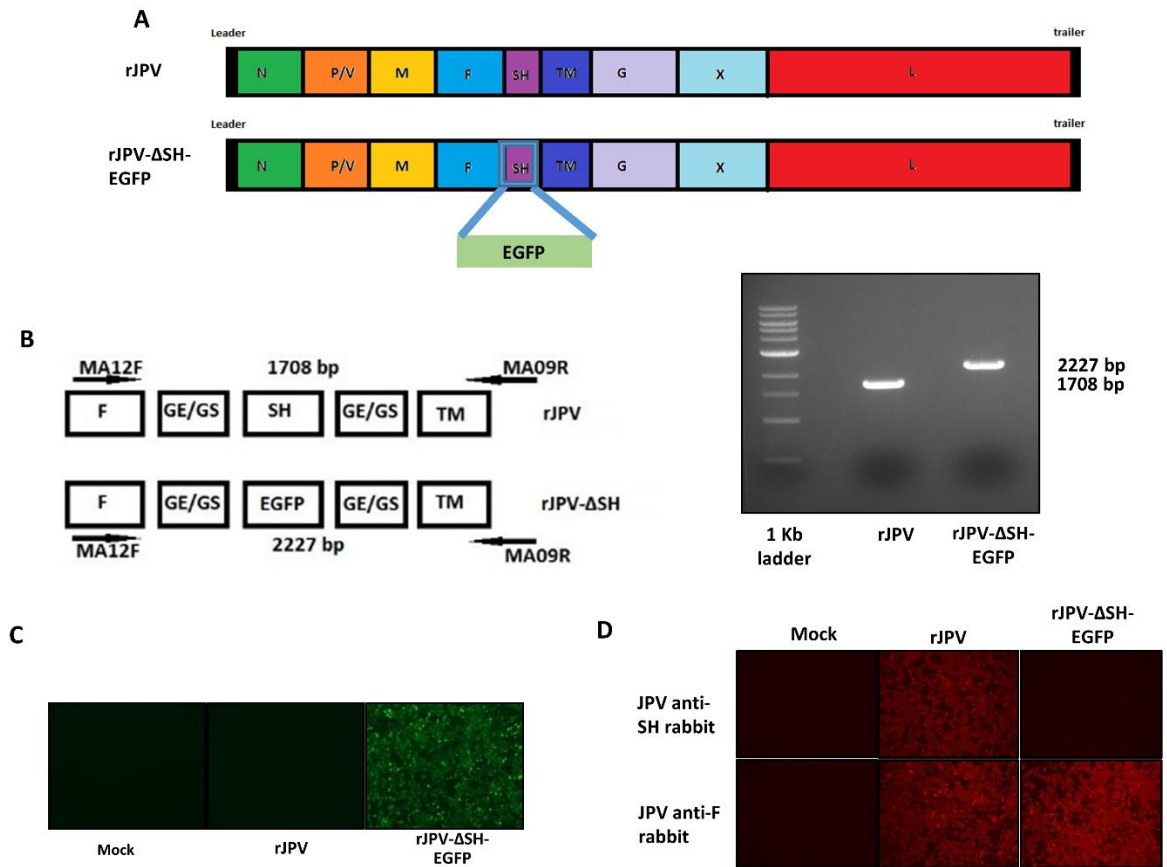


Figure 3.1. Recovery of recombinant virus rJPV- Δ SH-EGFP (A) Schematics of rJPV and rJPV- Δ SH-EGFP, indicating the location where the ORF of SH was replaced with EGFP. (B) To confirm the deletion of SH and the presence of EGFP in rJPV- Δ SH-EGFP, RT-PCR was performed using primers MA12F and MA09R to amplify the SH region. (C) EGFP expression of rJPV- Δ SH-EGFP. Vero cells were mock infected or infected with rJPV or rJPV- Δ SH-EGFP at an MOI of 5. At 2 d.p.i., fluorescence was examined using a NikonFXA fluorescence microscope (10x magnification). (D) Immunofluorescent staining of Vero cells infected with rJPV or rJPV- Δ SH-EGFP. Vero cells were mock infected or infected with rJPV or JPV- Δ SH-EGFP. At 2 d.p.i, cells were washed with PBS and fixed with 0.5% formaldehyde. The cells were permeabilized with 0.1% PBS-saponin solution incubated for 30 min with polyclonal

anti-F or -SH rabbit serum at a 1:100 dilution, and PE-labelled with goat anti-rabbit antibody. The cells were incubated for 30 min and examined and photographed using a Nikon FXA fluorescence microscope.

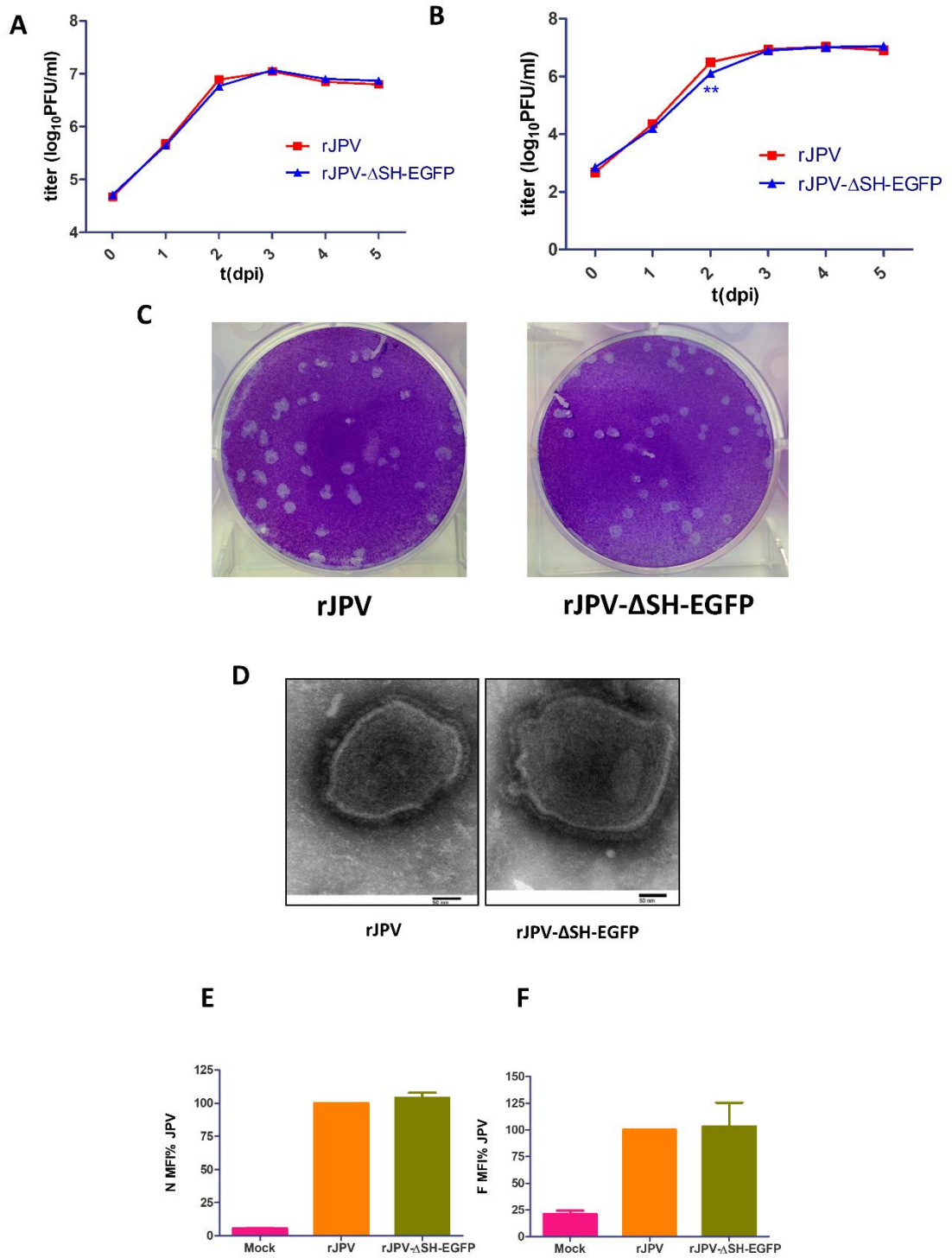


Figure 3.2. Comparison of rJPV and rJPV-ΔSH-EGFP in vitro (A) High MOI growth curve of rJPV and rJPV-ΔSH-EGFP. Vero cells in a 6 well plate were infected, in

triplicates, with rJPV or rJPV- Δ SH-EGFP at a MOI of 5, and the medium was harvested at 24-h intervals. Plaque assays were performed on Vero cells to determine the virus titer. (B) Low MOI growth curve of rJPV and rJPV- Δ SH-EGFP. Vero cells in a 6 well plate were infected, in triplicates, with rJPV or rJPV- Δ SH-EGFP at a MOI of 0.1, and the medium was harvested at 24-h intervals. Plaque assays were performed on Vero cells to determine the virus titer. (C) Plaques formed by rJPV and rJPV- Δ SH-EGFP in Vero cells. Plaques were stained with 0.5% crystal violet. (D) Morphology of rJPV and rJPV- Δ SH-EGFP. Viruses were grown in Vero cells and concentrated in a 20% sucrose gradient. Concentrated viruses dissolved in PBS were adsorbed onto electron microscopy grids and negatively stained with phosphotungstic acid. Bar, 50 nm. (2E & F) Expression of N and F in the virus-infected cells. L929 cells in the six-well plates were mock infected or infected with rJPV or rJPV- Δ SH-EGFP at a MOI of 5. The cells were collected at 2 d.p.i and fixed with 0.5% formaldehyde for 1 h. The fixed cells were resuspended in FBS-DMEM (50:50) and permeabilized with 70% ethanol overnight. The cells were washed once with PBS and then incubated with mouse anti-N monoclonal antibody and mouse anti-F monoclonal antibody. Secondary staining was performed using APC Goat anti-mouse IgG and the fluorescence intensity was measured with a flow cytometer. Samples are triplicates, and error bars show standard errors of the means.

Statistical significance between groups at each time point was calculated based on two-way ANOVA to compare the growth kinetics. (P<0.001 ***, P<0.01 **, P < 0.05 *)

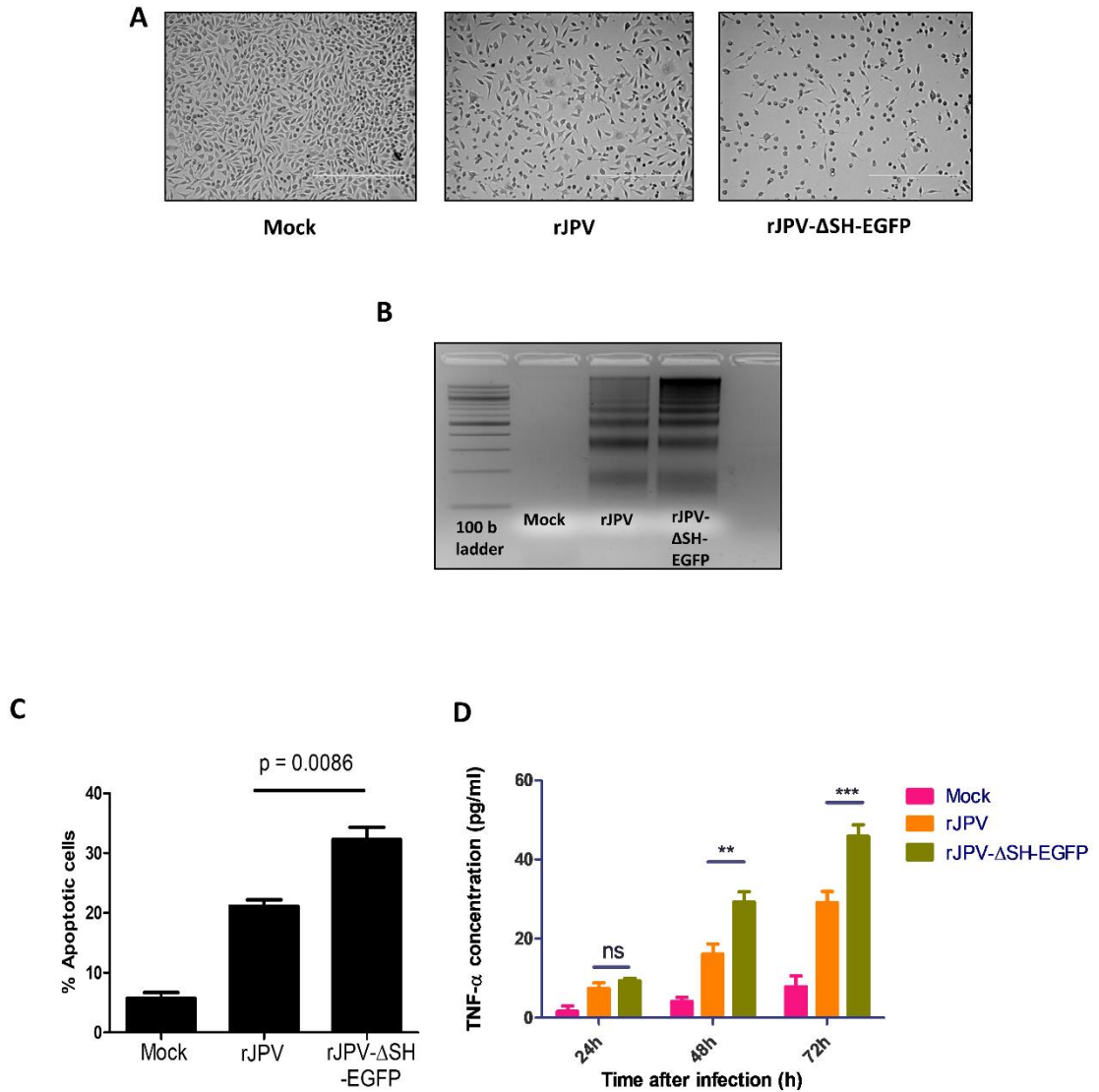


Figure 3.3. rJPV-ΔSH-EGFP induced more apoptosis in L929 cells (A) CPE induced by rJPV and rJPV-ΔSH-EGFP infection in L929 cells. L929 cells were mock infected or infected with rJPV or rJPV-ΔSH-EGFP at a MOI of 5. At 2 d.p.i., the cells were photographed. (B) DNA fragmentation assay in rJPV or rJPV-ΔSH-EGFP-infected cells. L929 cells were mock infected or infected with rJPV or rJPV-ΔSH-EGFP at an MOI of 5. The cells were collected at 2 d.p.i. (C) Induction of apoptosis by rJPV and rJPV-ΔSH-EGFP viruses. L929 cells were mock infected or infected with rJPV or rJPV-ΔSH-EGFP at an MOI of 5. The cells were collected for Pacific Blue™ Annexin

V Apoptosis Detection assay with 7-amino-actinomycin D (7-AAD) at 2 d.p.i. Statistical significance was calculated based on student t-test. (D) Concentrations of TNF- α produced from rJPV and rJPV- Δ SH-EGFP-infected cells. L929 cells were mock infected or infected with rJPV or rJPV- Δ SH-EGFP. The medium was collected at different time points after infection. The amounts of TNF- α were measured by ELISA. Samples are triplicates, and error bars show standard errors of the means. Statistical significance between groups at each time point was calculated based on two-way ANOVA. (P<0.001 ***, P<0.01 **, P < 0.05 *)

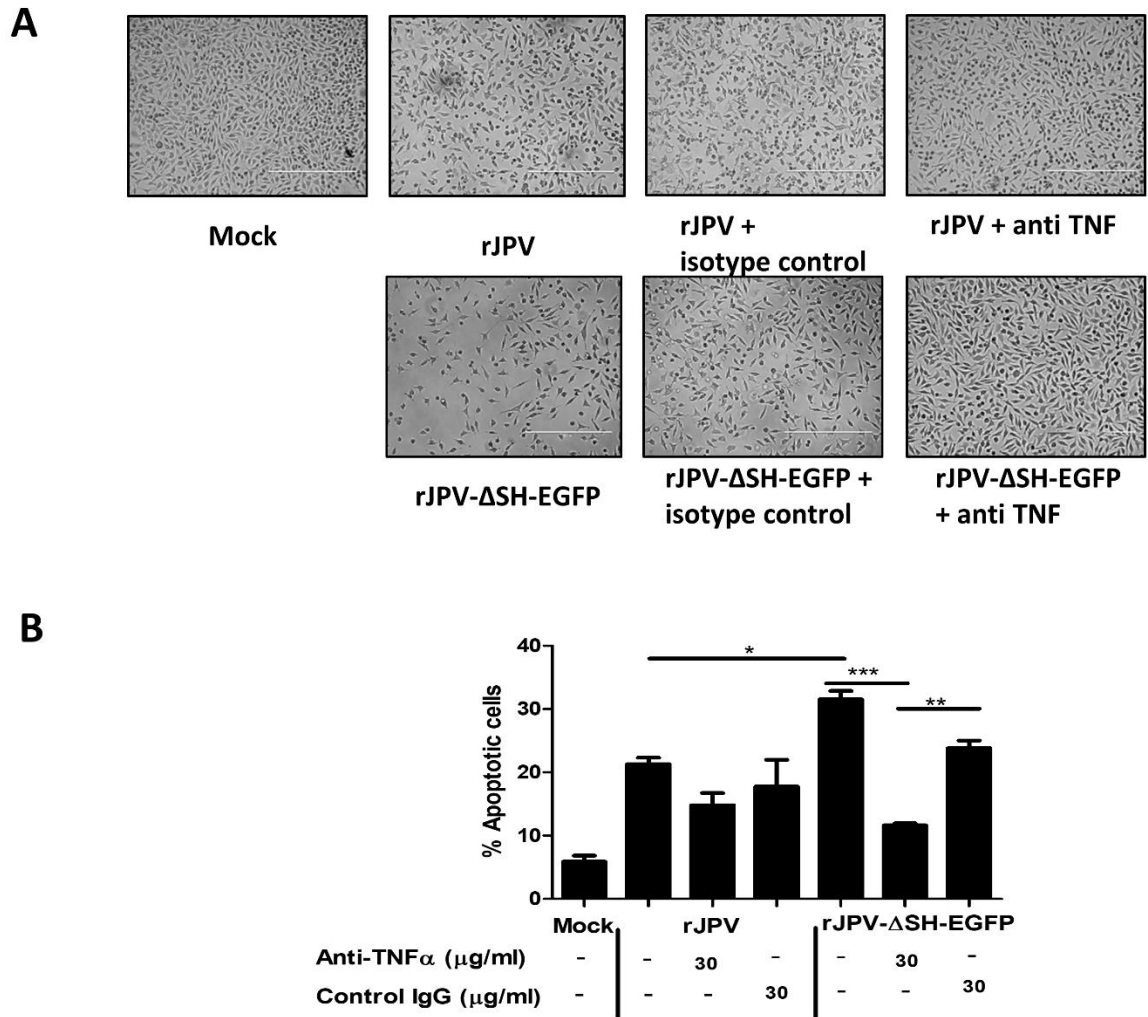
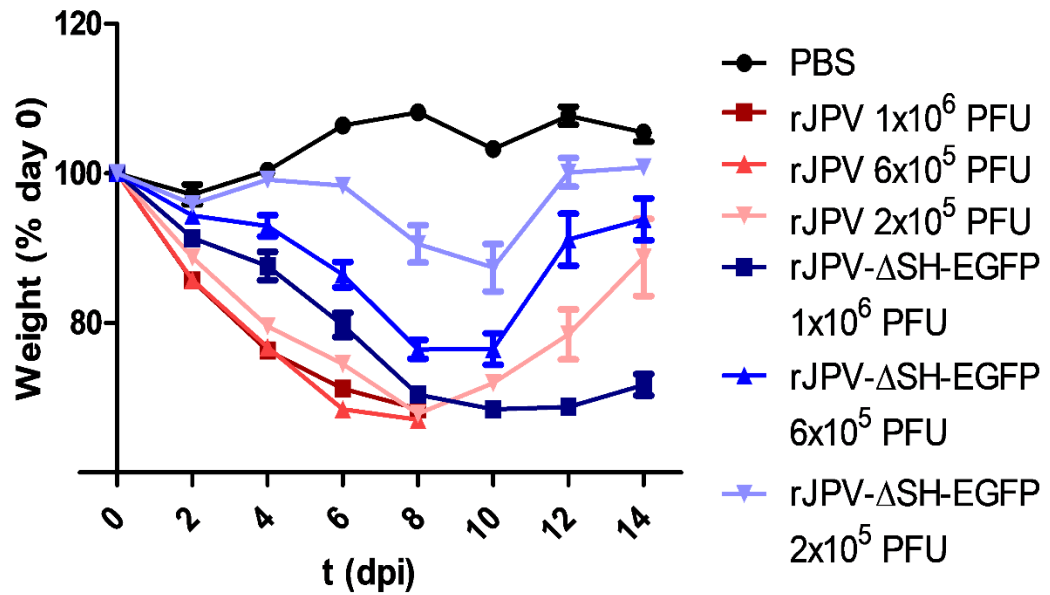


Figure 3.4. Inhibition of rJPV-ΔSH-EGFP-induced apoptosis by neutralizing antibody against TNF-α (A) Inhibition of CPE by the neutralizing antibody against TNF-α. L929 cells were mock infected or infected with rJPV or rJPV-ΔSH-EGFP at an MOI of 5 and incubated with no antibody, isotype control (30 μg/ml), or TNF-α neutralizing antibody (30 μg/ml) for 2 days. (B) Inhibition of apoptosis by neutralizing antibody against TNF-α. L929 cells were mock infected or infected with rJPV or rJPV-ΔSH-EGFP at an MOI of 5 and incubated with no antibody, control antibody (30 μg/ml), or neutralizing antibody (30 μg/ml) for 2 days. Pacific Blue™ Annexin V Apoptosis Detection assay

with 7-AAD was carried out at 2 d.p.i. Error bars show standard errors of the means. All infections were performed in triplicates. Statistical significance between groups at each time point was calculated based on one-way ANOVA. ($P < 0.001$ ***, $P < 0.01$ **, $P < 0.05$ *)

A



B

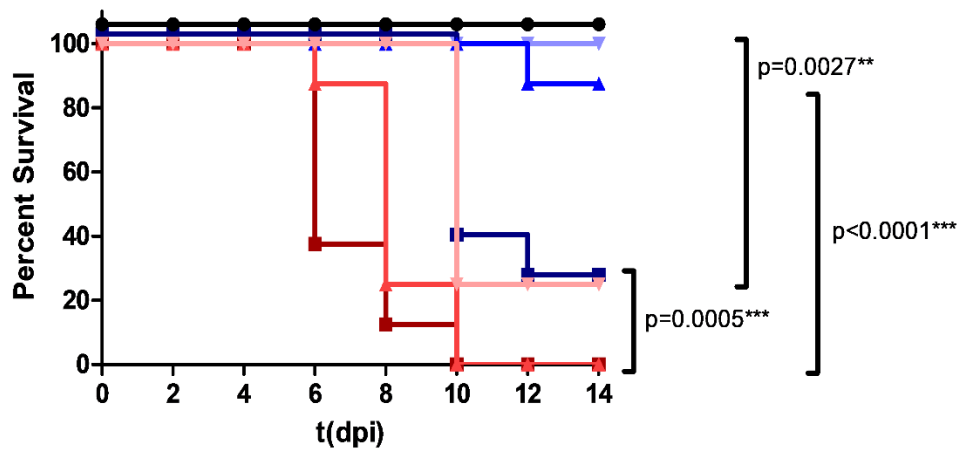


Figure 3.5. rJPV- Δ SH-EGFP is attenuated in BALB/c mice. BALB/c mice in 7 groups, each with 8 animals were infected with rJPV or rJPV- Δ SH-EGFP in three different doses such as 10^6 , 6×10^5 , and 2×10^5 PFU or 100 μ l of PBS intranasally. (A) Body weight loss. Mice were monitored daily, and weight loss was graphed as the average percentage of their original weight (on the day of infection). (B) Survival rate (n = 8).

Statistical analysis of survival curve was performed based on the log-rank (Mantel-Cox) test.

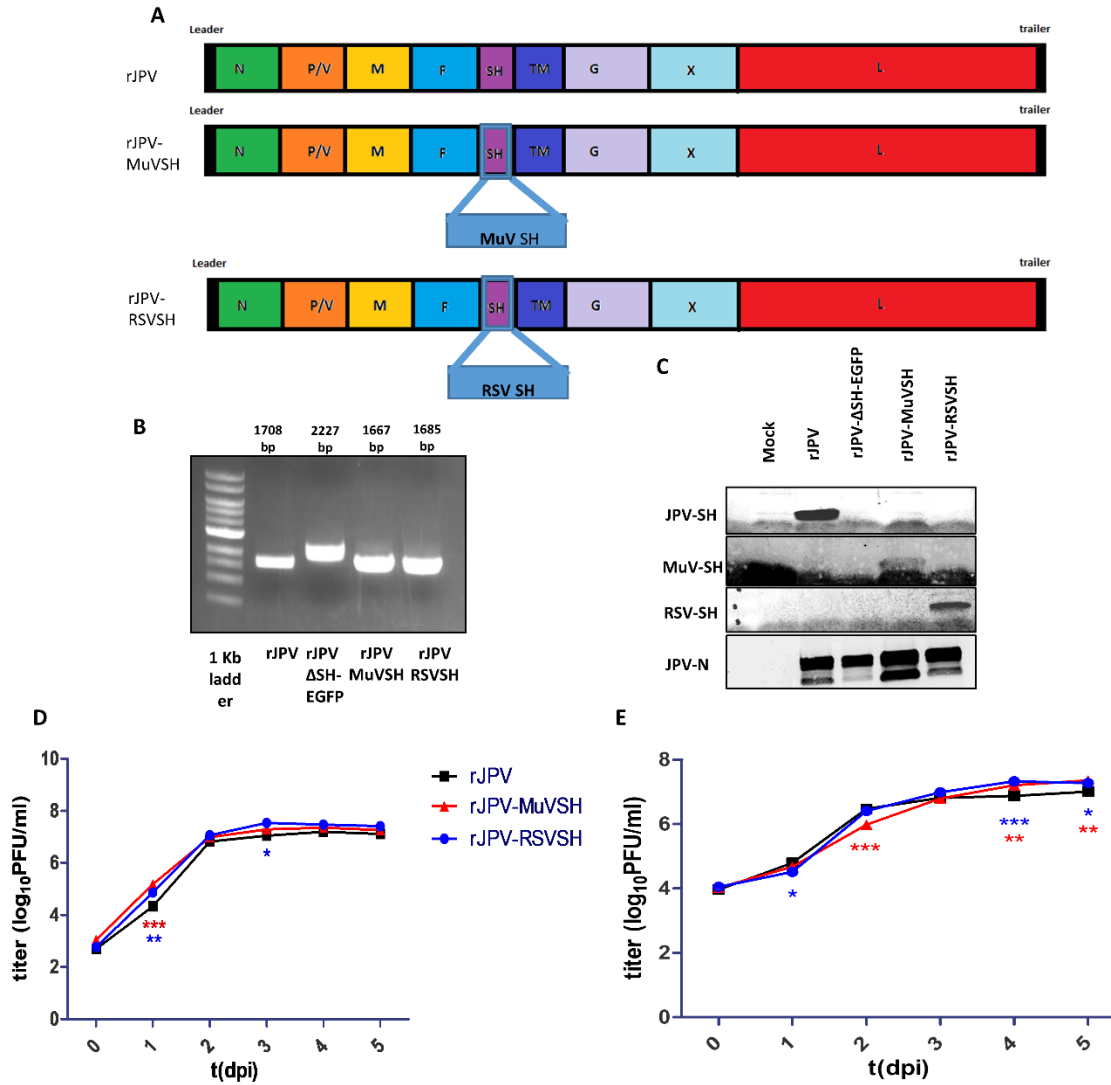


Figure 3.6. Recovery and growth characteristics of SH chimera viruses, rJPV-MuVSH and rJPV-RSVSH. (A) Schematics of rJPV, rJPV-MuVSH, and rJPV-RSVSH, indicating the location where the ORF of JPV SH was replaced with the SH of MuV or RSV (B) To confirm the presence of JPV SH, EGFP, MuVSH, and RSVSH in rJPV, rJPV-ΔSH-EGFP, rJPV-MuVSH, or rJPV-RSVSH respectively, RT-PCR was performed using primers MA12F and MA09R to amplify the SH region. (C) Viral protein expression levels of rJPV, rJPV-ΔSH-EGFP, rJPV-MuVSH, and rJPV-RSVSH. 6 well plates of Vero cells were mock infected or infected with rJPV, rJPV-

Δ SH-EGFP, rJPV-MuVSH, or rJPV-RSVSH at an MOI of 1. Cell lysates were subjected to immunoblotting with JPV anti-SH, MuV anti-SH, RSV anti-SH, or JPV anti-N. (D) Low MOI growth curve of rJPV, rJPV-MuVSH, and rJPV-RSVSH. Vero cells were infected with rJPV, rJPV-MuVSH, or rJPV-RSVSH at an MOI of 0.1, and the medium was harvested at 24-h intervals. Plaque assay was performed on Vero cells to determine the virus titer. (E) High MOI growth curve of rJPV, rJPV-MuVSH, and rJPV-RSVSH. Vero cells were infected with rJPV, rJPV-MuVSH, or rJPV-RSVSH at an MOI of 5, and the medium was harvested at 24-h intervals. Plaque assay was performed on Vero cells to determine the virus titer. Statistical significance between groups at each time point was calculated based on two-way ANOVA to compare the growth kinetics. (P<0.001 ***, P<0.01 **, P < 0.05 *)

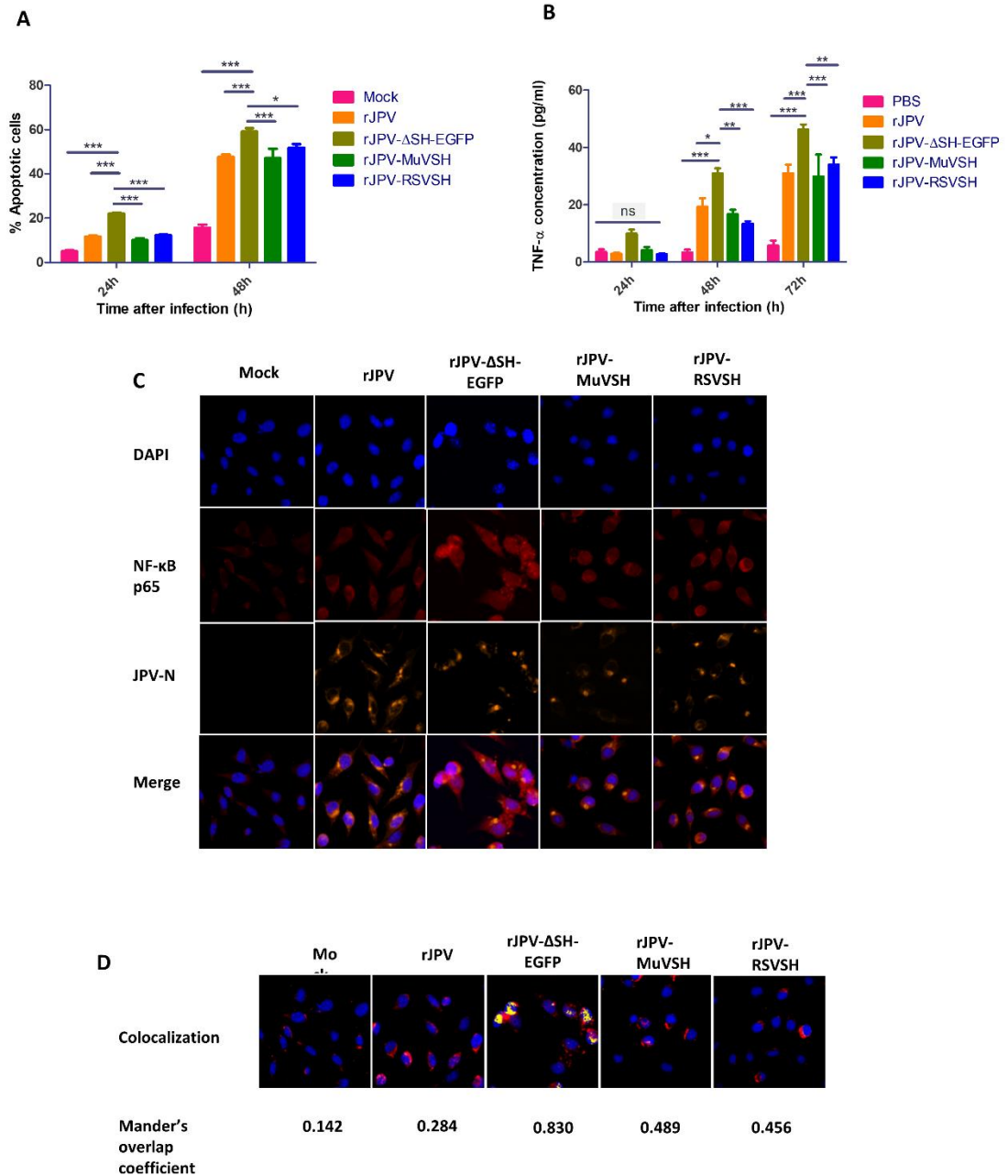


Figure 3.7. MuV SH and RSV SH reduce the level of apoptosis and TNF- α production

(A) Induction of apoptosis by rJPV-MuVSH and rJPV-RSVSH viruses. L929 cells were mock infected or infected with rJPV, rJPV- Δ SH-EGFP, rJPV-MuVSH, or rJPV-RSVSH at an MOI of 5. The cells were collected for Pacific Blue™ Annexin V Apoptosis Detection assay with 7-AAD at 24 h.p.i and 48 h.p.i. Statistical significance

between groups at each time point was calculated based on one-way ANOVA. (B) Concentrations of TNF- α produced from rJPV-MuVSH, and rJPV-RSVSH infected cells. L929 cells were mock infected or infected with rJPV, rJPV- Δ SH-EGFP, rJPV-MuVSH, or rJPV-RSVSH at an MOI of 5. The medium was collected at 24 h.p.i, 48 h.p.i., and 72 h.p.i. The amounts of TNF- α were measured by ELISA. Samples are triplicates, and error bars show standard errors of the means. Statistical significance between groups at each time point was calculated based on two-way ANOVA. (P<0.001 ***, P<0.01 **, P < 0.05 *) (C) Detection of NF- κ B p65 subunit expression in L929 cells by IFA. L929 cells were mock infected or infected with rJPV, rJPV- Δ SH-EGFP, rJPV-MuVSH, or rJPV-RSVSH at an MOI of 5. At 1 d.p.i, cells were fixed and stained with Zenon APC conjugated JPV N and anti-p65 antibody followed by staining with Cy3- conjugated secondary antibody. DAPI staining was performed with ProLong® Gold Antifade Mountant. Pictures were taken at a magnification of 40x. (D) Nuclear translocation of NF- κ B p65 subunit into the nucleus is expressed in terms of Mander's overlap coefficient.

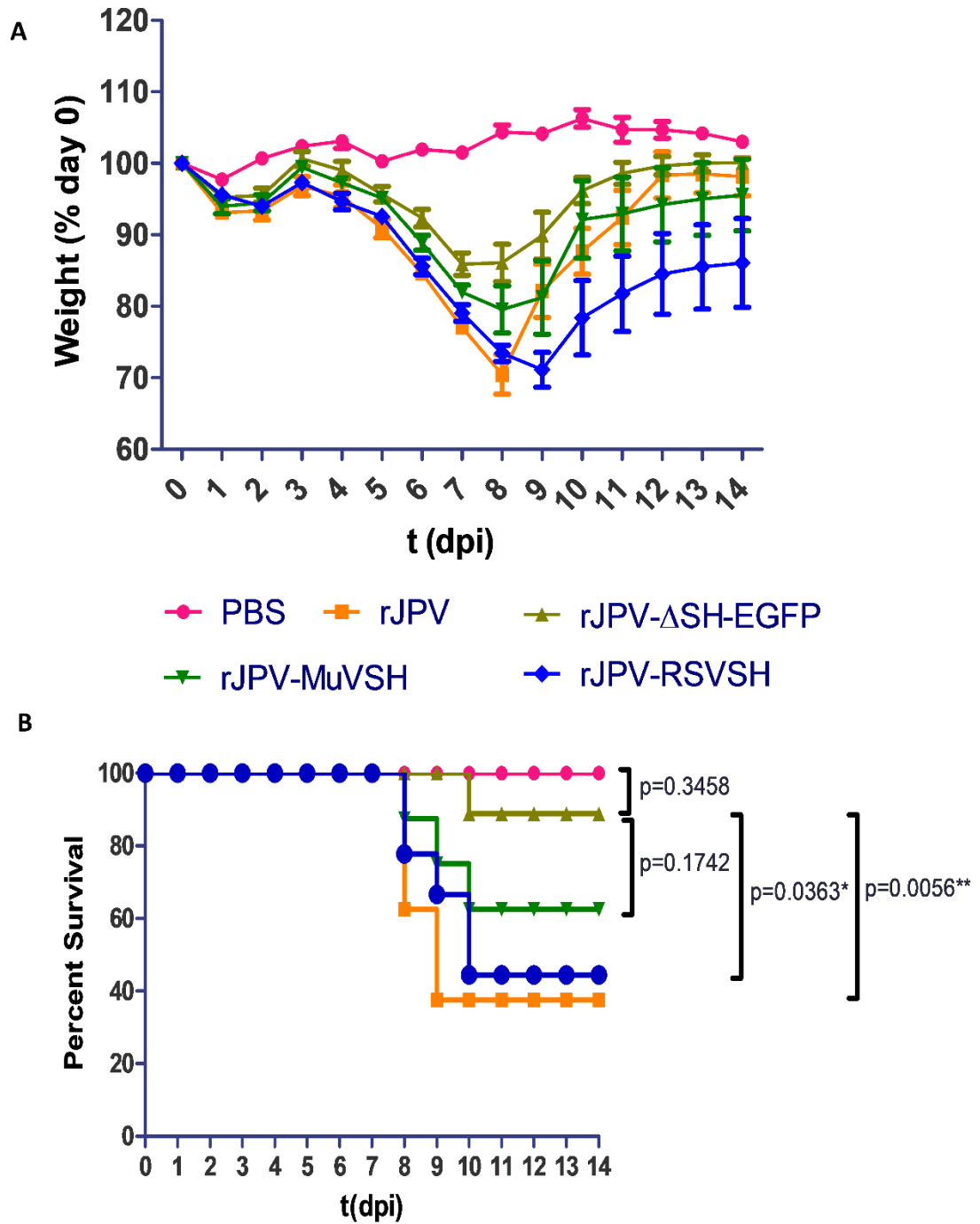
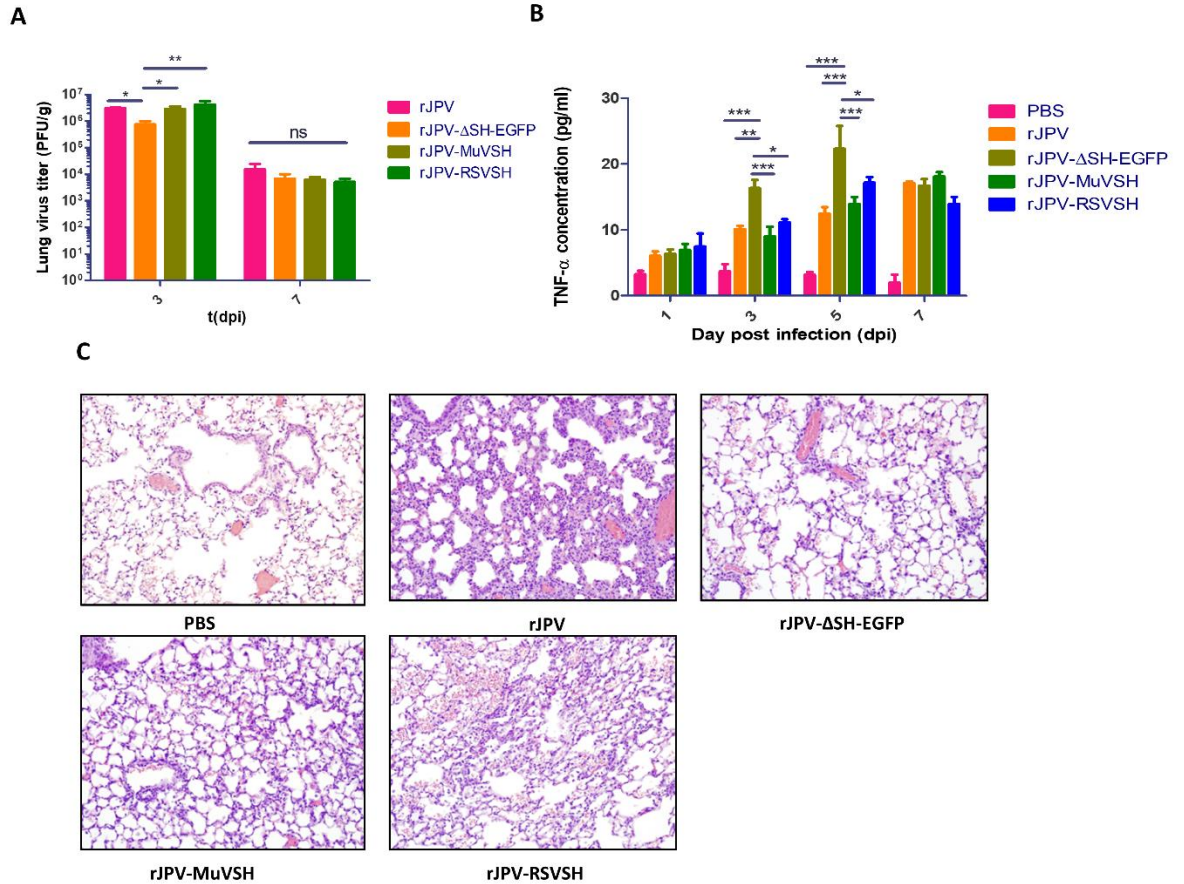


Figure 3.8. *rJPV-MuVSH* and *rJPV-RSVSH* are pathogenic in mice. BALB/c mice were intranasally infected with 100 μ l of PBS or 8×10^5 PFU of *rJPV*, *rJPV-ΔSH-EGFP*, *rJPV-MuVSH*, or *rJPV-RSVSH*. (A) Body weight loss. Mice were monitored daily, and weight loss was graphed as the average percentage of their original weight

(on the day of infection). (C) Survival rate (PBS n= 10, rJPV n= 8, rJPV- Δ SH-EGFP n = 9, rJPV-MuVSH, n= 8, rJPV-RSVSH, n= 9). Statistical analysis of survival curve was performed based on log-rank (Mantel-Cox) test.



*Figure 3.9. Infection of BALB/c mice with rJPV, rJPV-ΔSH-EGFP, rJPV-MuVSH, and rJPV-RSVSH. (A) Lung virus titers of mice. BALB/c mice were intranasally infected with 100 μl of rJPV, rJPV-ΔSH-EGFP, rJPV-MuVSH, or rJPV-RSVSH at a dose of 8×10^5 PFU. Mouse lungs were collected at 3 and 7 d.p.i. Virus titers were determined by plaque assay on Vero cells. (B) Concentrations of serum TNF-α in infected BALB/c mice. Sera were collected from infected animals at different time points after infection. Levels of TNF-α were measured using ELISA (n= 4). Statistical significance between groups at each time point was calculated based on two-way ANOVA. (P<0.001 ***, P<0.01 **, P < 0.05 *) (C) Histopathology of lungs. Lungs were collected from infected and mock-infected animals at 3 d.p.i and stained with H&E. Photomicrographs were taken at a magnification of 20x.*

CHAPTER 4

A RECOMBINANT J PARAMYXOVIRUS EXPRESSING HEMAGGLUTININ OF INFLUENZA A VIRUS H5N1 PROTECTED MICE AGAINST LETHAL HIGHLY PATHOGENIC AVIAN INFLUENZA VIRUS H5N1 CHALLENGE²

²Abraham M, Li Z, Tompkins SM, He B. To be submitted to *Journal of Virology*.

Abstract

H5N1, an avian influenza virus, is known to circulate in many Asian countries like Bangladesh, China, Cambodia, Indonesia, and Vietnam. The current FDA approved H5N1 vaccine only has a moderate level of efficacy. A safe and effective vaccine is needed to prevent the outbreaks of highly pathogenic avian influenza (HPAI) H5N1 in humans. Non-segmented Negative-Strand Viruses (NNSVs) are good candidates for vaccine development due to their stability and safety. J Paramyxovirus (JPV) is a non-segmented negative-strand virus, a member of the proposed genus *Jeilongvirus* of the family *Paramyxoviridae*. JPV is not known to cause disease in any species other than laboratory mouse. However, JPV specific antibodies were detected in humans and pigs. JPV has a high replication efficiency in the respiratory tract, so we decided to use JPV as a vector of developing an H5N1 vaccine for intranasal delivery. We incorporated H5N1 HA into the JPV genome by replacing the small hydrophobic (SH) gene to generate a recombinant, rJPV- Δ SH-H5 virus. A single intranasal administration of rJPV- Δ SH-H5 protected mice from a lethal HPAI H5N1 challenge.

Importance

H5N1 outbreak in Southeast Asia destroyed millions of birds. Transmission of H5N1 into humans resulted in deaths in many countries. We are developing a novel H5N1 vaccine using JPV as a vector. High replication efficiency of JPV in the respiratory tract is promising for the development of a protective systemic immune response.

Introduction

Influenza A virus causes thousands of hospitalizations and deaths in the United States. Influenza viruses are members of family *Orthomyxoviridae* with negative stranded segmented RNA genome. Among influenza viruses, Influenza A viruses are responsible for the epidemics in humans, swine and horses, as well as devastating outbreaks in poultry (75). Migratory waterfowl, including ducks, seabirds, or shorebirds are the natural hosts of influenza viruses and from where they jump the species barrier and cause disease in humans (76). H5N1 HPAI is primarily restricted within the poultry species, but it has emerged as a danger for humans by jumping into many mammalian hosts. Since 1997 H5N1 HPAI is responsible for 600 human infections with more than 300 deaths reported from broad geographical areas including Asia, middle-east, and Africa (77). Higher mortality rates and considering the possibility of the emergence of more virulent viruses from the avian source, make H5N1 viruses a significant public health threat. H5N1 HPAI viruses are not easily transmitted among humans or other mammals, but the spread of these viruses into new geographical regions and wild bird hosts may produce multiple clades with increased genetic diversity through genetic reassortment or antigenic drift. Eradication efforts were unsuccessful and led to the emergence of many antiviral resistant strains (78–80). The immunogenicity of the FDA approved H5N1 vaccine is low compared to the seasonal influenza vaccines. Inactivated virus vaccines given multiple times at a high concentration provided only mediocre protection (~50%) in clinical trials (81). Non-segmented negative-strand RNA viruses (NNSVs) are widely used as vaccine candidates. NNSV genomes are more stable than genomes of positive-stranded RNA

viruses. NNSV also do not have the possibility of causing modifications in host cellular DNA. These characteristics make NNSVs a safer choice for engineering vectored vaccines. Parainfluenza virus 5 (PIV5), is a member of the *Rubulavirus* genus of the family *Paramyxoviridae*, which is used as an excellent vector for vaccine development against many bacterial and viral diseases including HPAI H5N1. Recombinant PIV5 expressing HA of H5N1 was efficacious in protecting mice against HPAI H5N1 challenge at very low doses (82–85).

To develop a vaccine for humans, we have tried another NNSV to study the immunogenicity in animal models. JPV was isolated from mice in the early 1970s in Australia. Its genome structure was determined in 2005, and it has eight genes in the order of 3'-N-P/V/C-M-F-SH-TM-G-L-5' (10, 17). JPV has a large genome size of 18,954 nucleotides, which makes the insertion of large genes possible in the virus genome. JPV-LW, the virus initially sequenced, has many point mutations, but JPV-BH, a more virulent strain, has a close resemblance to the phenotype of virus isolated initially from Australia (1, 10). Deleting genes or gene segments to make an attenuated JPV-BH would be the best way to develop a stable and safe JPV based vaccine. We have seen that the deletion of the SH gene attenuates JPV (86). So, in this work, we generated a JPV-BH based H5N1 vaccine candidate by replacing the SH with HA.

Materials and Methods

Cells

Human Embryonic Kidney 293T (HEK293T), Baby Hamster Kidney (BHK) cells, and Vero cells (ATCC) were maintained in Dulbecco's modified Eagle's medium (DMEM) containing 10% fetal bovine serum (FBS), 100 IU/ml penicillin, and 100 µg/ml streptomycin. All cells were incubated at 37°C in 5% CO₂. Cells infected with viruses were grown in DMEM containing 2% FBS. Vero cells were used to perform plaque assays of JPV and BHK cells were used to perform plaque assays of PIV5.

Mice

6-week-old, female, BALB/c mice (Envigo) were used for the studies. Mice were infected with JPV and PIV5 in enhanced Biosafety Level 2 facilities in HEPA-filtered isolators. Mouse HPAI infections were performed in enhanced BSL3 facilities in HEPA-filtered isolators under the guidelines of institutional biosafety program at the University of Georgia and for the select agents approved by the CDC. All animal experiments were performed in accordance with the national guidelines provided by "The Guide for Care and Use of Laboratory Animals" and the University of Georgia Institutional Animal Care and Use Committee (IACUC). The Institutional Animal Care and Use Committee (IACUC) of the University of Georgia approved all animal experiments.

Influenza virus

Highly pathogenic A/Vietnam/1203/2004 (H5N1) was propagated in the allantoic cavity of embryonated hen eggs at 37°C for 24 h and were then aliquoted and stored at -80°C. Experiments involving HPAI were reviewed and approved by the institutional biosafety program at the University of Georgia and were conducted in enhanced biosafety level 3 (BSL3+) containment according to guidelines for the use of select agents approved by the CDC.

Construction of recombinant plasmids

Construction of a recombinant JPV-BH plasmid with a PvuI restriction site at the N gene was previously described (1). By using standard molecular biology techniques, the ORF of the SH gene was replaced by an HA gene of H5N1. The construct lacking the SH gene and containing the HA gene was designated as a pJPV- Δ SH-H5 plasmid. A plasmid containing the H5N1 HA gene without the cleavage site was used as the DNA template for PCR amplification (82). Sequences of primers used for the plasmid construction and the complete genome of pJPV- Δ SH-H5 is available on request.

Virus rescue and sequencing

To generate viable recombinant JPV containing HA gene (rJPV- Δ SH-H5), a full length pJPV- Δ SH-H5 plasmid, a plasmid expressing T7 polymerase (pT7P), and three plasmids encoding the N, P, and L proteins of JPV (pJPV-N, pJPV-P, and pJPV-L) were co-transfected into HEK293T cells at 95% confluency in a 6-cm plate with Jetprime (Polypus-Transfection, Inc., New York, NY). The amount of plasmids used

were as follows: 5 µg of full-length pJPV-ΔSH-EGFP plasmid, 1 µg of pT7P, 1 µg of pJPV-N, 0.3 µg of pJPV-P, and 1.5 µg of pJPV-L. Two days post-transfection, 1/10th of the HEK293T cells were co-cultured with 1 x 10⁶ Vero cells in a 10-cm plate. Seven days after coculture, media were centrifuged to remove the cell debris, and the supernatant was used for plaque assay in Vero cells to obtain single clones of recombinant JPV-ΔSH-H5. Vero cells were used to grow the plaque-purified virus. The full-length genomes of the plaque-purified rJPV-ΔSH-H5 virus were sequenced. Total RNA of rJPV-ΔSH-H5- infected Vero cells were purified using the RNeasy minikit (Qiagen, Valencia, CA). cDNA was prepared by using random hexamers. Sequences of all primers used for sequencing the whole genome of rJPV-ΔSH-H5 are available upon request. DNA sequences were determined by an Applied Biosystems sequencer (ABI, Foster City, CA).

Detection of protein expression

To confirm the rescue of JPV-ΔSH-H5, Vero cells were mock infected or infected with rJPV or rJPV-ΔSH-H5. Vero cells were mock infected or infected with rJPV or rJPV-ΔSH-H5 at an MOI of 0.1. At 2 d.p.i, cells were washed with phosphate-buffered saline (PBS) and fixed with 0.5% formaldehyde. The cells were permeabilized with 0.1% PBS-saponin solution and were incubated for 30 min with mouse monoclonal anti-F or –anti-H5N1 HA antibody at a 1:100 dilution (Genescript USA, Inc., Piscataway, NJ) and then fluorescein isothiocyanate (FITC)-labelled goat anti-mouse antibody was added to the cells. The cells were incubated for 30 min and were examined and photographed using a Nikon FXA fluorescence microscope.

Expression of H5N1 HA in the virus-infected cells was compared. Vero cells in the six-well plates were mock infected or infected with rJPV or rJPV- Δ SH-H5 at an MOI of 5. The cells were collected at 2 d.p.i and fixed with 0.5% formaldehyde for 1 h. The fixed cells were resuspended in FBS-DMEM (50:50) and permeabilized with 70% ethanol overnight. The cells were washed once with PBS and then incubated with mouse anti-H5N1 HA monoclonal antibody in PBS-1% BSA (1:200) for 1 h at 4°C. The cells were stained with APC Goat anti-mouse IgG from Biolegend (1:500) for 1 h at 4°C in the dark and then washed once with PBS-1% BSA. The fluorescence intensity was measured with a flow cytometer (Becton Dickinson LSR II).

Growth Kinetics

Vero cells in 6-well plates were infected with rJPV or rJPV- Δ SH-H5 at an MOI of 0.1. The cells were then washed with PBS and maintained in DMEM-2% FBS. The medium was collected at 0, 24, 48, 96, and 120 hours post infection (h.p.i). The titers were determined by plaque assay on Vero cells.

ELISA

HA (H5N1 HA)-specific serum antibody titers were measured using an IgG enzyme-linked immunosorbent assay (ELISA). Immulon 2 HB 96-well microtiter plates (ThermoLabSystems) were coated with 2 μ g/ml recombinant H5N1 HA protein and incubated at 4°C overnight. Plates were then washed with KPL wash solution (KPL, Inc.), and the wells were blocked with 200 μ l KPL wash solution with 5% nonfat dry milk and 0.5% BSA (blocking buffer) for 1h at room temperature. Serial dilutions of

serum samples were made (in blocking buffer), transferred to the coated plate, and incubated for 1h. To detect bound serum antibodies, 100 μ l of a 1:1000 dilution of Horseradish Peroxidase (HRP)-labeled goat anti-mouse IgG (KPL, Inc.) in blocking buffer was added per well and incubated for 1 h at room temperature. Plates were developed by adding 100 μ l of Sureblue Reserve TMB Microwell peroxidase substrate (1-component), and the reaction was allowed to develop at room temperature. After 3-5 minutes, the reaction was terminated with 100 μ l/well of 1N HCl. Optical density (OD) was measured at 450 nm on a Bio-Tek Powerwave XS plate reader.

Vaccination and Influenza A virus challenge in BALB/c mice

To test the immunogenicity of rJPV- Δ SH-H5, 6-week-old, female, BALB/c mice (Envigo) were infected with 100 μ l of PBS or 1×10^5 PFU each of rJPV- Δ SH-H5 or rPIV5-H5(82), intranasally. Plaque assays were performed for the back-titration of virus inoculum used for the vaccination. The weight of the mice was monitored for up to 14 days post vaccination (d.p.v.). Twenty-eight d.p.v., the mice were bled for serum H5N1 HA-specific IgG titer. On 73 d.p.v., mice were anesthetized and inoculated intranasally with 10 50% lethal infectious doses (LD_{50}) A/Vietnam/1203/04 (87) diluted in 50 μ l PBS. Mice were then monitored daily for morbidity and mortality with body weights measured every other day post challenge.

Results

Generation and *in vitro* analysis of a recombinant JPV expressing HA

To generate a recombinant JPV expressing HA of H5N1 (rJPV- Δ SH-H5), we replaced the SH coding sequence in a full-length JPV-BH plasmid with HA (Fig. 4.1). This plasmid, together with three other helper plasmids encoding N, P and L proteins, and a plasmid encoding T7 RNA polymerase, were co-transfected into HEK293T cells and co-cultured with Vero cells as described previously (1). Vero cells were used to select a plaque-purified clone of the rJPV- Δ SH-H5 virus. The full-length genome sequence of plaque-purified rJPV- Δ SH-H5 was confirmed by RT-PCR and Sanger sequencing.

Protein expression and *in vitro* growth kinetics

Expression of HA in rJPV- Δ SH-H5 infected Vero cells were confirmed using immunofluorescence assay with anti-mouse JPV F, and H5N1 HA monoclonal antibodies (Fig. 4.2A) and quantitative estimation of the mean fluorescence intensity (MFI) of H5N1 HA expression was determined using flow cytometry (Fig. 4.2B). To compare the growth kinetics of rJPV and rJPV- Δ SH-H5, Vero cells were infected with rJPV and rJPV- Δ SH-H5 at an MOI of 0.1. The medium was harvested at different time points, and titers of virus in media were determined by plaque assay. Although a similar growth pattern was observed for rJPV and rJPV- Δ SH-H5, rJPV had a significantly higher growth on 1 dpi and 2 dpi (Fig 4.3).

***In vivo* inoculation of rJPV-ΔSH-H5 and analysis of immune response**

To investigate the immune response generated by rJPV-ΔSH-H5, mice were vaccinated with 100 μl of PBS or 1x10⁵ PFU each of rJPV-ΔSH-H5 or rPIV5-H5 intranasally. The weight of animals was monitored for 14 dpi. No difference in the body weight was observed in mice vaccinated with rJPV-ΔSH-H5 or rPIV5-H5 compared to the PBS group (Fig 4.4A). Mice were bled at 28 dpi, and sera were used for ELISA to detect the H5 specific antibody response. However, rJPV-ΔSH-H5 induced a higher level of anti-H5-HA antibodies than rPIV5-H5 (Fig 4.4B).

Determining the efficacy of rJPV-ΔSH-H5 against HPAI H5N1 challenge in mice

The efficacy of rJPV-ΔSH-H5 against HPAI H5N1 was examined in mice with A/Vietnam/1203/04 strain. Mice were vaccinated with 100 μl of PBS or 1x10⁵ PFU each of rJPV-ΔSH-H5 or rPIV5-H5 intranasally. At 73-day post vaccination (dpv) mice were challenged with H5N1. All mice in the PBS group showed severe weight loss and all animals were dead by day 9 after challenge (Fig 4.5A). In contrast, all mice immunized with rJPV-ΔSH-H5 or rPIV5-H5 had survived with little weight loss (Fig 4.5B).

Discussion

Global influenza epidemics emerge seasonally causing 3–5 million cases of severe influenza infections annually, with 250,000–500,000 deaths globally. The reemergence of a pandemic H1N1 strain in 2009 (88), and the emergence of HPAI H5N1 and H7N9 influenza viruses (89, 90), confirms that influenza is one of the global threats in this

century. Even though influenza vaccines are available in the market since the 1930s, there are many limitations for these vaccines regarding availability and effectiveness. Currently licensed influenza vaccines are produced in chicken eggs, which requires a lot of time between the identification of vaccine strains and the availability. Other limitations include lengthy regulatory approval procedures, limited worldwide vaccine availability, limited efficacy in elderly and unprimed populations, and lack of cross-reactivity. The HPAI H5N1 virus was isolated for the first time from geese in Guangdong Province, China in 1996 (91). Since then, the virus has become endemic causing a significant loss to the poultry industry with many human infections. Viral-vectors such as adenoviruses and vaccinia viruses were frequently used to develop an H5N1 vaccine. Effect of pre-existing immunity and the requirement of multiple immunizations are the limitations of these vaccines (92, 93). Currently, the only FDA approved H5N1 vaccine also has to be administered multiple times at a high concentration to achieve a moderate level of efficacy compared to the conventional influenza vaccines. Traditional vaccines against H5N1 utilizing the HA or NA of the virus are poorly immunogenic with production issues (94).

PIV5-based H5N1 vaccine generated a good protective immunity with a single and low dose (10^3 PFU per mouse) (82, 95, 96). JPV, another paramyxovirus like PIV5 is not known for causing disease in any species other than laboratory mice. We have confirmed that point mutations in JPV make the virus highly attenuated in its natural host (1). Deletion of SH and V from the Mumps (Iowa strain) backbone has been employed for vaccine development. rMuV Δ SH Δ V, rMuV Δ V, and rMuV Δ SH were able to mount an immune response in mice. rMuV Δ SH Δ V was able to induce a

neutralizing titer and T cell response comparable to those induced by rMuV Δ SH and rMuV Δ V (97). Our previous research shows that deletion of SH improves the antigenic presentation and immunogenicity offered by the PIV5 vector (96). Roles of SH and V protein indicates various mechanisms used by paramyxoviruses to evade the host immune responses. The reverse genetic system of paramyxoviruses helps us to make recombinant attenuated viruses lacking the expression of these genes very easily. These Δ SH and Δ V paramyxoviruses are viable and grow similar to wild-type viruses *in vitro*, but most of them are attenuated *in vivo* (6, 36, 86). This quality makes them a good candidate to use as a modified live vaccine. We have previously shown that the deletion of SH or TM did not affect the viability and replication of JPV (16, 73, 86). We have also rescued a viable recombinant JPV lacking both SH and TM regions (Data not shown). Also, the deletion of SH improves the antigenic presentation and immunogenicity offered by the PIV5 vector (96). Deletion of genes or gene segments from a viral vector is safer than making point mutations in the genome, as latter has a possibility of reversion of virulence. TM is unique for jeilongviruses (62), and more studies are required to find the effect of deletion of TM from the JPV vector on immunogenicity.

In this work, we have used JPV-BH- Δ SH backbone for developing an H5N1 vaccine candidate due to the improved immunogenicity and safety observed compared to other paramyxoviruses. rJPV- Δ SH-H5 grew similar to rJPV in Vero cells and expressed the HA of H5N1. *In vivo* infection with rJPV- Δ SH-H5 or rPIV5-H5 resulted in no significant difference in the weight loss compared to the PBS control group. Higher HA-specific antibody response in vaccinated mice after a single dose of vaccine and

complete protection upon a lethal challenge with HPAI H5N1 shows that rJPV- Δ SH-H5 is a promising H5N1 vaccine candidate. Since JPV is a rodent virus, higher production of the HA-specific antibody may be due to the increased virus replication and transcription of JPV-encoded genes in mouse lungs. Experimental infection of jeilongviruses in other animals is needed to study the pathogenicity, tissue tropism, and serology associated with the infection by this group of paramyxovirus. Even though JPV specific antibodies were detected in pigs and humans, more studies with other animal models are needed to understand the protective immunity generated by JPV-vectored vaccines.

Acknowledgments

We appreciate the members of He laboratory for their helpful discussion and technical assistance. We thank the Animal Facility and Flow Cytometry facility of the College of Veterinary Medicine at the University of Georgia for their help and support.

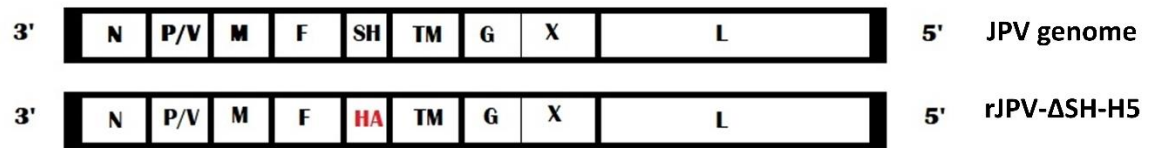


Figure 4.1. Recovery of recombinant virus rJPV-ΔSH-H5 (A) Schematics of rJPV and rJPV-ΔSH-H5, indicating the location where the ORF of SH was replaced with HA of H5N1.

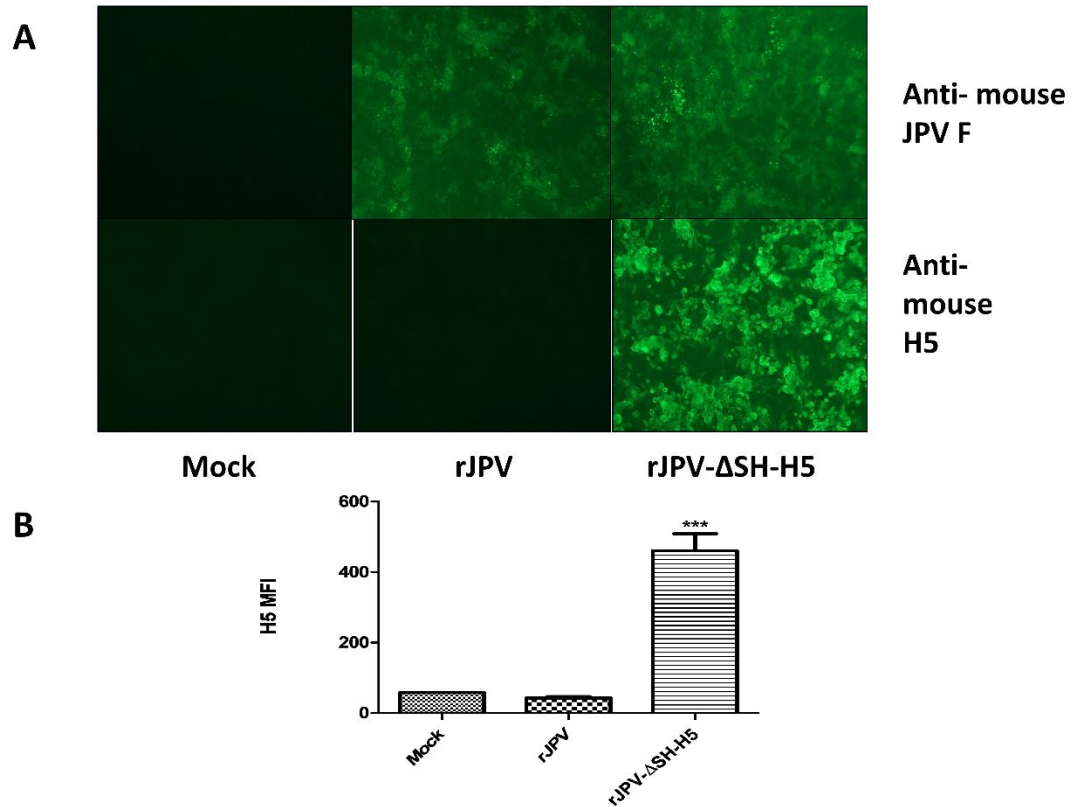


Figure 4.2. Gene expression of rJPV and rJPV- Δ SH-H5 in vitro. (A) Immunofluorescent staining of Vero cells infected with rJPV or rJPV- Δ SH-H5. Vero cells were mock infected or infected with rJPV or JPV- Δ SH-H5. At 2 d.p.i, cells were washed with PBS and fixed with 0.5% formaldehyde. The cells were permeabilized with 0.1% PBS-saponin solution incubated for 30 min with polyclonal anti-F or -H5N1 HA monoclonal antibody at a 1:100 dilution, and FITC-labelled with goat anti-mouse antibody. The cells were incubated for 30 min and examined and photographed using a Nikon FXA fluorescence microscope. (B) Expression of H5N1 HA in the virus-infected cells. Vero cells in the six-well plates were mock infected or infected with rJPV or rJPV- Δ SH-H5 at an MOI of 5. The cells were collected at 2 d.p.i and fixed with 0.5% formaldehyde for 1 h. The fixed cells were resuspended in FBS-DMEM

(50:50) and permeabilized with 70% ethanol overnight. The cells were washed once with PBS and then incubated with mouse anti-HA monoclonal antibody. Secondary staining was performed using APC Goat anti-mouse IgG, and the fluorescence intensity was measured with a flow cytometer. Samples are triplicates, and error bars show standard errors of the means.

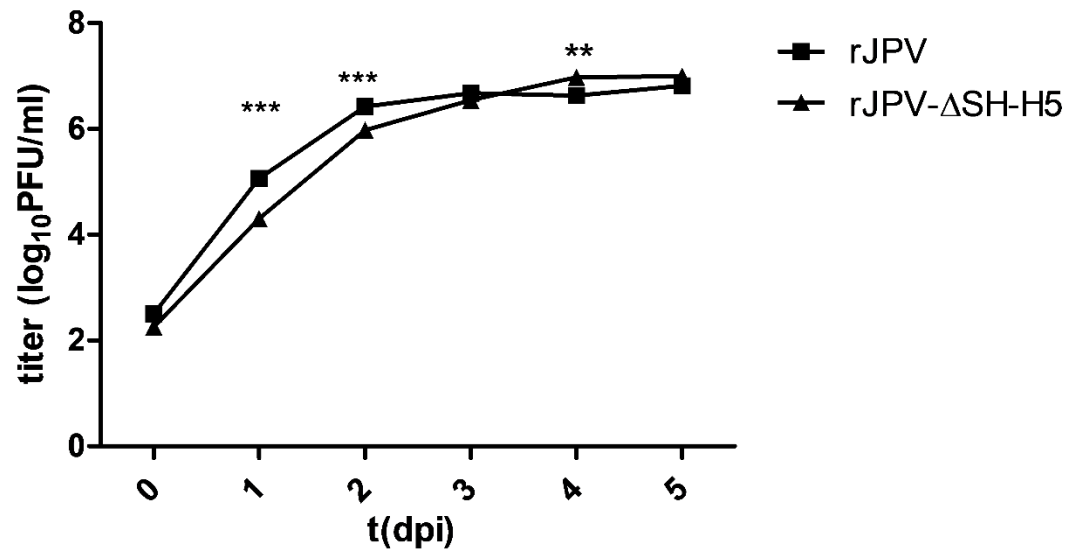


Figure 4.3. Comparison of rJPV and rJPV-ΔSH-H5 in vitro. Low MOI growth curve of rJPV and rJPV-ΔSH-H5. Vero cells in a 6 well plate were infected, in triplicates, with rJPV or rJPV-ΔSH-H5 at an MOI of 0.1, and the medium was harvested at 24-h intervals. Plaque assays were performed on Vero cells to determine the virus titer. Statistical significance between groups at each time point was calculated based on two-way ANOVA to compare the growth kinetics. (P<0.001 ***, P<0.01 **, P < 0.05 *)

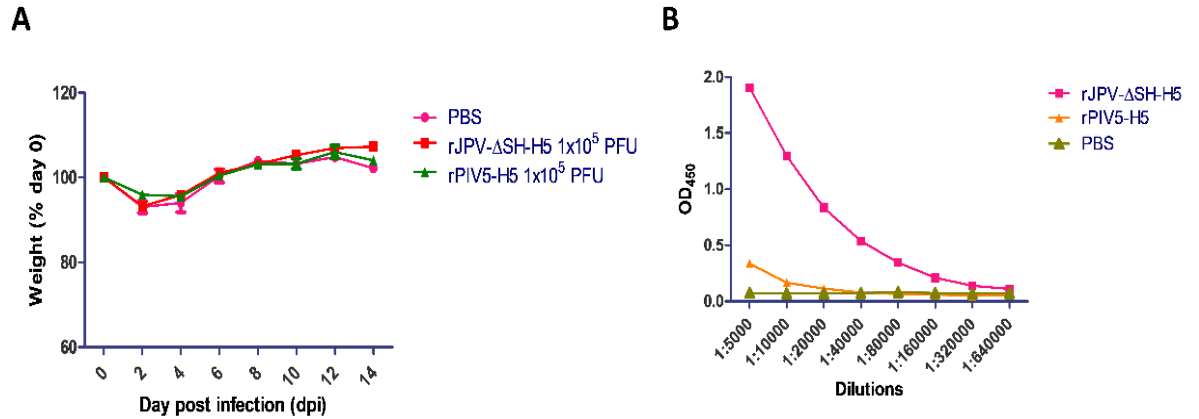


Figure 4.4. Immunization of BALB/c mice with of PBS, rJPV- Δ SH-H5, and rPIV5-H5.

(A) BALB/c mice were intranasally infected with 100 μ l of PBS, rJPV- Δ SH-H5, or rPIV5-H5 at a dose of 1×10^5 PFU (n=10 per group). Mice were monitored daily, and weight loss was graphed as the average percentage of their original weight (on the day of infection). (B) ELISA titers of immunized mice. BALB/c mice were intranasally immunized with PBS or rJPV- Δ SH-H5 or rPIV5-H5 at 10^5 PFU and bled on day 28 post immunization. The mouse blood samples were collected for analysis. Purified recombinant HA protein was used to coat the ELISA plates. OD450 values were measured using a plate reader.

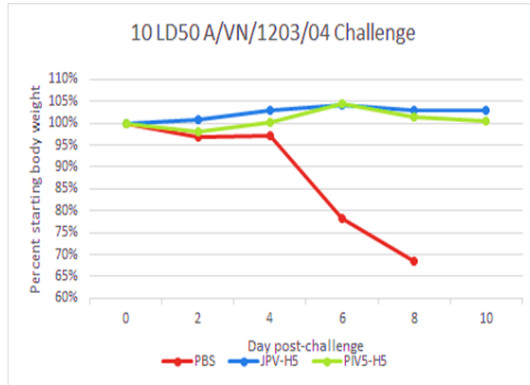
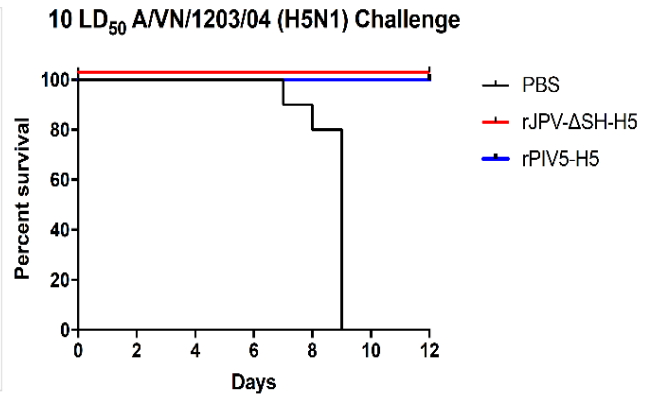
A**B**

Figure 4.5. Efficacy of *rJPV-ΔSH-H5* against HPAI H5N1 challenge in mice. The mice were inoculated with PBS, *rJPV-ΔSH-H5*, or *rPIV5-H5* ($n = 10$ per group) at a dose of 10^5 PFU per mouse. At 73 dpi, the mice were challenged with HPAI H5N1 at a dose of 10 LD₅₀. (A) Weights of mice challenged with H5N1. Weights were monitored daily after challenge for 10 days. Weight is graphed as the average percentages of original weight (the day of challenge). (B) Survival rate.

CHAPTER 5

CONCLUSIONS

Several paramyxoviruses that do not belong to the seven established genera were discovered from many species. Until recently, those paramyxoviruses were considered as ‘unclassified paramyxoviruses.’ Among them, JPV, BeiPV, and TImPV are rodent viruses with similar genome structure. Based on their similarities, a new genus called ‘*Jeilongvirus*’ has been proposed to group these viruses. Recently identified PMPV-1, MMLPV-1, MMLPV-2, and Rodent paramyxovirus are phylogenetically clustered together with JPV, BeiPV, and TImPV, signifying the expansion of this group of paramyxoviruses. Development of the reverse genetic system for a pathogenic JPV-BH strain helped us to study more about the pathogenesis of this group of viruses. This study mainly emphasizes the understanding of the functions of SH protein in virulence and the use of JPV as a vector for vaccine development.

Role of the small hydrophobic protein of JPV in virulence (Specific Aim 1)

Viruses have different strategies to evade the host immune response and to prolong their survival in the cell. One of these mechanisms seen in many paramyxoviruses is to inhibit the apoptosis or programmed cell death (98, 99). In Chapter 3, we studied the functions of JPV SH *in vitro*, as well as the role of SH of JPV, MuV, and RSV in the inhibition of apoptosis. SH protein present in paramyxoviruses and pneumoviruses shares little sequence homology. JPV and MuV SH proteins are type I membrane proteins, while RSV and PIV5 SH proteins are type II membrane proteins. In spite of

the lack of sequence homology and difference in orientation, the function of SH in blocking apoptosis remains same. Replacement of JPV SH with MuV or RSV SH restored the TNF- α -mediated apoptosis-blocking function in L929 cells. This result supports the findings of previous research on the role of SH proteins of RSV, PIV5, and MuV to block TNF- α signaling and induction of apoptosis (2, 6, 7). However, the infection of human cell lines with PIV5 did not inhibit TNF- α signaling upon the addition of exogenous TNF- α (100). This indicates that the differences in the virus replication and the effect of SH deletion vary depending on the cell types used. JPV as a rodent virus provides the best platform to study the functions of paramyxovirus SH gene *in vitro* using rodent cell lines and *in vivo* using laboratory mouse. Deletion of SH of JPV resulted in the increased TNF- α production and nuclear translocation of NF- κ B in L929 cells, but chimeric rJPV-MuVSH and rJPV-RSVSH had a decreased NF- κ B activation and TNF- α production.

Similarly, rJPV, rJPV-MuVSH, and rJPV-RSVSH were more pathogenic than rJPV- Δ SH. rJPV infection resulted in decreased lung virus titer and increased serum levels TNF- α . Expression of TNF- α in the JPV-infected respiratory cells is unknown. However, these studies show that the increased production of the pro-apoptotic cytokines like TNF- α might have increased the rate of apoptosis in the rJPV- Δ SH-EGFP infected lung cells, thereby limiting the spread of virus infection to the nearby cells resulting in attenuation. The mechanism of the inhibition of the TNF- α pathway by JPV SH is unknown. Our results indicate that SH of JPV or RSV or MuV has functional similarity in a JPV backbone. TNF- α mediated apoptotic pathway requires the binding of TNF- α to TNFR1 in the cell surface. Activated TNFR1 leads to apoptosis

and NF- κ B activation. TNFR1 contains a death domain that interacts with downstream proteins like TRADD and RIP1. These proteins mediate downstream signaling of the TNFR1. Steps in which the SH protein inhibits TNF- α -induced apoptotic pathway requires further studies.

Immunogenicity of JPV based vaccine candidates (Specific Aim 2)

Non-segmented negative-sense single-stranded viruses (NNSVs) are widely used as a vector to develop vaccines for humans, animals, and poultry. Many animal or avian NNSVs (like Vesicular stomatitis virus and Newcastle disease virus) are antigenically distinct from human pathogens, so have a high susceptibility to infect human population to develop a protective antigen-specific immune response. NNSVs stably express foreign genes without integrating with the host genome. Since NNSVs often can replicate efficiently in the respiratory tract of primates, it is ideal to induce mucosal and systemic immune response. JPV has a large genome with eight transcriptional units and facilitates the insertion of foreign genes into its genome. We have shown that the deletion of integral membrane proteins like SH attenuates the JPV in mice. Removal of the virulent genes by the reverse genetic system is an effective approach to create JPV-based vectored vaccines. Chapter 4 describes the development of a recombinant JPV by replacing its SH open reading frame with the HA of an HPAI H5N1. HA-specific antibodies generated by rJPV- Δ SH-H5 was higher than the PIV5 based vaccine. Both JPV and PIV5-based H5N1 HA candidates protected mice against an H5N1 challenge. However, the increased antibody response generated by a JPV vector may be useful for improving the immunogenicity of many other antigens. As a rodent virus, it is expected

that JPV generates a high antibody response in mice. Further testing of the vaccine in ferrets, NHPs, etc. will be needed to validate it as a vaccine platform for humans. The ability of JPV to infect other hosts to develop a protective immune response should be evaluated to create JPV-based vaccines for humans and livestock.

In this work, we were able to successfully delete JPV genes to develop viable recombinant JPV based vaccine. Many paramyxoviruses recently identified with a genome similarity of JPV have a proline/threonine/serine (P/T/S)-enriched ectodomain in their G protein. P/T/S-enriched region allows an extensive glycosylation site for the G protein, which is typical for the pneumoviruses (101, 102). In JPV, this feature is partially lost and an additional open reading frame ORF-X is located behind the ORF-G. ORF-X is not expressed in JPV-infected cells. Deleting the ORF-X may further improve the vaccine safety of JPV vector by terminating the possibility to restore the potential glycosylation sites of G upon successive *in vivo* infections. Since, JPV TM promotes cell-to-cell fusion, deleting the TM may also improve the safety of a JPV-based vaccine. Studies to elucidate the functions of jeilongvirus proteins and their interactions will help us to design more safe and effective JPV-based vaccines.

REFERENCES

1. Li Z, Xu J, Chen Z, Gao X, Wang L-F, Basler C, Sakamoto K, He B. 2013. The L gene of J paramyxovirus plays a critical role in viral pathogenesis. *J. Virol.* 87:12990–8.
2. He B, Lin GY, Durbin JE, Durbin RK, Lamb RA. 2001. The SH integral membrane protein of the paramyxovirus simian virus 5 is required to block apoptosis in MDBK cells. *J. Virol.* 75:4068–79.
3. Lin Y, Bright AC, Rothermel TA, He B. 2003. Induction of apoptosis by paramyxovirus simian virus 5 lacking a small hydrophobic gene. *J. Virol.* 77: 3371-83.
4. Li Z, Xu J, Patel J, Fuentes S, Lin Y, Anderson D, Sakamoto K, Wang L-F, He B. 2011. Function of the small hydrophobic protein of J paramyxovirus. *J. Virol.* 85:32–42.
5. Wilson RL, Fuentes SM, Wang P, Taddeo EC, Klatt A, Henderson AJ, He B. 2006. Function of small hydrophobic proteins of paramyxovirus. *J. Virol.* 80: 1700-09.
6. Xu P, Li Z, Sun D, Lin Y, Wu J, Rota PA, He B. 2011. Rescue of wild-type mumps virus from a strain associated with recent outbreaks helps to define the role of the SH ORF in the pathogenesis of mumps virus. *Virology* 417:126–136.
7. Fuentes S, Tran KC, Luthra P, Teng MN, He B. 2007. Function of the respiratory

- syncytial virus small hydrophobic protein. *J. Virol.* 81: 8361–66.
8. Lamb RA, Collins PL, Kolakofsky D, Melero JA, Nagai Y, Oldstone MBA, Pringle CR, Rima BK. 2005. Family paramyxoviridae, p. 655–668. In *Virus Taxonomy : The Classification and Nomenclature of Viruses*.
 9. Amarasinghe GK, Bào Y, Basler CF, Bavari S, Beer M, Bejerman N, Blasdel KR, Bochnowski A, Briese T, Bukreyev A, et al., 2017. Taxonomy of the order Mononegavirales. *Arch. Virol.* 162:1-12.
 10. Jun MH, Karabatsos N, Johnson RH. 1977. A new mouse paramyxovirus (J virus). *Aust. J. Exp. Biol. Med. Sci.* 55:645–647.
 11. Li Z, Yu M, Zhang H, Magoffin DE, Jack PJM, Hyatt A, Wang HY, Wang LF. 2006. Beilong virus, a novel paramyxovirus with the largest genome of non-segmented negative-stranded RNA viruses. *Virology* 346:219–228.
 12. Woo PCY, Lau SKP, Wong BHL, Wong AYP, Poon RWS, Yuen K-Y. 2011. Complete Genome Sequence of a Novel Paramyxovirus, Tailam Virus, Discovered in Sikkim Rats. *J. Virol.* 85:13473–13474.
 13. Woo PCY, Wong AYP, Wong BHL, Lam CSF, Fan RYY, Lau SKP, Yuen KY. 2016. Comparative genome and evolutionary analysis of naturally occurring Beilong virus in brown and black rats. *Infect. Genet. Evol.* 45:311–319.
 14. Magoffin DE, Mackenzie JS, Wang LF. 2007. Genetic analysis of J-virus and Beilong virus using minireplicons. *Virology* 364:103–111.
 15. Jack PJM, Anderson DE, Bossart KN, Marsh GA, Yu M, Wang LF. 2008.

Expression of novel genes encoded by the paramyxovirus J virus. *J. Gen. Virol.* 89:1434–41.

16. Li Z, Hung C, Paterson RG, Michel F, Fuentes S, Place R, Lin Y, Hogan RJ, Lamb RA, He B. 2015. Type II integral membrane protein, TM of J paramyxovirus promotes cell-to-cell fusion. *Proc. Natl. Acad. Sci. U S A.* 112:12504–09.
17. Jack PJM, Boyle DB, Eaton BT, Wang L-F. 2005. The Complete Genome Sequence of J Virus Reveals a Unique Genome Structure in the Family Paramyxoviridae. *J. Virol.* 79:10690–10700.
18. Jorgensen ED, Collins PL, Lomedico PT. 1987. Cloning and nucleotide sequence of newcastle disease virus hemagglutinin-neuraminidase mRNA: Identification of a putative sialic acid binding site. *Virology* 156:12–24.
19. Langedijk JP, Daus FJ, van Oirschot JT. 1997. Sequence and structure alignment of Paramyxoviridae attachment proteins and discovery of enzymatic activity for a morbillivirus hemagglutinin. *J. Virol.* 71:6155–67.
20. Poch O, Blumberg BM, Bougueleret L, Tordo N. 1990. Sequence comparison of five polymerases (L proteins) of unsegmented negative-strand RNA viruses: theoretical assignment of functional domains. *J. Gen. Virol.* 71:1153–1162.
21. Magoffin DE, Mackenzie JS, Wang LF. 2007. Genetic analysis of J-virus and Beilong virus using minireplicons. *Virology* 364:103–111.
22. Miller PJ, Boyle DB, Eaton BT, Wang LF. 2003. Full-length genome sequence of Mossman virus, a novel paramyxovirus isolated from rodents in Australia.

Virology 317:330–344.

23. Mesina JE, Campbell RS, Glazebrook JS, Copeman DB, Johnson RH. 1974. The pathology of feral rodents in North Queensland. *Tropenmed. Parasitol.* 25:116–27.
24. Jun MH. 1976. Studies on a virus isolated from wild mice (*Mus musculus*). M.Sc. thesis. James Cook University, Townsville, Queensland, Australia.
25. Banerjee AK, Barik S. 1992. Gene expression of vesicular stomatitis virus genome RNA. *Virology* 188: 417-428.
26. Cordey S, Roux L. 2006. Transcribing paramyxovirus RNA polymerase engages the template at its 3' extremity. *J. Gen. Virol.* 87:665–672.
27. Villiémox D, Cordey S, Mottet-Osman G, Roux L. 2005. Nature of a paramyxovirus replication promoter influences a nearby transcription signal. *J. Gen. Virol.* 86:171–180.
28. Abraham G, Rhodes DP, Banerjee AK. 1975. The 5' terminal structure of the methylated mRNA synthesized in vitro by vesicular stomatitis virus. *Cell* 5:51–58.
29. Fields BN, Knipe DM, Howley PM. 2013. Fields Virology, 6th Edition. Paramyxoviridae: the viruses and their replication. In *Fields Virology* p.3177
30. Plumet S, Duprex WP, Gerlier D. 2005. Dynamics of viral RNA synthesis during measles virus infection. *J. Virol.* 79:6900–8.
31. Egelman EH, Wu SS, Amrein M, Portner A, Murti G. 1989. The Sendai Virus

- Nucleocapsid Exists in at Least Four Different Helical States. *J. Virol.* 63:2233–2243.
32. Kolakofsky D, Pelet T, Garcin D, Hausmann S, Curran J, Roux L. 1998. Paramyxovirus RNA Synthesis and the Requirement for Hexamer Genome Length: the Rule of Six Revisited. *J. Virol.* 72:891–899.
 33. Kolakofsky D. 2016. Paramyxovirus RNA synthesis, mRNA editing, and genome hexamer phase: A review. *Virology* 498:94–98.
 34. Hausmann S, Jacques JP, Kolakofsky D. 1996. Paramyxovirus RNA editing and the requirement for hexamer genome length. *RNA* 2:1033–1045.
 35. Vidal S, Curran J, Kolakofsky D. 1990. A stuttering model for paramyxovirus P mRNA editing. *EMBO J.* 9:2017–22.
 36. Xu P, Luthra P, Li Z, Fuentes S, D’Andrea JA, Wu J, Rubin S, Rota P a, He B. 2012. The V protein of mumps virus plays a critical role in pathogenesis. *J. Virol.* 86:1768–76.
 37. Palosaari H, Parisien J-P, Rodriguez JJ, Ulane CM, Horvath CM. 2003. STAT protein interference and suppression of cytokine signal transduction by measles virus V protein. *J. Virol.* 77:7635–44.
 38. Rodriguez JJ, Wang L-F, Horvath CM. 2003. Hendra virus V protein inhibits interferon signaling by preventing STAT1 and STAT2 nuclear accumulation. *J. Virol.* 77:11842–5.
 39. Rodriguez JJ, Parisien J-P, Horvath CM. 2002. Nipah Virus V Protein Evades

Alpha and Gamma Interferons by Preventing STAT1 and STAT2 Activation and Nuclear Accumulation. *J. Virol.* 76:11476–11483.

40. Nanda SK, Baron MD. 2006. Rinderpest Virus Blocks Type I and Type II Interferon Action: Role of Structural and Nonstructural Proteins. *J. Virol.* 80:7555–7568.
41. Andrejeva J, Childs KS, Young DF, Carlos TS, Stock N, Goodbourn S, Randall RE. 2004. The V proteins of paramyxoviruses bind the IFN-inducible RNA helicase, mda-5, and inhibit its activation of the IFN- promoter. *Proc. Natl. Acad. Sci.* 101:17264–17269.
42. Audsley MD, Marsh GA, Lieu KG, Tachedjian M, Joubert DA, Wang LF, Jans DA, Moseley GW. 2016. The immune evasion function of J and beilong virus V proteins is distinct from that of other paramyxoviruses, consistent with their inclusion in the proposed genus Jeilongvirus. *J. Gen. Virol.* 97:581–592.
43. de Graaf M, Herfst S, Aarbiou J, Burgers PC, Zaaraoui-Boutahar F, Bijl M, van IJcken W, Schrauwen EJA, Osterhaus ADME, Luider TM, Scholte BJ, Fouchier RAM, Andeweg AC. 2013. Small Hydrophobic Protein of Human Metapneumovirus Does Not Affect Virus Replication and Host Gene Expression In Vitro. *PLoS One.* 8:e58572.
44. Hiebert SW, Paterson RG, Lamb RA. 1985. Identification and predicted sequence of a previously unrecognized small hydrophobic protein, SH, of the paramyxovirus simian virus 5. *J. Virol.* 55:744-51.
45. Hiebert SW, Richardson CD, Lamb RA. 1988. Cell surface expression and

orientation in membranes of the 44-amino-acid SH protein of simian virus 5. *J. Virol.* 62:2347–2357.

46. Takeuchi K, Tanabayashi K, Hishiyama M, Yamada a. 1996. The mumps virus SH protein is a membrane protein and not essential for virus growth. *Virology* 225:156–162.
47. Jin H, Zhou H, Cheng X, Tang R, Munoz M, Nguyen N. 2000. Recombinant respiratory syncytial viruses with deletions in the NS1, NS2, SH, and M2-2 genes are attenuated in vitro and in vivo. *Virology* 273:210–218.
48. Karron RA, Buonagurio DA, Georgiu AF, Whitehead SS, Adamus JE, Clements-Mann M Lou, Harris DO, Randolph VB, Udem SA, Murphy BR, Sidhu M. 1997. Respiratory syncytial virus (RSV) SH and G proteins are not essential for viral replication in vitro: clinical evaluation and molecular characterization of a cold-passaged. *Proc. Natl. Acad. Sci.* 94:13961–6.
49. Franz S, Rennert P, Woznik M, Grützke J, Lüdde A, Arriero Pais EM, Finsterbusch T, Geyer H, Mankertz A, Friedrich N. 2017. Mumps Virus SH protein inhibits NF- κ B activation by interacting with TNFR1, IL-1R1, and TLR3 complexes. *J. Virol.* 91:e01037-17.
50. Whitehead SS, Bukreyev a, Teng MN, Firestone CY, St Claire M, Elkins WR, Collins PL, Murphy BR. 1999. Recombinant respiratory syncytial virus bearing a deletion of either the NS2 or SH gene is attenuated in chimpanzees. *J. Virol.* 73:3438–3442.
51. Russell RF, McDonald JU, Ivanova M, Zhong Z, Bukreyev A, Tregoning JS.

2015. Partial Attenuation of Respiratory Syncytial Virus with a Deletion of a Small Hydrophobic Gene Is Associated with Elevated Interleukin-1 β Responses. *J. Virol.* 89:8974–81.
52. Taylor G, Wyld S, Valarcher JF, Guzman E, Thom M, Widdison S, Buchholz UJ. 2014. Recombinant bovine respiratory syncytial virus with deletion of the SH gene induces increased apoptosis and pro-inflammatory cytokines in vitro, and is attenuated and induces protective immunity in calves. *J. Gen. Virol.* 95:1244–1254.
53. Pennica D, Nedwin GE, Hayflick JS, Seeburg PH, Derynck R, Palladino MA, Kohr WJ, Aggarwal BB, Goeddel D V. 1984. Human tumour necrosis factor: Precursor structure, expression and homology to lymphotoxin. *Nature* 312:724–729.
54. Jin Z, El-Deiry WS. 2005. Overview of cell death signaling pathways. *Cancer Biol. Ther.* 4: 139-163.
55. Micheau O, Tschopp J. 2003. Induction of TNF receptor I-mediated apoptosis via two sequential signaling complexes. *Cell* 114:181–190.
56. Varfolomeev E, Goncharov T, Fedorova A V, Dynek JN, Zobel K, Deshayes K, Fairbrother WJ, Vucic D. 2008. c-IAP1 and c-IAP2 are critical mediators of tumor necrosis factor alpha (TNF α)-induced NF-kappaB activation. *J. Biol. Chem.* 283:24295–24299.
57. Ea CK, Deng L, Xia ZP, Pineda G, Chen ZJ. 2006. Activation of IKK by TNF α Requires Site-Specific Ubiquitination of RIP1 and Polyubiquitin Binding by

NEMO. *Mol. Cell.* 22:245–257.

58. Wang C, Deng L, Hong M, Akkaraju GR, Inoue JI, Chen ZJ. 2001. TAK1 is a ubiquitin-dependent kinase of MKK and IKK. *Nature* 412:346–351.
59. Sidhu MS, Chan J, Kaelin K, Spielhofer P, Radecke F, Schneider H, Masurekar M, Dowling PC, Billeter MA, Udem SA. 1995. Rescue of Synthetic Measles Virus Minireplicons: Measles Genomic Termini Direct Efficient Expression and Propagation of a Reporter Gene. *Virology* 208:800–807.
60. Fuerst TR, Niles EG, Studier FW, Moss B. 1986. Eukaryotic transient-expression system based on recombinant vaccinia virus that synthesizes bacteriophage T7 RNA polymerase. *Proc. Natl. Acad. Sci. U S A* 83:8122–6.
61. He B, Paterson RG, Ward CD, Lamb RA. 1997. Recovery of infectious SV5 from cloned DNA and expression of a foreign gene. *Virology* 237:249–260.
62. Vanmechelen B, Bletsa M, Laenen L, Lopes AR, Vergote V, Beller L, Deboutte W, Korva M, Avšič Županc T, Goüy de Bellocq J, Gryseels S, Leirs H, Lemey P, Vrancken B, Maes P. 2018. Discovery and genome characterization of three new Jeilongviruses, a lineage of paramyxoviruses characterized by their unique membrane proteins. *BMC Genomics*. 19: 617.
63. Bao Y, Chetvernin V, Tatusova T. 2014. Improvements to pairwise sequence comparison (PASC): a genome-based web tool for virus classification. *Arch. Virol.* 159: 3293–3304.
64. Alkhovsky S, Butenko A, Eremyan A, Shchetinin A. 2018. Genetic characterization of bank vole virus (BaVV), a new paramyxovirus isolated from

kidneys of bank voles in Russia. *Arch. Virol.* 163:755-759.

65. Kurth A, Kohl C, Brinkmann A, Ebinger A, Harper JA, Wang LF, Mühldorfer K, Wibbelt G. 2012. Novel paramyxoviruses in free-ranging European bats. *PLoS One* 7:e38688.
66. Leroy EM, Kumulungui B, Pourrut X, Rouquet P, Hassanin A, Yaba P, Délicat A, Paweska JT, Gonzalez JP, Swanepoel R. 2005. Fruit bats as reservoirs of Ebola virus. *Nature* 438:575–576.
67. Li W, Shi Z, Yu M, Ren W, Smith C, Epstein JH, Wang H, Crameri G, Hu Z, Zhang H, Zhang J, McEachern J, Field H, Daszak P, Eaton BT, Zhang S, Wang LF. 2005. Bats are natural reservoirs of SARS-like coronaviruses. *Science* 310:676–679.
68. Yob JM, Field H, Rashdi AM, Morrissy C, van der Heide B, Rota P, bin Adzhar A, White J, Daniels P, Jamaluddin A, Ksiazek T. 2001. Nipah virus infection in bats (order Chiroptera) in peninsular Malaysia. *Emerg. Infect. Dis.* 7:439–441.
69. Middleton DJ, Morrissy CJ, van der Heide BM, Russell GM, Braun MA, Westbury HA, Halpin K, Daniels PW. 2007. Experimental Nipah Virus Infection in Pteropid Bats (*Pteropus poliocephalus*). *J. Comp. Pathol.* 136:266–272.
70. Halpin K, Young PL, Field HE, Mackenzie JS. 2000. Isolation of Hendra virus from pteropid bats: A natural reservoir of Hendra virus. *J. Gen. Virol.* 81:1927–1932.
71. Ghatage D, Gosavi S, Hazarey V, Ganvir S. 2012. Apoptosis: Molecular

mechanism. *J. Orolfac. Sci.* 4: 103-107.

72. Wilson RL, Fuentes SM, Wang P, Taddeo EC, Klatt A, Henderson AJ, He B. 2006. Function of small hydrophobic proteins of paramyxovirus. *J. Virol.* 80:1700–1709.
73. Li Z, Xu J, Patel J, Fuentes S, Lin Y, Anderson D, Sakamoto K, Wang L-F, He B. 2011. Function of the small hydrophobic protein of J paramyxovirus. *J. Virol.* 85:32-42.
74. Miller LC, Tainter ML. 1944. Estimation of the ED50 and Its Error by Means of Logarithmic-Probit Graph Paper. *Proc. Soc. Exp. Biol. Med.* 57:261–264.
75. Webster RG. 1997. Influenza virus: transmission between species and relevance to emergence of the next human pandemic. *Arch Virol. Suppl.* 13:105-13.
76. Alexander DJ. 2000. A review of avian influenza in different bird species. *Veterinary Microbiology.* 74:3-13.
77. Van Kerkhove MD, Mumford E, Mounts AW, Bresee J, Ly S, Bridges CB, Otte J. 2011. Highly pathogenic avian influenza (H5N1): Pathways of exposure at the animal-human interface, a systematic review. *PLoS One.* 6:e14582.
78. Banner D, Kelvin AA. 2012. The current state of H5N1 vaccines and the use of the ferret model for influenza therapeutic and prophylactic development. *J. Infect. Dev. Ctries.* 6:465-469.
79. Neumann G, Chen H, Gao GF, Shu Y, Kawaoka Y. 2010. H5N1 influenza viruses: Outbreaks and biological properties. *Cell Res.* 20:51-61.

80. Sambhara S, Poland GA. 2010. H5N1 Avian Influenza: Preventive and Therapeutic Strategies Against a Pandemic. *Annu. Rev. Med.* 61:187-98.
81. Treanor JJ, Campbell JD, Zangwill KM, Rowe T, Wolff M. 2006. Safety and Immunogenicity of an Inactivated Subvirion Influenza A (H5N1) Vaccine. *N. Engl. J. Med.* 354:1343-1351.
82. Li Z, Mooney AJ, Gabbard JD, Gao X, Xu P, Place RJ, Hogan RJ, Tompkins SM, He B. 2013. Recombinant parainfluenza virus 5 expressing hemagglutinin of influenza A virus H5N1 protected mice against lethal highly pathogenic avian influenza virus H5N1 challenge. *J. Virol.* 87:354–62.
83. Mooney AJ, Li Z, Gabbard JD, He B, Tompkins SM. 2013. Recombinant parainfluenza virus 5 vaccine encoding the influenza virus hemagglutinin protects against H5N1 highly pathogenic avian influenza virus infection following intranasal or intramuscular vaccination of BALB/c mice. *J. Virol.* 87:363–71.
84. Li Z, Gabbard JD, Johnson S, Dlugolenski D, Phan S, Tompkins SM, He B. 2015. Efficacy of a parainfluenza virus 5 (PIV5) - Based H7N9 vaccine in mice and guinea pigs: Antibody titer towards HA was not a good indicator for protection. *PLoS One* 10:e0120355.
85. Chen Z, Gupta T, Xu P, Phan S, Pickar A, Yau W, Karls RK, Quinn FD, Sakamoto K, He B. 2015. Efficacy of parainfluenza virus 5 (PIV5)-based tuberculosis vaccines in mice. *Vaccine.* 33:7217-7224.
86. Abraham M, Arroyo-Diaz NM, Li Z, Zengel J, Sakamoto K, He B. 2018. Role

of small hydrophobic (SH) protein of J paramyxovirus (JPV) in virulence. *J. Virol.* 92: e00653-18.

87. Govorkova EA, Rehg JE, Krauss S, Yen H-L, Guan Y, Peiris M, Nguyen TD, Hanh TH, Puthavathana P, Long HT, Buranathai C, Lim W, Webster RG, Hoffmann E. 2005. Lethality to Ferrets of H5N1 Influenza Viruses Isolated from Humans and Poultry in 2004. *J. Virol.* 79:2191-8.
88. Neumann G, Noda T, Kawaoka Y. 2009. Emergence and pandemic potential of swine-origin H1N1 influenza virus. *Nature.* 459:931-9.
89. de Jong JC, Claas ECJ, Osterhaus ADME, Webster RG, Lim WL. 1997. A pandemic warning? *Nature.* 389:554.
90. Gao R, Cao B, Hu Y, Feng Z, Wang D, Hu W, Chen J, Jie Z, Qiu H, Xu K, Xu X, Lu H, Zhu W, Gao Z, Xiang N, Shen Y, He Z, Gu Y, Zhang Z, Yang Y, et al. 2013. Human Infection with a Novel Avian-Origin Influenza A (H7N9) Virus. *N. Engl. J. Med.* 368:1888-1897.
91. Xu X, Subbarao K, Cox NJ, Guo Y. 1999. Genetic characterization of the pathogenic influenza A/Goose/Guangdong/1/96 (H5N1) virus: Similarity of its hemagglutinin gene to those of H5N1 viruses from the 1997 outbreaks in Hong Kong. *Virology.* 261:15-9.
92. Zhang J. 2012. Advances and future challenges in recombinant adenoviral vectored H5N1 influenza vaccines. *Viruses.* 4: 2711–2735.
93. Sebastian S, Lambe T. 2018. Clinical Advances in Viral-Vectored Influenza Vaccines. *Vaccines.* 6:E29.

94. Stephenson I, Nicholson KG, Wood JM, Zambon MC, Katz JM. 2004. Confronting the avian influenza threat: Vaccine development for a potential pandemic. *Lancet Infect. Dis.* 4:499-509.
95. Li Z, Gabbard JD, Mooney A, Gao X, Chen Z, Place RJ, Tompkins SM, He B. 2013. Single-dose vaccination of a recombinant parainfluenza virus 5 expressing NP from H5N1 virus provides broad immunity against influenza A viruses. *J. Virol.* 87:5985–93.
96. Li Z, Gabbard JD, Mooney A, Chen Z, Tompkins SM, He B. 2013. Efficacy of parainfluenza virus 5 mutants expressing hemagglutinin from H5N1 influenza A virus in mice. *J. Virol.* 87:9604-9.
97. Xu P, Chen Z, Phan S, Pickar A, He B. 2014. Immunogenicity of novel mumps vaccine candidates generated by genetic modification. *J. Virol.* 88:2600-10.
98. Takeuchi R, Tsutsumi H, Osaki M, Haseyama K, Mizue N, Chiba S. 1998. Respiratory syncytial virus infection of human alveolar epithelial cells enhances interferon regulatory factor 1 and interleukin-1beta-converting enzyme gene expression but does not cause apoptosis. *J. Virol.* 72:4498-502.
99. Thomas KW, Monick MM, Staber JM, Yarovinsky T, Brent Carter A, Hunninghake GW. 2002. Respiratory syncytial virus inhibits apoptosis and induces NF- κ B activity through a phosphatidylinositol 3-kinase-dependent pathway. *J. Biol. Chem.* 277:492-501.
100. Young VA, Parks GD. 2003. Simian virus 5 is a poor inducer of chemokine secretion from human lung epithelial cells: identification of viral mutants that

activate interleukin-8 secretion by distinct mechanisms. *J. Virol.* 77:7124-30.

101. Wertz GW, Collins PL, Huang Y, Gruber C, Levine S, Ball LA. 1985. Nucleotide sequence of the G protein gene of human respiratory syncytial virus reveals an unusual type of viral membrane protein. *Proc. Natl. Acad. Sci. U S A.* 82:4075-9.
102. Collins PL, Melero JA. 2011. Progress in understanding and controlling respiratory syncytial virus: Still crazy after all these years. *Virus Res.* 162:80-99.
103. Abraham G, Banerjee A K. 1976. Sequential transcription of the genes of vesicular stomatitis virus. *Proc. Natl. Acad. Sci. U S A.* 73:1504-8.
104. Tokusumi T, Iida A, Hirata T, Kato A, Nagai Y, Hasegawa M. 2002. Recombinant Sendai viruses expressing different levels of a foreign reporter gene. *Virus Res.* 86:33-8.
105. Zhao H, Peeters BPH. 2003. Recombinant Newcastle disease virus as a viral vector: Effect of genomic location of foreign gene on gene expression and virus replication. *J. Gen. Virol.* 84:781-8.
106. von Messling V, Milosevic D, Cattaneo R. 2004. Tropism illuminated: lymphocyte-based pathways blazed by lethal morbillivirus through the host immune system. *Proc. Natl. Acad. Sci. U S A.* 101: 14216–14221.
107. Zhang Z, Zhao W, Li D, Yang J, Zsak L, Yu Q. 2015. Development of a newcastle disease virus vector expressing a foreign gene through an internal ribosomal entry site provides direct proof for a sequential transcription

- mechanism. *J. Gen. Virol.* 96:2028-35.
108. Hall MP, Unch J, Binkowski BF, Valley MP, Butler BL, Wood MG, Otto P, Zimmerman K, Vidugiris G, MacHleidt T, Robers MB, Benink HA, Eggers CT, Slater MR, Meisenheimer PL, Klaubert DH, Fan F, Encell LP, Wood K V. 2012. Engineered luciferase reporter from a deep sea shrimp utilizing a novel imidazopyrazinone substrate. *ACS Chem. Biol.* 7:1848-57.
 109. Panchal RG, Kota KP, Spurgers KB, Ruthel G, Tran JP, Boltz RC, Bavari S. 2010. Development of high-content imaging assays for lethal viral pathogens. *J. Biomol. Screen.* 15:755-65.
 110. Hoenen T, Groseth A, Callison J, Takada A, Feldmann H. 2013. A novel Ebola virus expressing luciferase allows for rapid and quantitative testing of antivirals. *Antiviral Res.* 99:207–213.
 111. Johansen LM, Brannan JM, Delos SE, Shoemaker CJ, Stossel A, Lear C, Hoffstrom BG, DeWald LE, Schornberg KL, Scully C, Lehár J, Hensley LE, White JM, Olinger GG. 2013. FDA-approved selective estrogen receptor modulators inhibit ebola virus infection. *Sci. Transl. Med.* 5:190ra79.
 112. Panchal RG, Kota KP, Spurgers KB, Ruthel G, Tran JP, Boltz RC, Bavari S. 2010. Development of high-content imaging assays for lethal viral pathogens. *J. Biomol. Screen.* 15:755-65.
 113. Zhou M, Kitagawa Y, Yamaguchi M, Uchiyama C, Itoh M, Gotoh B. 2013. Expedient neutralization assay for human metapneumovirus based on a recombinant virus expressing Renilla luciferase. *J. Clin. Virol.* 56:31–36.

114. Hu Q, Chen W, Huang K, Baron MD, Bu Z. 2012. Rescue of recombinant peste des petits ruminants virus: Creation of a GFP-expressing virus and application in rapid virus neutralization test. *Vet. Res.* 43:48
115. Banyard AC, Simpson J, Monaghan P, Barrett T. 2010. Rinderpest virus expressing enhanced green fluorescent protein as a separate transcription unit retains pathogenicity for cattle. *J. Gen. Virol.* 91:2918–2927.
116. De Swart RL, Ludlow M, De Witte L, Yanagi Y, Van Amerongen G, McQuaid S, Yüksel S, Geijtenbeek TBH, Duprex WP, Osterhaus ADME. 2007. Predominant infection of CD150+ lymphocytes and dendritic cells during measles virus infection of macaques. *PLoS Pathog.* 3:1771–1781.
117. De Vries RD, Lemon K, Ludlow M, McQuaid S, Yüksel S, Van Amerongen G, Rennick LJ, Rima BK, Osterhaus ADME, De Swart RL, Duprex WP. 2010. In Vivo Tropism of Attenuated and Pathogenic Measles Virus Expressing Green Fluorescent Protein in Macaques. *J. Virol.* 84:4714–4724.
118. Ludlow M, Nguyen DT, Silin D, Lyubomska O, de Vries RD, von Messling V, McQuaid S, De Swart RL, Duprex WP. 2012. Recombinant Canine Distemper Virus Strain Snyder Hill Expressing Green or Red Fluorescent Proteins Causes Meningoencephalitis in the Ferret. *J. Virol.* 86:7508-19.
119. Rudd PA, Cattaneo R, von Messling V. 2006. Canine Distemper Virus Uses both the Anterograde and the Hematogenous Pathway for Neuroinvasion. *J. Virol.* 80:9361-70.
120. Wertz GW, Moudy R, Ball LA. 2002. Adding genes to the RNA genome of

vesicular stomatitis virus: positional effects on stability of expression. *J. Virol.* 76: 7642–7650.

121. Marschalek A, Finke S, Schwemmler M, Mayer D, Heimrich B, Stitz L, Conzelmann K-K. 2009. Attenuation of Rabies Virus Replication and Virulence by Picornavirus Internal Ribosome Entry Site Elements. *J. Virol.* 83:1911-9.
122. Ammayappan A, Nace R, Peng K-W, Russell SJ. 2013. Neuroattenuation of Vesicular Stomatitis Virus through Picornaviral Internal Ribosome Entry Sites. *J. Virol.* 87:3217-28.
123. Hashimoto K, Ono N, Tatsuo H, Minagawa H, Takeda M, Takeuchi K, Yanagi Y. 2002. SLAM (CD150)-Independent Measles Virus Entry as Revealed by Recombinant Virus Expressing Green Fluorescent Protein. *J. Virol.* 76:6743–6749.
124. Hotard AL, Shaikh FY, Lee S, Yan D, Teng MN, Plemper RK, Crowe JE, Moore ML. 2012. A stabilized respiratory syncytial virus reverse genetics system amenable to recombination-mediated mutagenesis. *Virology.* 434:129-36.

APPENDIX A

J PARAMYXOVIRUS (JPV) REPORTER VIRUSES GENERATED BY
INCORPORATING A REPORTER GENE INTO THE VIRAL GENOME
THROUGH THE INTERNAL RIBOSOMAL ENTRY SITE (IRES) REVEALS THE
IN VIVO REPLICATION DYNAMICS OF JPV

Abraham M, Li Z, He B. To be submitted to *Journal of Virology*.

Abstract

J Paramyxovirus (JPV) was first isolated from moribund mice with hemorrhagic lung lesions in Australia in 1972. It is a rodent paramyxovirus classified under genus *Jeilongvirus*. To understand the real-time infection dynamics, we have created replication-competent JPV reporter viruses suitable for *in vivo* bioluminescent imaging in a mouse model. We have used a small and bright NanoLuc luciferase (nL) gene to create the reporter viruses, rJPV-SH-IRES-nL and rJPV-M-IRES-nL, using the reverse genetics system of JPV. Full-Length sequencing of the cDNA of a single virus clone of rJPV-SH-IRES-nL or rJPV-M-IRES-nL confirmed the identity of mutation-free reporter viruses. Infection of Vero cells with reporter viruses revealed that the luciferase activity is in correlation with the concentration and growth kinetics of rJPV-SH-IRES-nL or rJPV-M-IRES-nL. A sublethal intranasal challenge of mice with rJPV-SH-IRES-nL or rJPV-M-IRES-nL enables the visualization of virus spread and clearance on anesthetized mice using IVIS (In vivo Imaging System) Lumina XR imaging system. These findings provide a novel approach to study JPV replication and spread.

Importance

Antibodies against J Paramyxovirus have been detected in rodents, pigs, and humans, suggesting that J Paramyxovirus (JPV) has a broad host range and zoonotic potential. More studies are needed to understand the pathogenic mechanism of *Jeilongviruses*. Our work demonstrates that a recombinant JPV with a luciferase gene is an excellent candidate to study the tissue tropism and replication of JPV by live animal imaging. One of the main advantages of tracking virus infection with a reporter virus is the ability to use the same animal repeatedly to visualize the spread of infection for a long time, which significantly reduces the number of animals required for conducting an *in vivo* experiment.

Introduction

J Paramyxovirus (JPV), a non-segmented negative-sense single-stranded RNA virus (NNSV), is a member of a proposed genus *Jeilongvirus* of the family *Paramyxoviridae*. It was isolated from moribund mice (*Mus musculus*) with hemorrhagic lung lesions in northern Queensland, Australia in 1972. (1, 10, 17, 86). JPV has a large genome of 18,954 nucleotides consisting of eight genes in the order 3'-N-P/V/C-M-F-SH-TM-G-L-5'. JPV has an increased genome size due to the presence of two additional integral membrane proteins, small hydrophobic (SH) and transmembrane (TM), and a second open reading frame (ORF-X) of the G gene (15). JPV genome initially sequenced in 2005, has been named as JPV-LW. By developing a JPV reverse genetic system, a recombinant JPV-LW (rJPV-LW) was generated from the cDNA clone with the sequences of JPV-LW. rJPV-LW contains one extra nucleotide difference in ORF G and three nucleotide differences in ORF X compared to the JPV-LW GenBank submission sequence (17). The rJPV-LW infection did not cause any weight loss or clinical signs in mice (4). A new isolate, JPV-BH, is pathogenic in mice and cause severe fibrinonecrotizing lesions in the lungs. JPV-BH has a same number of nucleotides as JPV-LW and contains one nucleotide difference in the leader (Le) sequence and three nucleotide differences in the L gene compared to JPV-LW (1).

JPV, Tailam virus (TlmpV), and Beilong virus (BeiPV) have similarity in genome coding potential and amino acid identity of putative proteins, put these viruses together in *Jeilongvirus* genus. (12, 13). The genome replication machinery of JPV and BeiPV can be interchanged (21), which also suggests that JPV and BeiPV are closely related. TlmpV was isolated from Sikkim rats (*Rattus andamanensis*) in a molecular

epidemiology study (12). RNA sequences of *jeilongviruses* were isolated from bats (65). Bats are the natural reservoirs of deadly paramyxoviruses like Nipah and Hendra (68–70). As of now, very little information is available about the host specificity, tissue tropism, and molecular basis of pathogenicity of *jeilongviruses*. It is quite possible that a paramyxovirus with human importance may emerge in future from this group.

The presence JPV-BH with a laboratory mouse model system and a reverse genetics system will help to determine the functions of novel genes like TM as well as the pathogenesis and transmission of *jeilongviruses*. In this work, we have generated replication-competent JPV reporter viruses by incorporating NanoLuc® Luciferase gene into the JPV-BH genome. Due to the sequential transcription of NNSVs, a fusion of a reporter gene into the viral genome as an additional transcriptional unit (ATU) will cause a potential impact on the virus life cycle through the attenuated expression of the downstream viral genes (103–107). We decided to pursue the approach of using an internal ribosomal entry site (IRES) to link a reporter gene to the viral gene by avoiding the need for adding a reporter gene as an ATU.

In this study, we used a very small and highly bright luciferase, NanoLuc® Luciferase (nL) to construct a replication-competent JPV reporter virus for our *in vivo* imaging. nL is a 19-kDa luciferase with more than 100 fold light output than renilla and firefly luciferase (108). nL is very easy to clone into the JPV genome due to its small size, and the extreme brightness of the nL-based reporter virus makes the imaging of the internal organs of animals very clear.

Materials and methods

Cells

Human Embryonic Kidney 293T (HEK293T, ATCC, CRL-1573) and Vero cells (ATCC) were maintained in Dulbecco's modified Eagle's medium (DMEM) containing 10% fetal bovine serum (FBS), 100 IU/ml penicillin, and 100 µg/ml streptomycin. All cells were incubated at 37°C in 5% CO₂. Cells infected with viruses were grown in DMEM containing 2% FBS. Vero cells were used to perform plaque assays.

Mice

6-week-old, female, BALB/c mice (Envigo) were used for the studies. Mice were infected with JPV in enhanced Biosafety Level 2 facilities in HEPA-filtered isolators. All animal experiments were performed in accordance with the national guidelines provided by "The Guide for Care and Use of Laboratory Animals" and the University of Georgia Institutional Animal Care and Use Committee (IACUC). The Institutional Animal Care and Use Committee (IACUC) of the University of Georgia approved all animal experiments.

Construction of recombinant JPV plasmids expressing a reporter gene (NanoLuc® Luciferase)

The internal ribosomal entry site (IRES) from encephalomyocarditis virus (EMCV) and the coding sequence of NanoLuc® Luciferase were fused as a single fragment by PCR amplification. This PCR fusion product (IRES-nL) was cloned into the full-length JPV

vector. For constructing pJPV-SH-IRES-nL plasmid, IRES-nL fusion product was inserted after the stop codon of SH gene. For constructing pJPV-M-IRES-nL plasmid, IRES-nL was inserted after the stop codon of M gene.

Virus rescue and sequencing

To generate viable recombinant JPV reporter viruses, a full length plasmid of pJPV-SH-IRES-nL or pJPV-M-IRES-nL, a plasmid expressing T7 polymerase (pT7P), and three plasmids encoding the N, P, and L proteins of JPV (pJPV-N, pJPV-P, and pJPV-L) were co-transfected into HEK293T cells at 95% confluency in a 6-cm plate with Jetprime (Polypus-Transfection, Inc., New York, NY). The amount of plasmids used were as follows: 5 µg of full-length pJPV-ΔSH-EGFP plasmid, 1 µg of pT7P, 1 µg of pJPV-N, 0.3 µg of pJPV-P, and 1.5 µg of pJPV-L. Two days post-transfection, 1/10th of the HEK293T cells were co-cultured with 1 x 10⁶ Vero cells in a 10-cm plate. Seven days after coculture, media were centrifuged to remove the cell debris, and the supernatant was used for plaque assay in Vero cells to obtain single clones of rJPV-SH-IRES-nL or rJPV-M-IRES-nL. Vero cells were used to grow the plaque-purified virus.

The full-length genomes of plaque-purified rJPV-SH-IRES-nL and rJPV-M-IRES-nL were sequenced. Total RNA of rJPV-SH-IRES-nL and rJPV-M-IRES-nL- infected Vero cells were purified using the RNeasy minikit (Qiagen, Valencia, CA). cDNA was prepared using random hexamers. DNA sequences were determined by an Applied Biosystems sequencer (ABI, Foster City, CA).

Growth Kinetics

Vero cells in 6-well plates were infected with rJPV, rJPV-SH-IRES-nL or rJPV-M-IRES-nL at an MOI of 0.1 and maintained in DMEM-2% FBS. The medium was collected at 0, 24, 48, 72, 96, and 120 post-infection (h.p.i). The titers were determined by plaque assay on Vero cells.

Nano-Glo assay

A Nano-Glo viral titer assay was developed to compare the nL activity and the viral titer estimation in PFU/ml. Vero cells in 6-well plates were infected with rJPV, rJPV-SH-IRES-nL or rJPV-M-IRES-nL at an MOI of 0.1 and maintained in DMEM-2% FBS. The medium was collected at 0, 24, 48, 96, and 120 hours post infection (h.p.i). nL activity was measured with the Nano-Glo assay system (Promega), and luminescence was detected with a plate reader.

Detection of viral protein expression

Expression of JPV N, M, F and G in the virus-infected cells was compared. Vero cells in the six-well plates were mock infected or infected with rJPV or rJPV- Δ SH-EGFP at an MOI of 5. The cells were collected at 2 d.p.i and fixed with 0.5% formaldehyde for 1 h. The fixed cells were resuspended in FBS-DMEM (50:50) and permeabilized with 70% ethanol overnight. The cells were washed once with PBS and then incubated with mouse anti-N monoclonal antibody, anti-M monoclonal antibody, anti-F monoclonal antibody or anti-G monoclonal antibody in PBS-1% BSA (1:200) for 1 h at 4°C. The cells were stained with APC Goat anti-mouse IgG from Biolegend (1:500) for 1 h at

4°C in the dark and then washed once with PBS-1% BSA. The fluorescence intensity was measured with a flow cytometer (Becton Dickinson LSR II). For a better comparison of the protein expression, the peak of fluorescence intensity against each monoclonal antibody elicited by mock or virus-infected cells was merged into a single graph using FlowJo software.

Infection of mice with JPV reporter viruses

All animal experiments were carried out strictly following the protocol approved by the University of Georgia IACUC. To study the pathogenesis of rJPV-SH-IRES-nL and rJPV-M-IRES-nL, 6-week-old BALB/c mice (Envigo) were infected with 100 µl of PBS or 8×10^5 of rJPV, rJPV-SH-IRES-nL or rJPV-M-IRES-nL, intranasally. The weight of the mice was monitored for up to 14 d.p.i. Mice were euthanized at 3 and 7 d.p.i to collect lungs to determine the virus titer.

In vivo imaging was performed on anesthetized mice. Nano-Glo® Luciferase Assay Substrate (Promega) was diluted 1:20 in PBS and 100 µl was used to inject retro-orbitally. Bioluminescent images were acquired with IVIS Lumina XR machine. The analysis was performed using the Living Image software (PerkinElmer), and flux measurements were acquired from regions of interest automatically gated to the signal contours. All data in composite images utilized the same scale.

Results

Development and *in vitro* analysis of bioluminescent JPV reporter viruses

To study the real-time replication dynamics of JPV infection, two full-length JPV-BH plasmids (pJPV-SH-IRES-nL and pJPV-M-IRES-nL) with a reporter gene, nL was constructed (Fig A.1). These plasmids, together with three other helper plasmids encoding N, P and L proteins, and a plasmid encoding T7 RNA polymerase, were co-transfected into HEK293T cells and co-cultured with Vero cells as described previously (1). After obtaining the rescued virus, the full-length genome sequences of plaque-purified rJPV-SH-IRES-nL and rJPV-M-IRES-nL were confirmed by RT-PCR and Sanger sequencing.

To compare the growth kinetics of rJPV-SH-IRES-nL and rJPV-M-IRES-nL with rJPV, Vero cells were infected with rJPV, rJPV-SH-IRES-nL, and rJPV-M-IRES-nL at an MOI of 0.1. The medium was harvested at different time points, and titers of virus in media were determined by plaque assay. Compared to rJPV-SH-IRES-nL and rJPV-M-IRES-nL, rJPV had a significantly higher growth on 1 dpi and 2 dpi (Fig A.2A & Fig A.3A). Luciferase activity in the cell culture media of reporter viruses-infected Vero cells was comparable to the growth kinetics of the virus (Fig A.2B & Fig A.3B).

Altered JPV protein expression in Vero cells infected with JPV reporter viruses

To compare the protein expression of rJPV-SH-IRES-nL and rJPV-M-IRES-nL with rJPV, Vero cells were infected with rJPV, rJPV-SH-IRES-nL, and rJPV-M-IRES-nL at an MOI of 5. Mouse monoclonal antibodies against JPV N, M, F, and G were used

to detect the protein expression in terms of Mean Fluorescence Intensity (MFI). Infection of Vero cells with rJPV, rJPV-SH-IRES-nL and rJPV-M-IRES-nL showed similar gene expression of N. N is the first gene transcribed in JPV infection. So we used the expression level of N to standardize the gene expression of other downward genes. Expression of JPV G protein was reduced in rJPV-SH-IRES-nL infection in Vero cells. However, no statistically significant differences were seen in the expression of JPV N, M, and F genes located towards the 3' end of the insertion site. Expression of JPV F and G protein was reduced in rJPV-M-IRES-nL infection in Vero cells. But, no statistically significant differences were seen in the expression of JPV N and M genes located towards the 3' end of the insertion site. (Fig. A.4). These results suggest a decreased gene expression of genes that are located after the insertion site of IRES-nL.

Real-time *in vivo* imaging of JPV infection

To track the real-time replication of JPV in animals and also to determine the pathogenesis of JPV reporter viruses, BALB/c mice were intranasally infected with 100 μ l of PBS or 8×10^5 PFU of rJPV, rJPV-SH-IRES-nL, and rJPV-M-IRES-nL. Mice were monitored for 14 days. rJPV infection resulted in more significant weight loss (Fig. A.5A) than rJPV-SH-IRES-nL and rJPV-M-IRES-nL, suggesting the attenuation of reporter viruses. High virus load was observed in mice infected with rJPV at 3 d.p.i, but interestingly, no difference was seen in the virus loads between the groups at 7 d.p.i (Fig. A.5B). BALB/c mice infected with reporter viruses were subjected to longitudinal weighing and *in vivo* imaging (Fig. A.5C & A.5D). Bioluminescence was detected as

early as 1 dpi indicating the early replication of JPV in both lungs. Increase in the flux intensity of the bioluminescence correlated with the weight loss of mice infected with the reporter viruses. Flux intensity was higher at 3 and 5 dpi on mice infected with both rJPV-SH-IRES-nL and rJPV-M-IRES-nL. These results are comparable with the lung titer of the virus at 3 dpi. Determining the flux intensity of infection with a bioluminescent reporter virus is an ideal way to replace the determination of lung virus titer by sacrificing animals. Bioluminescence was not able to detect from regions other than the lungs, showing the high tropism of JPV to the respiratory system. Plaque assay with homogenates prepared from heart, liver, brain, spleen, and intestine did not show any presence of JPV at 3 dpi (Data not shown). Despite the replication efficiency and corresponding weight loss in mice infected with reporter viruses, their pathogenicity is highly reduced *in vivo*.

Discussion

Even though extensive hemorrhagic lung lesions were observed in mice from which JPV was isolated for the first time, experimental infection of mice and rats with JPV did not cause any clinical signs (10). rJPV-LW has been rescued based on the published genome sequence of JPV, but the intranasal infection did not cause disease in mice (4, 17). Nucleotide differences in the Le sequence and L of JPV resulted in a pathogenic JPV-BH strain with a different phenotype upon experimental infection in mice indicates that the rapid mutations in the JPV and other *jeilongviruses* will result in the evolution of virulent virus strains. Genome structure and aminoacid identity of JPV, TImPV, and BeiPV suggest the possibility of the emergence of other *jeilongviruses* with

varying degree of pathogenicity and host specificity. Due to the pathogenic nature of JPV-BH and the availability of a laboratory mouse model, we can use JPV-BH as a candidate to study the molecular basis of pathogenesis of *jeiloviruses*.

Reverse genetics system of NNSVs allows the generation of recombinant viruses with a single amino acid mutation to the addition or deletion of genes and gene segments. Reporter-expressing viruses with a foreign reporter gene insertion in the viral genome have many benefits for *in vitro* and *in vivo* applications. Reporter viruses are widely used for the anti-viral drug screening (109–112) and for the development of rapid neutralization test to detect the antibody titer (23, 24). Reporter viruses are also used in pathogenesis studies and to gain insights on the dissemination of viruses through the host (106, 115–119).

Bioluminescence was able to detect from 1 dpi in both lungs of mice infected with JPV reporter viruses. Flux increased until 3 dpi to 5 dpi and then diminished, showing an early onset of high replication in the lungs. We previously observed that a high viral titer of JPV up to 5 dpi (1). Moreover, in our previous study, we demonstrated that low viral titer at 3 dpi correlated with the attenuation in mice infected with rJPV- Δ SH-EGFP virus (86). Interestingly, both reporter viruses used in this study were attenuated *in vitro* and *in vivo* (Fig A.2 and A.3). Recombinant Newcastle Disease Virus (rNDV) with alkaline phosphatase reporter gene at various locations had a slow replication in chicken embryo fibroblast. There was a greater attenuation in NDV when the insertion was between the N and P protein (105). Similar results were also seen in Vesicular Stomatitis Virus (VSV), where the insertion of a non-coding transcriptional unit between the N and P reduced the virulence (120). Attenuation of NNSVs after the

addition of IRES sequence into the genome has been previously reported in Rabies and VSV (121, 122). While the reason for the attenuation is unknown, we observed that the insertion of IRES-nL into the JPV reduces the expression gradient of the downstream viral genes (Fig A.4). Using IRES to incorporate the nL gene into the JPV genome helped to maintain the total number of transcriptional units same as that of the wildtype JPV. The coding region of the reporter gene is fused with the IRES region without the conserved Gene End (GE) and Gene Start (GS) regions on the 3' end. It remains unclear why the expression of downstream genes has reduced even though we added nL gene as an extended ORF using the IRES sequence, allowing a cap-independent translation of reporter gene.

Taking into consideration the low JPV titer in lungs and Vero cells, it is clear that the attenuation is related to the slow replication of the virus and the reduced viral protein expression. It was discovered that the L gene of JPV is critical for the pathogenesis (1). Meanwhile, the insertion of IRES-nL decreased the expression of downstream genes; it is possible that the level of L gene-specific mRNA is reduced in cells infected with reporter viruses. Interestingly, the expression of a reporter gene before the first gene showed little attenuation in some paramyxoviruses. Measles virus expressing GFP as an additional transcriptional unit upstream of the N protein showed minimal attenuation *in vitro* and *in vivo* (116, 123). Similarly, very little *in vitro* attenuation was observed in a recombinant RSV expressing a reporter gene before the NS1 gene (124). Generation of a reporter virus which preserves the normal expression gradient of viral genes and molar ratio of viral proteins may be essential to prevent the attenuation.

Acknowledgments

We appreciate the members of He laboratory for their helpful discussion and technical assistance. We thank Dr. Andre Mehle (University of Wisconsin – Madison) for the valuable advice of reporter protein expression. We appreciate the Animal Facility and Flow Cytometry facility of the College of Veterinary Medicine at the University of Georgia for their help and support.

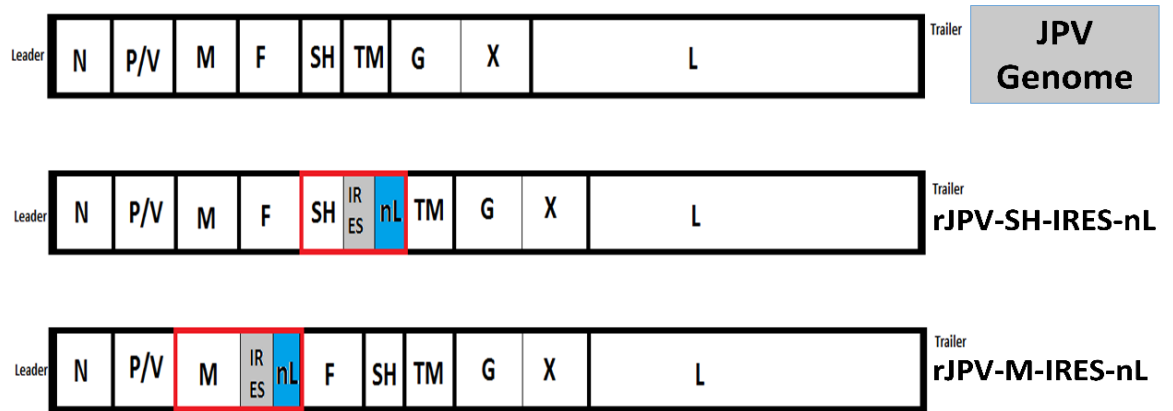


Figure A.1. Recovery of JPV reporter viruses, rJPV-SH-IRES-nL and rJPV-M-IRES-nL. Schematics of rJPV, rJPV-SH-IRES-nL and rJPV-M-IRES-nL, indicating the location where the nL is inserted.

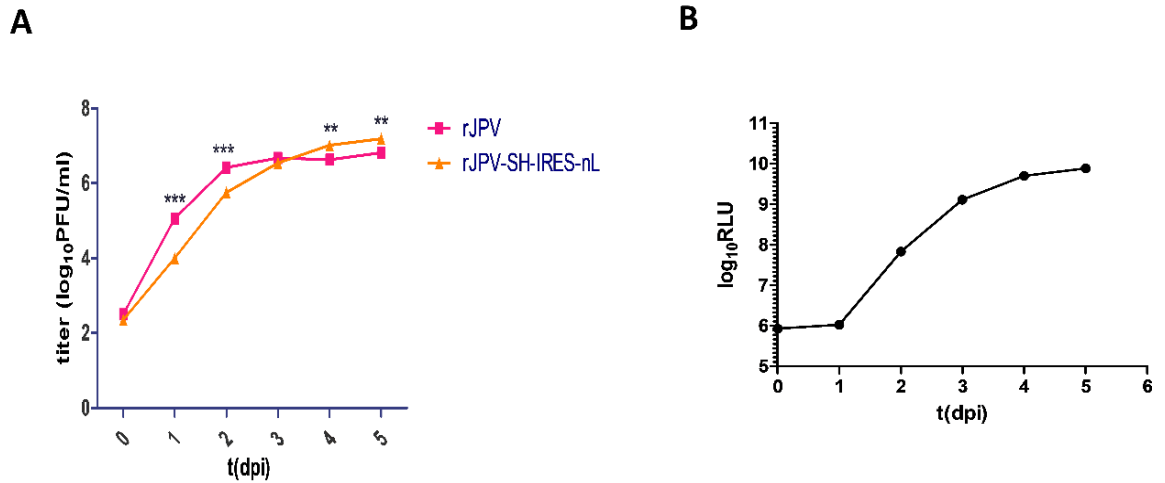


Figure A.2. Growth characteristics and luciferase expression of rJPV-SH-IRES-nL.

(A) Low MOI growth curve of rJPV and rJPV-SH-IRES-nL. Vero cells were infected with rJPV and rJPV-SH-IRES-nL at an MOI of 0.1, and the medium was harvested at 24-h intervals. Plaque assay was performed on Vero cells to determine the virus titer. Statistical significance between groups at each time point was calculated based on two-way ANOVA to compare the growth kinetics. ($P < 0.001$ ***, $P < 0.01$ **, $P < 0.05$ *).

(B) Vero cells in 6-well plates were infected with rJPV and rJPV-SH-IRES-nL at an MOI of 0.1 and maintained in DMEM-2% FBS. The medium was collected at 0, 24, 48, 96, and 120 hours post infection (h.p.i). nL activity was measured with the Nano-Glo assay system (Promega), and luminescence was detected with a plate reader.

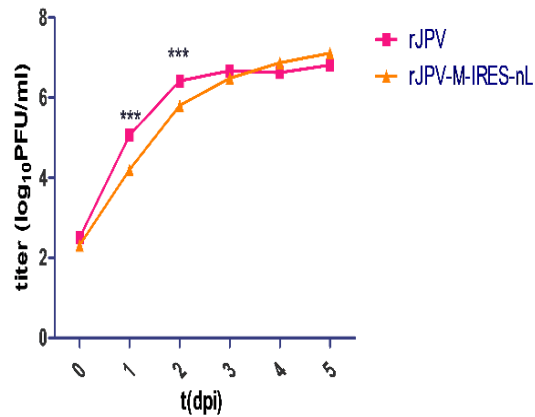
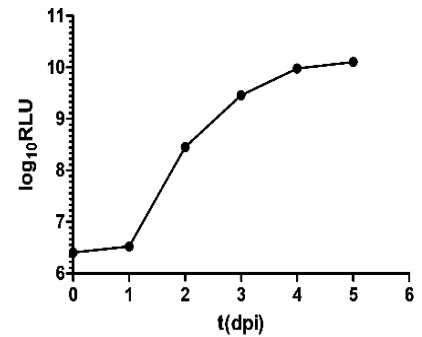
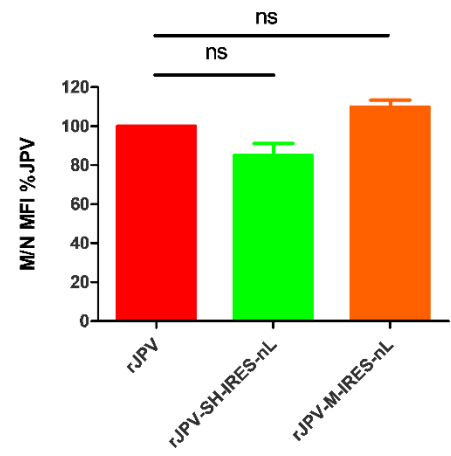
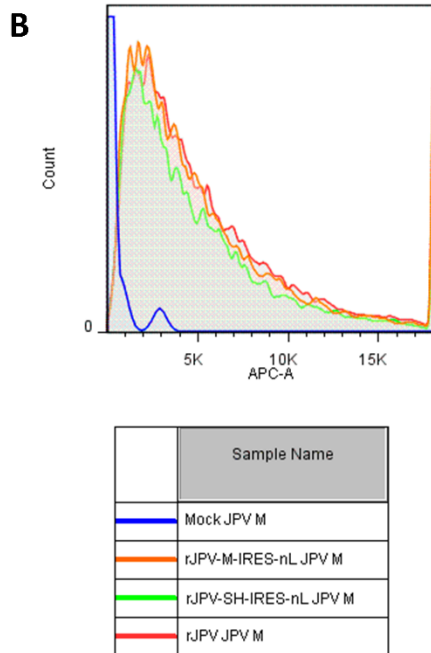
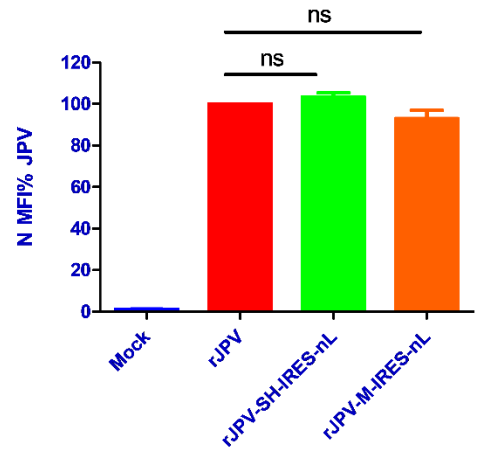
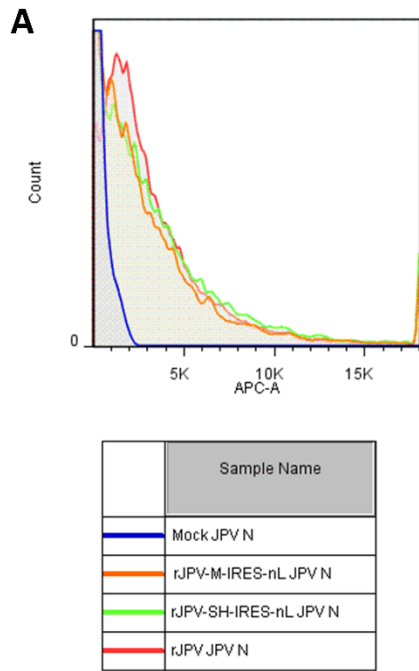
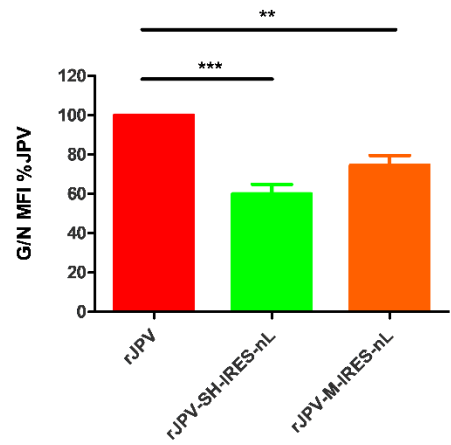
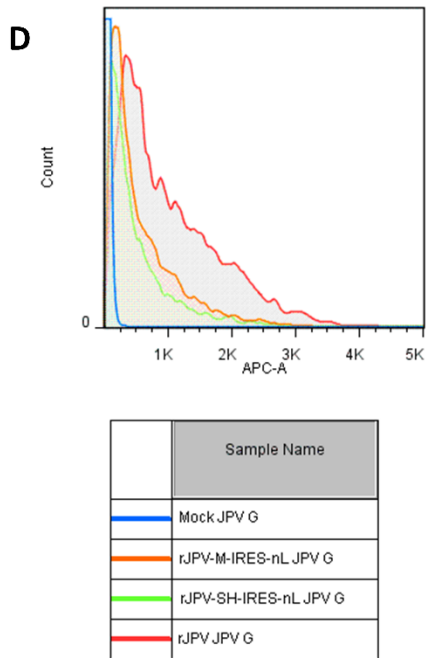
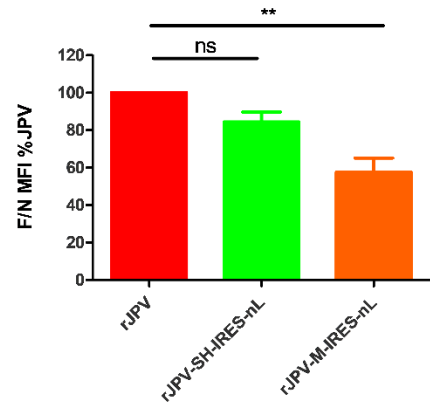
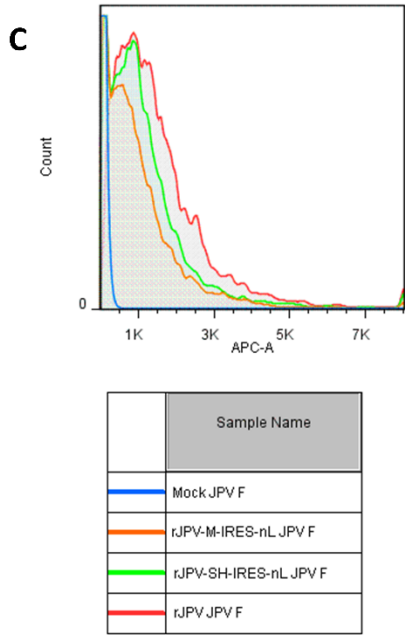
A**B**

Figure A.3. Growth characteristics and luciferase expression rJPV-M-IRES-nL. (A)

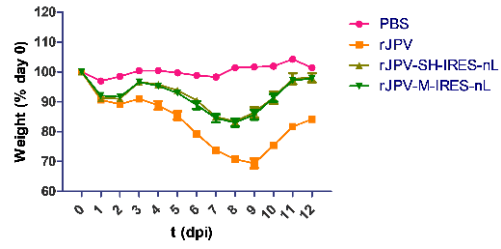
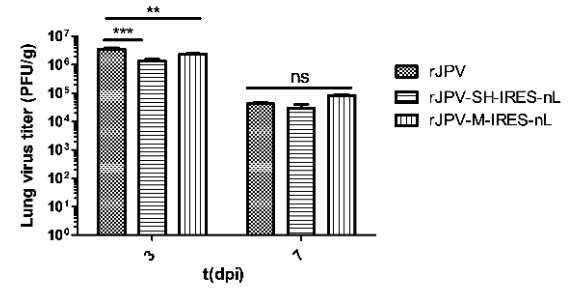
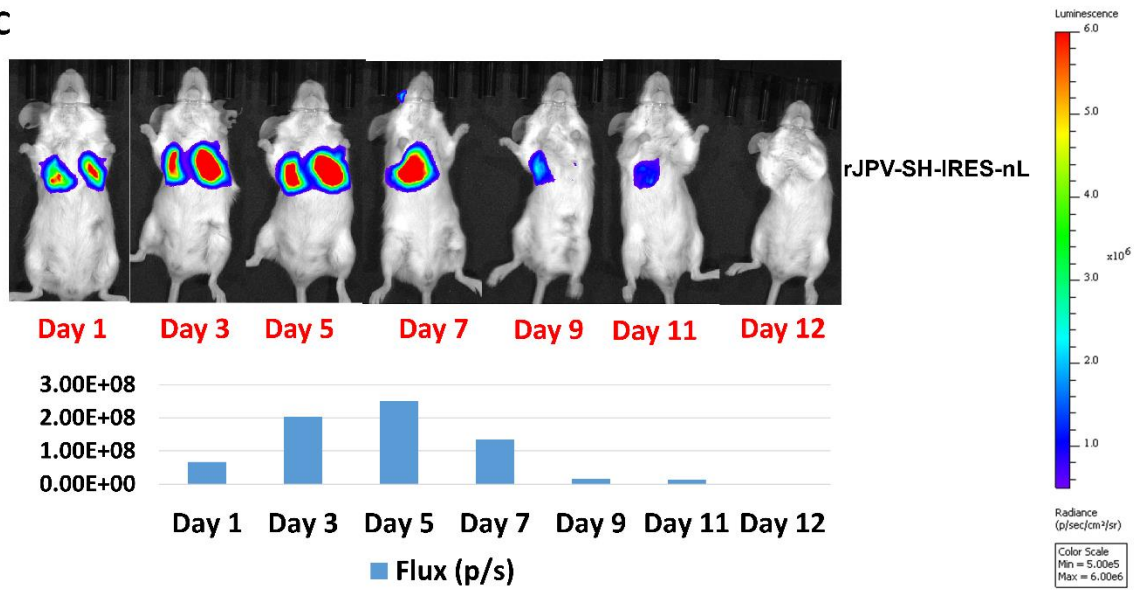
Low MOI growth curve of rJPV and rJPV-M-IRES-nL. Vero cells were infected with rJPV and rJPV-M-IRES-nL at an MOI of 0.1, and the medium was harvested at 24-h intervals. Plaque assay was performed on Vero cells to determine the virus titer. Statistical significance between groups at each time point was calculated based on two-way ANOVA to compare the growth kinetics. ($P < 0.001$ ***, $P < 0.01$ **, $P < 0.05$ *).

(B) Vero cells in 6-well plates were infected with rJPV and rJPV-M-IRES-nL at an MOI of 0.1 and maintained in DMEM-2% FBS. The medium was collected at 0, 24, 48, 96, and 120 hours post infection (h.p.i). nL activity was measured with the NanoGlo assay system (Promega), and luminescence was detected with a plate reader.





*Figure A.4. Gene expression of JPV reporter viruses, rJPV-SH-IRES-nL and rJPV-M-IRES-nL in Vero cells. (A) Expression of N, (B) Expression of M, (C) Expression of F, and (D) Expression of G in the virus-infected cells. Vero cells in the six-well plates were mock infected or infected with rJPV or rJPV-SH-IRES-nL or rJPV-M-IRES-nL at an MOI of 5. The cells were collected at 2 d.p.i and fixed with 0.5% formaldehyde for 1 h. The fixed cells were resuspended in FBS-DMEM (50:50) and permeabilized with 70% ethanol overnight. The cells were washed once with PBS and then incubated with mouse anti-N, anti-M, anti-F, and anti-G monoclonal antibodies. Secondary staining was performed using APC Goat anti-mouse IgG and the fluorescence intensity was measured with a flow cytometer. Samples are triplicates, and error bars show standard errors of the means. Statistical significance between groups at each time point was calculated based on two-way ANOVA to compare the growth kinetics. (P<0.001 ***, P<0.01 **, P < 0.05 *)*

A**B****C**

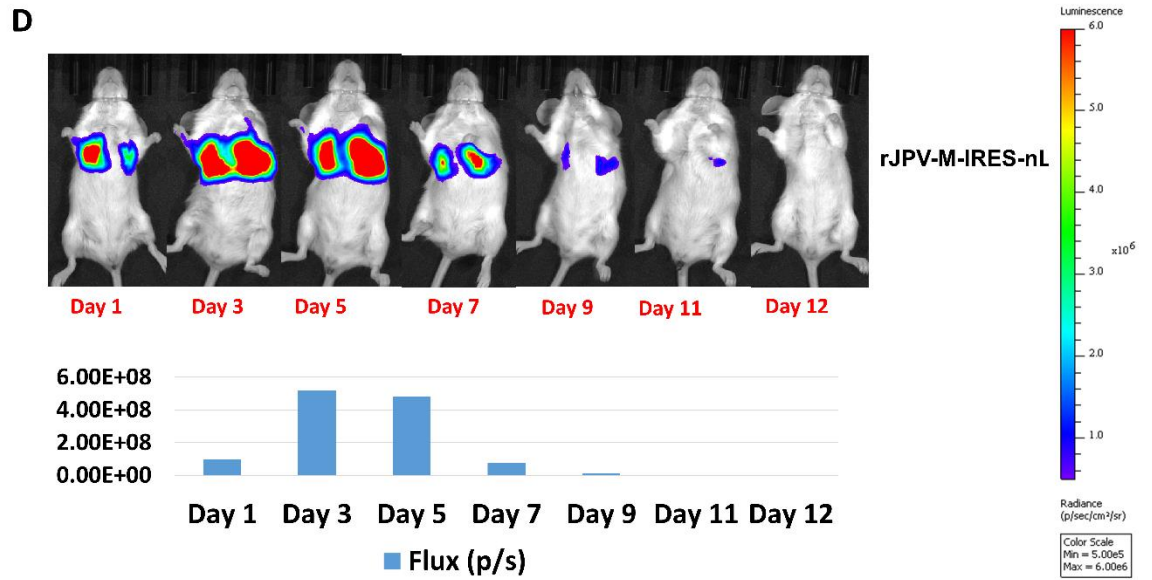


Figure A.5. Infection of BALB/c mice with of rJPV reporter viruses and visualization of JPV replication in vivo. BALB/c mice were intranasally infected with 100 μ l of PBS or rJPV, rJPV-SH-IRES-nL and rJPV-M-IRES-nL at a dose of 8×10^5 PFU. Mice were monitored daily, and weight loss was graphed as the average percentage of their original weight (on the day of infection). (B) Mouse lungs were collected at 3 and 7 d.p.i. Virus titers were determined by plaque assay on Vero cells. (C & D) BALB/c mice were infected with 8×10^5 PFU of rJPV-SH-IRES-nL and rJPV-M-IRES-nL and monitored for bioluminescence of nL using an IVIS camera. Flux measurements were acquired using the Living Image software (PerkinElmer).